

This electronic thesis or dissertation has been downloaded from the King's Research Portal at <https://kclpure.kcl.ac.uk/portal/>



## **An integrated imaging and modelling approach for the management of aortic dissection**

Noorani, Alia Shahzadi

*Awarding institution:*  
King's College London

The copyright of this thesis rests with the author and no quotation from it or information derived from it may be published without proper acknowledgement.

### **END USER LICENCE AGREEMENT**



**Unless another licence is stated on the immediately following page** this work is licensed

under a Creative Commons Attribution-NonCommercial-NoDerivatives 4.0 International

licence. <https://creativecommons.org/licenses/by-nc-nd/4.0/>

You are free to copy, distribute and transmit the work

Under the following conditions:

- Attribution: You must attribute the work in the manner specified by the author (but not in any way that suggests that they endorse you or your use of the work).
- Non Commercial: You may not use this work for commercial purposes.
- No Derivative Works - You may not alter, transform, or build upon this work.

Any of these conditions can be waived if you receive permission from the author. Your fair dealings and other rights are in no way affected by the above.

### **Take down policy**

If you believe that this document breaches copyright please contact [librarypure@kcl.ac.uk](mailto:librarypure@kcl.ac.uk) providing details, and we will remove access to the work immediately and investigate your claim.

# **An integrated imaging and modelling approach for the management of aortic dissection**

**Alia Noorani**

**MBBS (Hons.) BSc. (Hons.) MRCS (England)**

**Dissertation submitted for the degree of Doctor of Medicine**

**University of London, England**

**2015**

The tragedies of life are largely arterial.

Sir William Osler 1908

# Abstract

Aortic dissection is a complex dynamic disease and is the commonest manifestation of the acute aortic syndrome. Outcomes for this disease have not changed significantly despite advances in therapy. Several negative prognostic indicators have been identified but these are generally morphological entities. It is likely that aortic haemodynamics in this pathological state are complex and more than likely contribute to morphological changes seen over time. This is of particular concern in patients who are deemed stable and yet go on to develop complications. A one size fits all strategy is unrealistic in this cohort of patients.

There have been considerable advances in non-invasive diagnostic techniques and although CT is reliable, quick and readily available, MRI provides excellent anatomical detail and application of black blood techniques has the potential to provide vessel wall and therefore tear morphology. Additionally, MRI delivers dynamic functional data. Coupled with computational fluid dynamics there is significant potential to develop a method of non-invasively assessing the haemodynamics in aortic dissection.

The aorta is a complex organ that is subject to a variety of forces thereby undergoing deformation throughout the cardiac cycle. In the setting of a dissection with a fragile intimal flap the variation of motion of the flap can be significant. Dual phase imaging may have the potential to understand the dynamic variability in aortic motion and the deformation it experiences.

In this work, four studies based on the aforementioned factors were undertaken with the aim of highlighting the need for individualised management strategy in aortic dissection.



# Table of Contents

<b>Abstract .....</b>	<b>3</b>
<b>Acknowledgements .....</b>	<b>7</b>
<b>Common Abbreviations .....</b>	<b>9</b>
<b>Chapter 1 .....</b>	<b>10</b>
<b>Overview .....</b>	<b>10</b>
<b>Chapter 2 .....</b>	<b>11</b>
<b>Aortic dissection: The clinical problem .....</b>	<b>11</b>
<b>2.1 Clinical Background .....</b>	<b>11</b>
2.1.1 History .....	11
2.1.2 Pathogenesis, Frequency and Aetiology .....	12
<b>2.2 Classification .....</b>	<b>19</b>
<b>2.3 Presentation .....</b>	<b>22</b>
<b>2.4 Diagnosis .....</b>	<b>23</b>
<b>2.5 Clinical Management .....</b>	<b>25</b>
2.5.1 Management of hypertension .....	25
2.5.2 Surgical management of ascending aortic dissection .....	26
2.5.3 Surgical management of descending aortic dissection .....	29
<b>2.6 Prognosis .....</b>	<b>31</b>
<b>2.7 Fate of the false lumen .....</b>	<b>34</b>
<b>2.8 Follow-up .....</b>	<b>34</b>
<b>2.9 Clinical issues .....</b>	<b>35</b>
<b>Chapter 3 .....</b>	<b>38</b>
<b>3.1 Imaging Modalities in Aortic Dissection .....</b>	<b>38</b>
3.1.1 Challenges .....	38
3.1.2 Computed Tomography .....	40
3.1.3 Magnetic Resonance Imaging .....	42
3.1.4 Echocardiography .....	47
<b>Chapter 4 .....</b>	<b>49</b>
<b>4.1 Computational Fluid Dynamics and Simulation .....</b>	<b>49</b>
4.1.1 CFD in dissection studies .....	50
<b>Chapter 5 .....</b>	<b>53</b>
<b>Aims .....</b>	<b>53</b>
<b>Chapter 6 .....</b>	<b>54</b>
<b>General Materials and Methods .....</b>	<b>54</b>
<b>6.1. Overview .....</b>	<b>54</b>
6.1.1 Validation study .....	54
6.1.2 Follow-up study .....	55
6.1.3 Black blood study .....	55
6.1.4 Dual phase study .....	55

6.2 Ethical approval .....	55
<b>Chapter 7 .....</b>	<b>57</b>
7.1 General Computational Fluid Dynamics Methods .....	57
7.1.1 CRIMSON .....	57
7.1.2 Simulation .....	66
<b>Chapter 8 .....</b>	<b>67</b>
8.1 Validation study Methods .....	67
8.1.1 Equipment details.....	67
8.1.2 Set up for pressure wire recording study.....	68
8.1.3 Subjects .....	70
<b>Chapter 9 .....</b>	<b>71</b>
9.1 Follow up study: Imaging methods.....	71
<b>Chapter 10 .....</b>	<b>73</b>
10.1 Black blood study of aortic wall morphology .....	73
10.1.1 In-vivo experiments .....	73
10.1.2 Pilot study: optimizing parameters to ensure flow-independence .....	76
10.1.3 Data analysis and statistics.....	77
<b>Chapter 11 .....</b>	<b>79</b>
11.1 Dual phase study for aortic motion and strain: imaging methods .....	79
11.1.1 Study population .....	79
11.1.2 Image acquisition .....	79
11.1.3 Image segmentation.....	80
11.1.4 Image analysis .....	81
11.1.5 Analysis of aortic motion and strain .....	86
<b>Chapter 12 .....</b>	<b>87</b>
<b>Results .....</b>	<b>87</b>
12.1 TEVAR Study Results.....	87
12.1.1 TEVAR- Patient 1 .....	89
12.1.2 TEVAR- Patient 2.....	92
12.1.3 TEVAR Patient 3 .....	95
12.1.4 Patient 4 .....	97
12.2 Recording of pressure wire results .....	100
<b>Chapter 13 .....</b>	<b>102</b>
<b>Results .....</b>	<b>102</b>
13.1 Follow up study results.....	102
13.1.1 Follow up patient 1 .....	104
13.1.2 Follow up patient 2 .....	113
13.1.3 Follow up patient 3 .....	118
13.1.4 Follow up patient 4 .....	120
<b>Chapter 14 .....</b>	<b>123</b>

Results .....	123
14.1 Black blood study results.....	123
<b>Chapter 15 .....</b>	<b>128</b>
Results .....	128
15.1 Dual Phase results.....	128
15.1.1 Circumferential change: volunteers.....	132
15.1.2 Circumferential change: patients.....	133
15.1.3 Aortic strain: healthy volunteers .....	138
15.1.4 Aortic strain: dissection patients.....	141
<b>Chapter 16 .....</b>	<b>145</b>
Discussion.....	145
16.1 Follow up study .....	145
<b>Chapter 17 .....</b>	<b>147</b>
Discussion.....	147
17.1 Black blood study .....	147
<b>Chapter 18 .....</b>	<b>149</b>
Discussion.....	149
18.1 Dual phase study .....	149
<b>Chapter 19 .....</b>	<b>153</b>
Conclusion .....	153
19.1 Proposed patient pathway for long term management of acute, residual (chronic) Type B dissections.....	153
<b>Chapter 20 .....</b>	<b>157</b>
Limitations.....	157
20.1 TEVAR Study .....	157
20.2 Follow up study .....	157
20.3 Black blood .....	158
20.4 Dual phase.....	159
<b>References.....</b>	<b>160</b>
<b>List of Tables.....</b>	<b>174</b>
<b>List of Figures .....</b>	<b>175</b>
<b>Appendix.....</b>	<b>183</b>
A1 Patient invitation letters: pressure wire study.....	183
A1 Patient invitation letters - MRI study .....	184
A2 Patient information - invasive study .....	185
A2 Patient information- MRI study .....	194
A3 Research protocol- invasive study .....	203
A3 Research protocol- MRI study.....	212
A4 Consent form- invasive study .....	218
A4 Consent form- MRI study.....	220

# Acknowledgements

This body of work represents the translation of some of my ideas and interests into experiments and then results onto paper. There were many challenges and obstacles along the way but without the support of several kind individuals, none of this work would have been possible.

First and foremost, to all the patients who so very kindly agreed to participate in my study, thank you for driving the field of research in aortic dissection. You all made the effort to attend the hospital on numerous occasions and tolerated hours in the scanner to help me produce this body of work. Without you there would be no project. I am forever humbled and grateful for your generosity.

I am indebted to my supervisor Alberto Figueroa who championed my ideas and thoughts. Despite all the shortcomings thank you for believing in the work for which I am grateful.

My heartfelt appreciation to Desmond Dillon-Murphy, who is living proof that every cloud has a silver lining and that optimism, goes a long way. Without Des's expertise and knowledge on engineering and software applications I would have been lost. Thank you for your unwavering help, patience, and support and of course, the friendship.

My deepest gratitude to Dr Markus Henningsson and his knowledge of MRI physics. Thank you for spending uncountable hours helping me develop ideas into practical experiments.

To all my consultants and my training programme director at Papworth Hospital; thank you for allowing me the time to undertake this work, for all the encouragement and for instilling in me the drive to succeed. You have all been inspirational.

I am grateful for the grant support I received from the Royal College of Surgeons of England and Heart Research UK. Without their generosity I would not have been able to undertake any of this work.

To my family who I hope will be proud, but also glad that the months I have spent obsessing and worrying have come to an end (for now!).

My father Anwar and my mother Khurshid, who have always insisted that nothing was impossible, and that there are no limits; thank you for all your wise words, your time and above all your love and support. Almost nothing in my life would be possible without you two. You are what dreams are made of. You are my inspiration.

An enormous thank you to my sister Ayesha, for the inspiration, the persistent encouragement, and generosity. Without your time and efforts nothing would be possible. We have come such a long way together. I hope I can repay the favour one day.

Thank you also to Alma, without whom nothing would have been practically possible. You have been a fairy godmother.

Finally, two of the most important men in my life; my husband Emin, who has for the last 10 years been a steady rock in my chaotic life, who has stood by every decision I have made no matter how ridiculous. Thank you for all your understanding, your patience, your kindness and your unshakable belief in us. It has not been easy finishing this work, but it would have been impossible without you by my side. My son Rafa: thank you for your patience even at two years of age, and for reminding me, that there is a lot more to life. Never forget, there is nothing more important in the world to me than you, you are my sunshine.

# Common Abbreviations

AA- aortic arch

AAo- ascending aorta

aCNR- apparent contrast to noise ratio

BMT- best medical therapy

CAD - computer aided design

CE-MRA - contrast enhanced magnetic resonance angiography

CFD- computational fluid dynamics

DTA- descending aorta

FOV- field of view

GBCA- gadolinium based contrast agent

IR- inversion recovery

MRA- magnetic resonance angiogram

MDCT- multidetector computed tomography

PC-MRI - phase contrast Magnetic Resonance Imaging

TAAD- Type A aortic dissection

TBAD- Type B aortic dissection

TE- echo time

TR- repetition time

TEVAR- thoracic endovascular aortic repair

TOE- transoesophageal echocardiogram

TTE- transthoracic echocardiogram

T2PSIR- T2-phase sensitive inversion recovery

T2IR- T2- inversion recovery

# Chapter 1

## Overview

Aortic dissection is a major cardiovascular emergency and the commonest aortic catastrophe. A tear in the intima leads to formation of a false lumen between the intima and the media. This false lumen is an alternative channel for blood flow and can lead to several fatal complications such as end organ ischaemia, aortic rupture and cardiac tamponade. Management of this disease depends on the morphology of the dissection, in particular, whether it involves the ascending (Stanford Type A, Debakey I and II) or descending aorta (Stanford Type B or Debakey Type III) as well as the presence of associated complications including end organ ischaemic events, rapid aortic growth and aortic rupture.

Emergency surgery is the treatment of choice for dissection involving the ascending aorta although not every patient may be a candidate for surgery in view of pre-existing co-morbidities or a moribund preoperative state. Patients with dissection involving the descending aorta are generally managed with strict pharmacological blood pressure control, although surgery becomes necessary in those who develop complications.

Outcomes of patients with chronic, non-surgically treated descending aortic dissection (as well as surgically repaired ascending aortic dissection with a residual dissection in the descending aorta) are variable, with more than 1 in 4 patients dead at 5 years from their original presentation. Predictors of outcomes are therefore needed to improve the prognosis in this population. Several negative prognostic factors are already known and one of these is false lumen expansion leading to aortic rupture. Haemodynamics within the false lumen may hold the answer to why some patients remain stable and whilst others do not. A non-invasive method of determining these haemodynamic parameters will provide important insight into this complex disease and a greater understanding of how to best manage it at an early stage and in the long term.

# Chapter 2

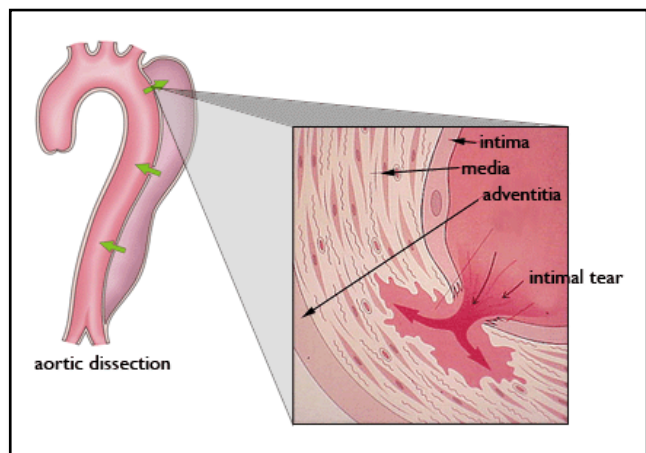
## Aortic dissection: The clinical problem

### 2.1 Clinical Background

#### 2.1.1 History

Acute aortic dissection is a life threatening medical emergency and the commonest manifestation of the acute aortic syndrome, an umbrella term for those conditions that carry a real and inherent risk of aortic rupture, including penetrating aortic ulcer, intramural haematoma and aortic dissection. Of these conditions, aortic dissection is the commonest, (62-88%) followed by intramural haematoma (10-30%) and penetrating ulcer (2-8%). (1)

Aortic dissection is a disease of the media. Cystic medical necrosis weakens the aortic integrity with a tear developing in the aortic intima and formation of a false lumen, Figure 1. Frank Nichols, physician to the then King of England, George II, made the first



description of acute aortic dissection in 1760. On the morning of October

FIGURE 1 AN INTIMAL TEAR RESULTS IN A TRUE AND FALSE LUMEN FOR BLOOD FLOW (2)

25<sup>th</sup> 1760, following a drink of hot chocolate, the 76-year-old King as per usual, retired to the toilet. Several minutes later, his valet heard a noise louder than 'the royal wind' and rushed into the toilet to discover the King lying face down on the floor, with a laceration to the forehead. After laying the King onto his bed, his daughter Amelia was sent for and it was she, who discovered that he was dead. Dr Nichols was instructed to embalm the royal corpse. During this process he made the discovery of a tear in the right ventricle and a transverse



fissure in the inner layer of the aorta which had allowed blood to leak out into the external layer of the aorta, and eventually into the pericardium, causing tamponade (3). However, it was not till 1954 when the all-star team of Denton Cooley and Michael DeBakey in Houston, Texas performed the first successful case of repair of a descending aortic dissection (4,5)

## **2.1.2 Pathogenesis, Frequency and Aetiology**

### ***2.1.2.1 Pathogenesis***

The human aorta, consisting of the ascending aorta, arch and descending aorta is a complex structure complicated by obliquity and asymmetry. The ascending aorta has two portions; the aortic root or a lower portion that extends from the aortic valve to the sinotubular junction, including the aortic annulus and sinuses of Valsalva and an upper part that extends from the sinotubular junction to the origin of the innominate artery. The origin of the innominate artery is the landmark for the beginning of the aortic arch (Figure 2).

The aortic root provides support to the aortic valve leaflets as well as the sinuses of Valsalva from where the coronary arteries originate. The majority of dissections and intramural haematomas of the ascending aorta originate from within a few centimetres of the aortic valve.

The descending aorta begins just distal to the origin of the left subclavian artery at the aortic isthmus. The isthmus is particularly vulnerable to deceleration forces during trauma as here the relatively mobile ascending aorta and arch become relatively fixed to the thoracic cage. As a result, most descending aortic dissections and intramural hematomas have their origin just distal to the left subclavian artery.

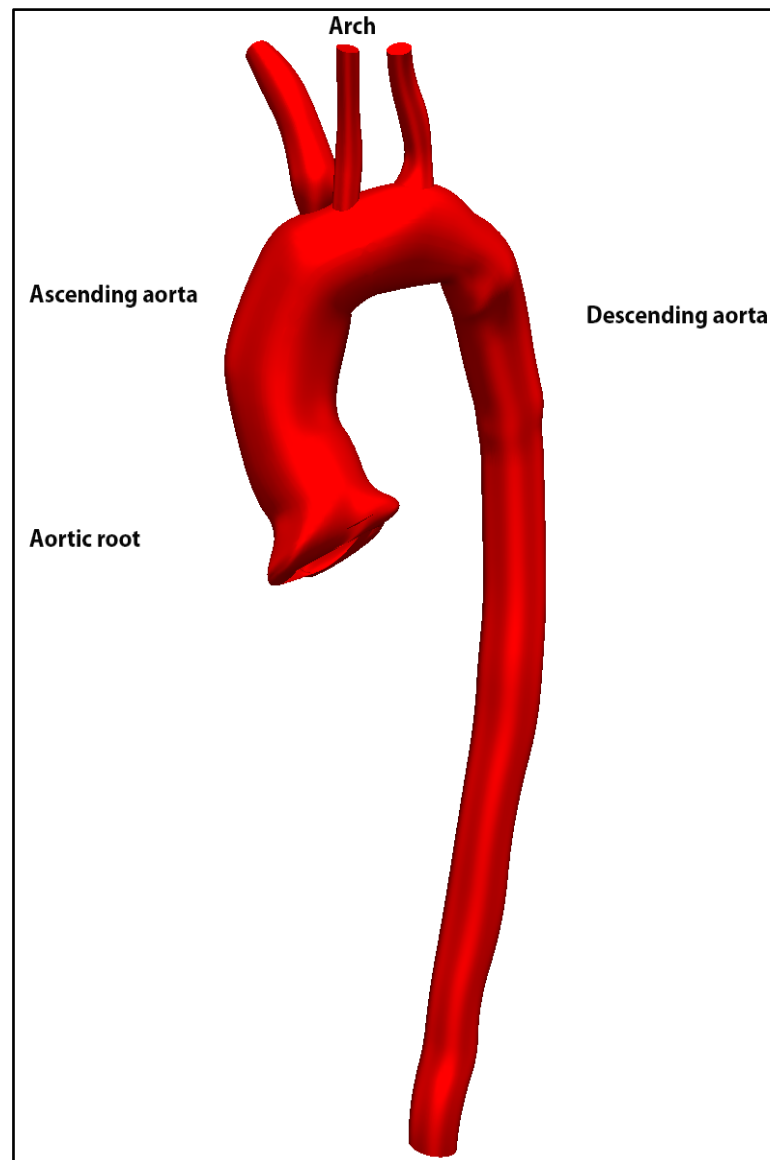


FIGURE 2 SEGMENTS OF THE AORTA. THE AORTIC ROOT EXTENDS FROM THE AORTIC ANNULUS TO THE SINOTUBULAR JUNCTION. THE ASCENDING AORTA COMMENCES AT THE SINOTUBULAR JUNCTION AND EXTENDS TO THE ORIGIN OF THE INNOMINATE ARTERY. THE ARCH OF THE AORTA EXTENDS FROM THE ORIGIN OF THE INNOMINATE ARTERY TO THE LEFT SUBCLAVIAN ARTERY. THE DESCENDING AORTA EXTENDS FROM THE LEFT SUBCLAVIAN TO THE DIAPHRAGMATIC HIATUS WHERE IT CROSSES TO BECOME THE ABDOMINAL AORTA

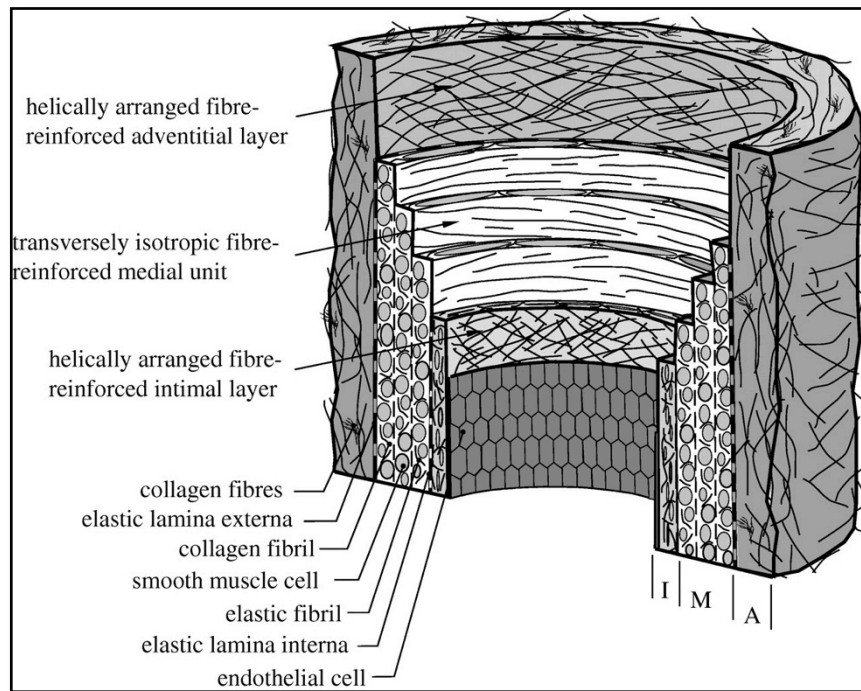


FIGURE 3 COMPONENTS OF THE ARTERIAL WALL (6). THE MONOLAYERED INTIMA IS A THIN BASAL MEMBRANE WITH A SUBENDOTHELIAL LAYER, THE THICKNESS OF WHICH VARIES WITH AGE AND DISEASE. THE MEDIA IS COMPOSED OF SMOOTH MUSCLE CELLS, A NETWORK OF ELASTIC AND COLLAGEN FIBRILS AND ELASTIC LAMINAE WHICH SEPARATE THE MEDIA INTO A NUMBER OF FIBRE-REINFORCED LAYERS. THE ADVENTITIA IS THE OUTERMOST LAYER AND PRIMARILY CONSISTS OF THICK BUNDLES OF COLLAGEN FIBRILS.

Figure 3 shows the structure of the aorta consists of three distinct anatomic layers; the innermost tunica intima, the muscular media and the outer layer, the tunica externa or adventitia.

The intima is a metabolically active mono-layered structure consisting of endothelial cells, with a loose connective tissue base that allows movement of the intima relative to the muscular media accommodating changes in the cardiac cycle. In contrast, the media consists of many lamellar elastic fibres, interposed with collagenous fibres and smooth muscle. These anatomic features allow for distensibility, stretch and aortic integrity as well as modulation of vascular tone in response to shear stresses induced by the blood flow. The

outermost adventitia is a tough layer of collagen and connective tissue that enhances overall aortic integrity. The dominant component is elastin in the thoracic aorta and collagen in the descending aorta.

Aortic dissection is primarily a disease of the aortic media, where cystic necrosis leads to compromise in the aortic integrity. Eventually, a tear develops in the intima, allowing a new channel for blood flow, the false lumen, to form between the aortic media and intima. Often pressurized, the false lumen can propagate proximally towards the aortic valve, leading to acute aortic insufficiency, coronary artery compromise and even aortic rupture. Conversely, it may propagate distally, affecting the branches of the thoracic as well as the abdominal aorta along the way, leading to ischaemic cerebral, visceral or limb complications.

Other manifestations of the acute aortic syndrome, such as intramural haematoma and penetrating aortic ulcer have a similar pathogenesis, presentation and natural history to acute dissection. Intramural hematoma develops from haemorrhage within the aortic wall (ruptured vasa vasora), commonly within the descending thoracic aorta. Although lacking a demonstrable tear, it is nonetheless thought to be a precursor to dissection, with a similar prognosis. Penetrating ulcers usually occur in elderly patients within a heavily atherosclerotic descending aorta, and can be a precursor to dissection. Generally, large (greater than 3 cm in diameter) and symptomatic ulcers should be managed surgically. (4)

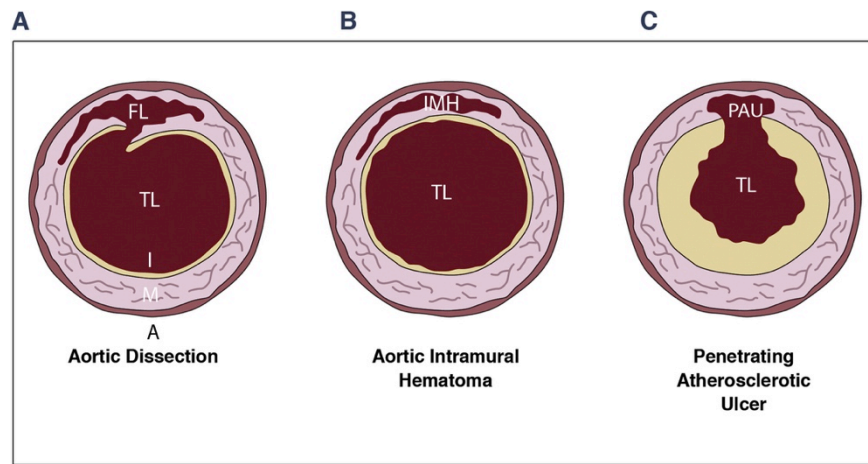


FIGURE 4 MANIFESTATIONS OF THE ACUTE AORTIC SYNDROME. TL= TRUE LUMEN, FL= FALSE LUMEN, PAU = PENETRATING AORTIC ULCER, IMH = INTRAMURAL HAEMATOMA (7)

### **2.1.2.2 Frequency**

The incidence of acute aortic dissection is 4-10 per 100 000 in the UK and the USA, although since this is not a reportable disease and fewer autopsies are being performed, actual numbers may in fact be much higher.

### **2.1.2.3 Aetiology**

Aortic dissection is a complex disease with a multifactorial aetiology and any weakening of aortic structure may predispose the patient to dissection.

**Age:** Aortic dissection is commoner in patients between 60-75 years (40%) than in younger patients or those older than 75 years. The aetiology in younger patients tends to reflect aorto-vascular or connective tissue disease in contrast to atherosclerosis that affects the older population. (8)

**Sex:** Prevalence studies have demonstrated a male predilection of 3:1.

**Hypertension:** Hypertension is the most important predisposing factor for aortic dissection affecting up to 70% of patients. Data from The International Registry of Acute Aortic

Dissections (IRAD) has identified a history of hypertension as being an independent risk factor for Type A aortic dissection in aortic diameters less than 5.5cm. (9)

Systolic hypertension exacerbates the haemodynamic forces acting upon the mobile ascending and the relative fixed aortic arch and descending aorta thereby affecting aortic integrity in the acute setting. A study by Juvonen et al demonstrated that higher mean arterial and diastolic pressures were independent risk factors for the development of aortic rupture in chronic, medically treated Type B dissection. (10)

Genetic predisposition: A number of genetic connective tissue disorders have been linked to aortic dissection. Although these form a smaller subset of the affected patient population, they make up the majority of younger patients (< 40 years) presenting with dissection. The incidence of acute aortic dissection depends on the genetic variant present.

- a. Marfan syndrome: Marfan syndrome is the commonest of all connective tissue disorders, with an estimated incidence of 1 in 5000 to 2-3 in 10 000. It was first described by the French physician Bernard Marfan in 1896 and occurs as a result of a variety of missense mutations on chromosome 15. These mutations affect the gene encoding for fibrillin-1, an elastin-matrix glycoprotein essential for the formation of microfibrils or elastic fibres vital for connective tissue function (11). Transmission is in an autosomal dominant fashion with complete penetrance. A myriad of clinical problems can occur with this disease, of which cardiac, musculoskeletal and ocular complications are the commonest. Approximately 70% of patients with Marfan syndrome develop thoracic aortic dissection.
- b. Loeys-Dietz syndrome: Loeys-Dietz syndrome was first described in 2005. It is an autosomal dominant disorder caused by mutations in the genes encoding the transforming growth factor beta receptor (TGF $\beta$ R) (12). The main characteristics of Loeys-Dietz syndrome include arterial tortuosity, especially affecting the head and neck vessels, hypertelorism, a bifid uvula, and aneurysm formation, most commonly

affecting the aortic root. Some 30% of patients with Loeys-Dietz syndrome develop thoracic aortic dissection. (8)

- c. Ehlers-Danlos syndrome: Ehlers-Danlos syndrome encompasses a heterogeneous group of inherited connective tissue disorders characterised by joint hypermobility, cutaneous fragility and hyperextensibility (13). In the United States, the prevalence of this condition is approximately 1 in 400 000. The collagen defect has only been identified in 6 of the 11 types Ehlers-Danlos syndrome.
- d. Non-syndromic mutations in other genes (MYH11 and ACTA2) and single nucleotide polymorphism, in MMP3 and MMP9 have also been linked to the development of aortic dissection.

**Congenital cardiac anomalies:** A bicuspid aortic valve (BAV) is the commonest inherited congenital cardiac anomaly, affecting up to 1-2% of the population and is responsible for the majority of cases of aortic stenosis under the age of 60 years (14). A co-inherited defect in the aortic media leads to enhanced apoptosis resulting in its weakening and subsequent dilatation. Patients with bicuspid aortic valve are at 5-18 times the risk of developing aortic dissection.

**Iatrogenic causes:** Although rare, aortic dissection is thought to occur in up to 5% of cardiac surgical procedures (in particular aortic valve surgery) as well as in percutaneous revascularisation interventions. (15)

**Inflammatory conditions:** Inflammatory conditions affecting the aorta (and other arteries) include Takayasu's arteritis, giant cell arteritis, rheumatoid arthritis and syphilitic aortitis. Subsequent weakening and dilatation of the aorta can cause dissection.

Miscellaneous causes: Any acute sustained increase in arterial blood pressure can lead to aortic dissection. Systolic blood pressure surges of up to 300mmHg have been well documented in weight lifters, and these are an 'at risk' group (16). In addition, sudden acute hypertension caused by emotional stressors has also been implicated. Finally, cocaine has also been known to result in aortic dissection.

## 2.2 Classification

Disease classification is an essential component of risk stratification and patient management. Classification of aortic dissection is important and helps to differentiate between cases requiring prompt surgical intervention and those, which can be managed conservatively.

Acute aortic dissection is classified either by the location of the primary intimal tear or the involvement of the ascending aorta. (Figure 5) The DeBakey (I, II, III) classification was devised in 1965 and is based on the origin of the primary intimal tear. (5) The Stanford classification method was proposed in 1970 and sought to simplify the original DeBakey classification in that the *location* of the intimal tear did not contribute to the classification. (17)



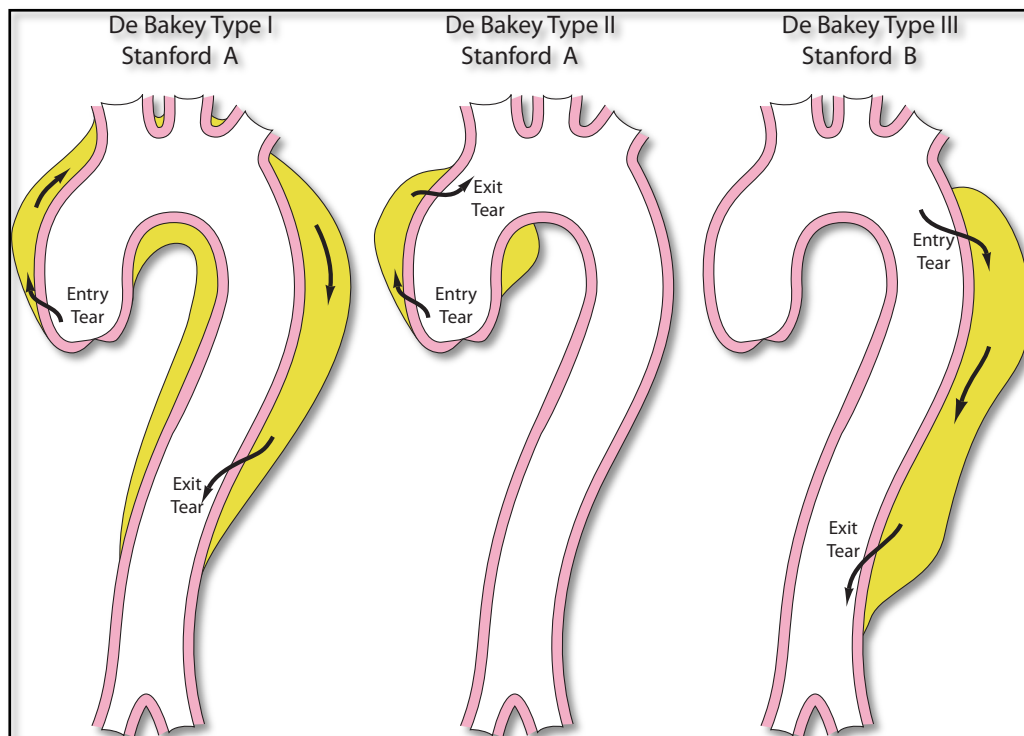


FIGURE 5 CLASSIFICATION OF AORTIC DISSECTION, DEBAKEY AND STANFORD. IN STANFORD TYPE A THE ASCENDING AORTA IS INVOLVED IN THE DISSECTION. IN STANFORD TYPE B THE DESCENDING AORTA IS INVOLVED. IN THE DEBAKEY SYSTEM THE LOCATION OF THE TEAR IS IMPORTANT, AND IN TYPE I AND II THE TEAR IS LOCATED IN THE ASCENDING AORTA WHEREAS IN TYPE III THE TEAR IS IN THE DESCENDING AORTA.

In DeBakey Type I and II aortic dissection, the intimal tear is located in the ascending aorta, whereas in Type III it is located distal to the left subclavian artery. (5,17)

By contrast, in the Stanford system, the origin of the tear does not matter and instead any involvement of the ascending aorta classifies the dissection as Type A whereas its non-involvement classifies it as Type B. Typically in DeBakey Type I and II subtypes, the dissection originates in the ascending aorta and propagates distally whereas in Type III the dissection originates in the descending thoracic aorta, distal to the left subclavian artery and extends distally, or rarely proximally and retrograde into the arch and ascending aorta (17,18).

Based on these factors, it is a given that Stanford Type A dissection and DeBakey Type I and II, by virtue of involving the ascending aorta require surgical intervention to prevent aortic rupture whereas Type B and Type III can be managed conservatively unless complications ensue.

Dissection involving the arch is a controversial area. As management of these generally tends to be pharmacological, without surgical intervention, many recommend that this entity fall into the Type B Stanford category. (19)

## 2.3 Presentation

The classical presentation for aortic dissection is a patient with acute, tearing, central chest pain radiating to the intra-scapular region. Other presenting features may include signs of acute left ventricular failure from aortic insufficiency, ischaemic manifestations from involvement of any of the branches of the aorta such as coronary compromise leading to acute myocardial infarction, stroke from extension into the supra-aortic branches, mesenteric infarction if the infra-diaphragmatic aorta is involved and death from aortic rupture or tamponade.

Neurological deficit has been reported in up to 17% of cases with Type A aortic (TAAD) dissection, and acute aortic regurgitation and unequal peripheral pulses in up to 32% of presenting cases. Other clinical features may include hypertension, usually in Type B dissection (TBAD) and hypotension in up to 25% of TAAD cases. Silent dissection without any symptoms can occur in up to 10% of patients, and commonly in diabetic patients (18).

## 2.4 Diagnosis

A prompt diagnosis is crucial. Any history of central chest pain is, in the first instance investigated with an ECG and biochemical myocardial enzyme testing to exclude myocardial infarction. A chest radiograph is performed to rule out pleural or pulmonary diseases. Commonly now, a triple rule-out test in the form of an ECG-gated computed tomography angiogram (CTA) is performed upon presentation. This effectively images the pulmonary and coronary circulation in addition to the aorta. In doing so, this method excludes catastrophic causes of chest pain originating from these sites including myocardial infarction, pulmonary embolus and aortic dissection. (20). Quite often patients may undergo transthoracic echocardiography, although this is only really effective in imaging the first few centimetres of the ascending aorta in a patient with good echo windows.

Although a dissection flap may not be evident, a false lumen, a dilated aorta and aortic insufficiency may be seen in these cases. Transoesophageal echocardiography (TOE) provides excellent views of the ascending, arch and proximal descending aorta although this is not routinely performed in the acute setting due to the potential adverse haemodynamic effects from the stress of the procedure.

TOE does have a role in the perioperative setting to delineate flap anatomy and the functional state of the aortic valve. Figure 6 shows the perioperative TOE images from a patient with acute TAAD and Figure 7 shows the CT images in the same situation.

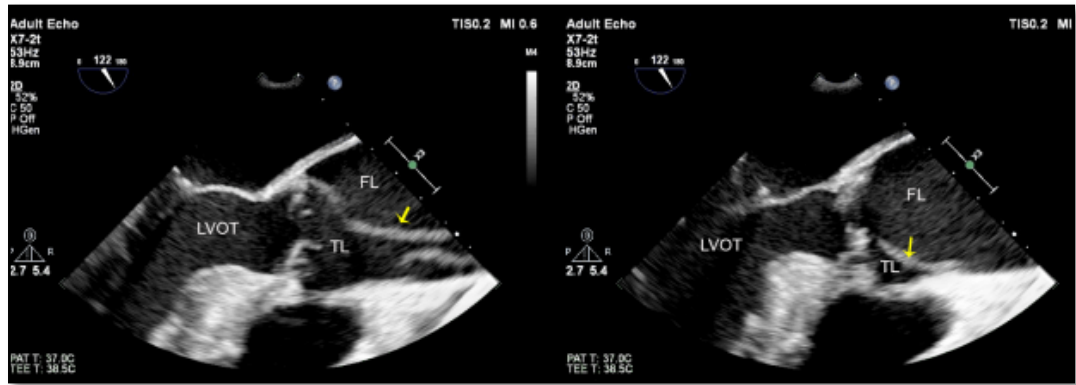


FIGURE 6 TOE IMAGES FROM A PATIENT WITH ACUTE TAAD. YELLOW ARROW INDICATES POSITION OF INTIMAL FLAP. FL=FALSE LUMEN, TL=TRUE LUMEN, LVOT= LEFT VENTRICULAR OUTFLOW TRACT

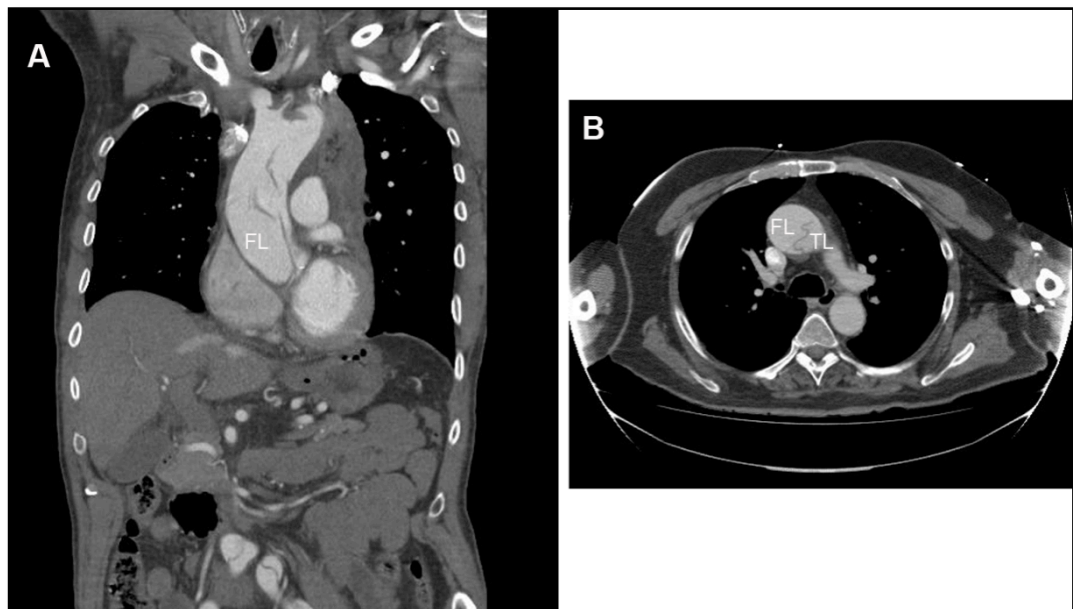


FIGURE 7 CT ANGIOGRAM (A&B) IMAGES FROM A PATIENT WITH ACUTE TAAD. YELLOW ARROW INDICATES POSITION OF INTIMAL FLAP. FL= FALSE LUMEN, TL= TRUE LUMEN.

## 2.5 Clinical Management

Immediate treatment measures once a diagnosis of aortic dissection is made include prompt resuscitation and aggressive blood pressure control (if hypertension is present). The aim is to maintain the systolic blood pressure lower than 100mmHg with the use of beta-blockade, and if required, vasodilators. Once haemodynamic stability is achieved, the patient is referred to a specialist team for optimal further management. Stanford TAAD requires prompt surgery, to treat acute heart failure from valvular insufficiency and prevent death from rupture and tamponade, whereas Stanford TBAD unless complicated by rapid growth, rupture or organ ischaemia can be managed conservatively, with aggressive anti-hypertensive agents.

### 2.5.1 Management of hypertension

Normotension is essential in this subgroup of patients as it aims to prevent additional shearing forces on the aortic wall, which propagate the dissection further. Intravenous beta-blockade is a first line therapy (labetalol, esmolol), titrated to maintain the systolic blood pressure below 100mmHg and a target heart rate between 60-80bpm. A fine balance exists between normotension and hypotension and bradycardia caused by the beta blockade. It is vital to maintain adequate cardiac output and tissue perfusion. Close monitoring of end organ perfusion by means of hourly urine output documentation is essential. In general, vasodilators such as glyceryl trinitrate (GTN) and isosorbide dinitrate (Isoket) are avoided as first line agents, and instead are added once beta blockade therapy has been established. The reflex tachycardia caused by dilating agents as well as the increase in pulse pressure can cause a sudden increase in the shear force on the aorta due to the fast rate of change of pressure ( $\Delta p/\Delta t$  where  $p$ = pressure and  $t$ = time), thereby potentiating tear propagation. Conversely, beta-blockers decrease the pulse pressure and therefore the  $\Delta p/\Delta t$  along with lowering the heart rate. Calcium channel antagonists can also be used but are contraindicated in patients with a history of second or third degree heart block.

## **2.5.2 Surgical management of ascending aortic dissection**

The mortality from acute TAAD is in the order of 1% per hour. (21). Urgent surgery is recommended for patients with acute TAAD, although not all patients are suitable candidates for a major operative procedure. Following transfer to the operating room, under general anaesthesia with endotracheal intubation and ventilation, preparations are made for cardiopulmonary bypass.

Circulatory control and bypass can be achieved via median sternotomy and central aortic access under TOE guidance to ensure cannulation of the true lumen or via peripheral cannulation (femoral arterial and venous or axillary arterial cannulation).

Benefits of peripheral cannulation include control of the circulation prior to entering the chest, and risk of aortic rupture without central arterial access. Axillary cannulation allows for antegrade pump flow and selective antegrade cerebral perfusion should it be desired, during periods of hypothermic circulatory arrest.

Femoral cannulation although easier in practice due to the widespread familiarity with the anatomy of this region and superficial location of the artery may be complicated by retrograde extension of the dissection, or high arterial line pressures and poor flow in the case of an extensive thoracic and abdominal extension of the dissection. In either case, although surgical practices vary, a 10mm woven vascular graft is sewn onto the desired peripheral artery and connected onto the arterial line from the cardiopulmonary bypass circuit.

General considerations for surgery for ascending aortic dissection are identification and resection of the primary tear, stabilisation of the aortic wall (using adjuncts such as glue, Bioglue, CryoLife, GA, USA) prevention of aortic rupture, protection of end-organs (in particular the brain) and correction of malperfusion syndromes by ensuring resection of the primary ascending aortic tear (21).

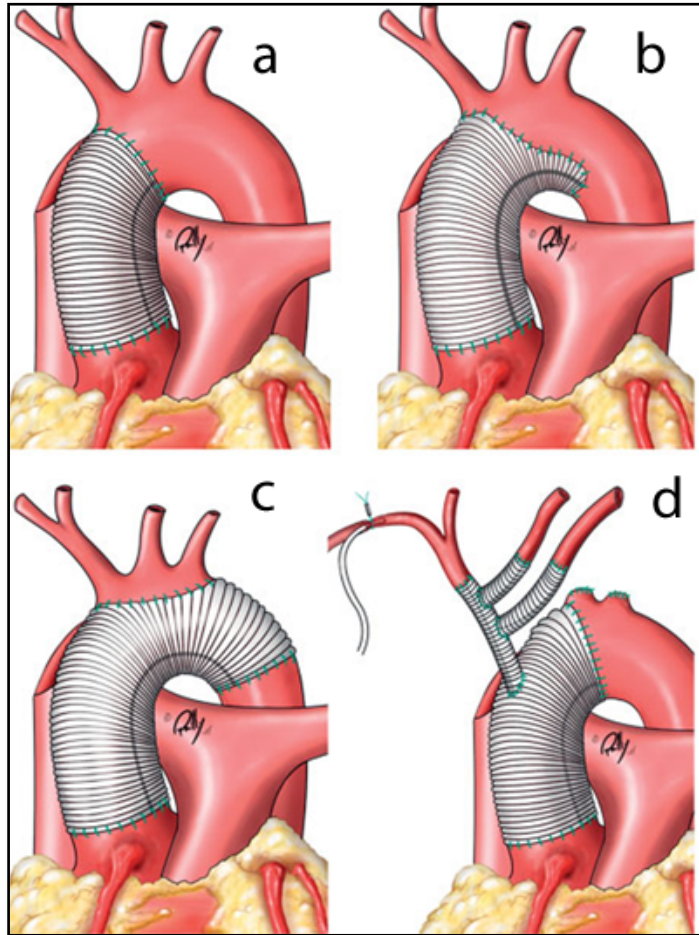


FIGURE 8 OPERATIONS FOR TAAD. A) REPLACEMENT OF THE SUPRA-COMMISSURAL ASCENDING AORTA. B) HEMI-ARCH REPLACEMENT. C) ARCH REPLACEMENT. D) TRIFURCATED GRAFT AND ARCH DEBRANCHMENT (21)



A variety of cannulation options exist but essentially venous drainage occurs from the right atrium, with arterial return either into the distal aorta (true lumen cannulation is directed via TOE using a Seldinger technique) or via the femoral or axillary artery as described above. Hypothermia is initiated once the patient is on cardiopulmonary bypass to allow for an 'open' distal anastomosis without an aortic cross clamp, under deep hypothermic circulatory arrest. Under cardioplegic arrest the distal ascending aorta is inspected, looking specifically for the intimal tear.

Aortic valvular function and anatomy should have been already assessed by perioperative TOE if time allows, as well as by visual inspection. Bioglue (CryoLife, GA, USA) or similar adjuncts are used to approximate and secure the true and false lumens and replacement of the ascending aorta is performed usually using a synthetic graft, although various additional procedures may also be required (valve repair/re-suspension/replacement/hemi-arch replacement) as shown in .

### 2.5.3 Surgical management of descending aortic dissection

The development of ischaemic complications, uncontrollable hypertension, on-going pain indicative of aortic growth and aneurysm formation as well as aortic rupture and are poor prognostic indicators in patients with TBAD and merit intervention.

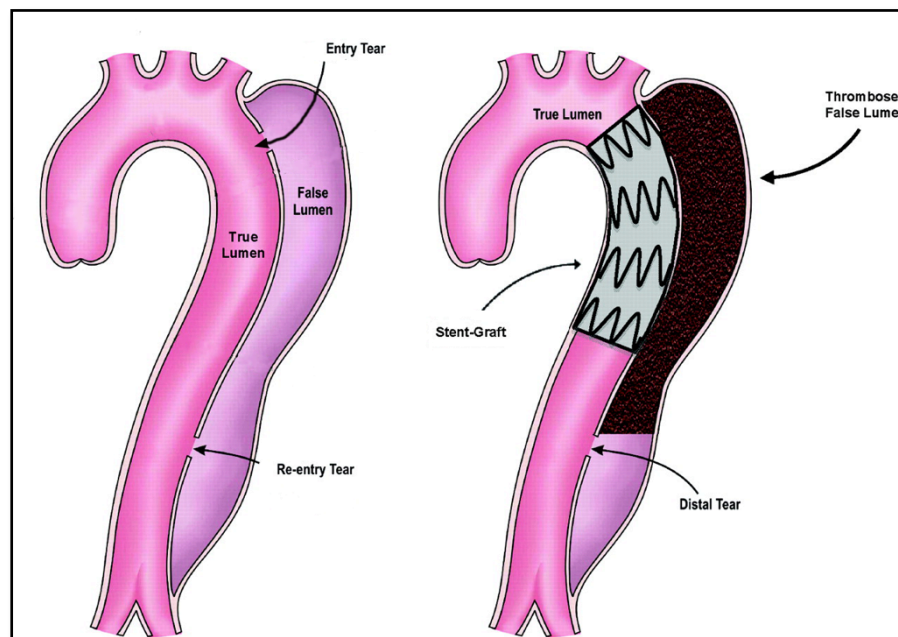


FIGURE 9 TEVAR AIMS TO SEAL OFF THE ENTRY TEAR AND PROMOTE AORTIC REMODELLING. (24)

THE OBJECTIVE OF THE THORACIC STENT GRAFT IS TO OCCLUDE THE ENTRY TEAR, THEREBY SEALING THE FALSE LUMEN, PROMOTING THROMBOSIS (

Figure 9 This is associated with a more favourable outcome. (24,25) Current indications for thoracic endovascular aortic repair (TEVAR) include the presence of symptoms, aortic diameter greater than 5.5cm or a growth rate of over 1 cm per year. (26)

In the multi-centre Investigation of Stent Grafts in patients with TBAD (INSTEAD), a prospective multicentre, European randomized trial, optimal medical therapy was compared

with endovascular stent graft placement for stable TBADs. At one year, no significant all-cause mortality was found. At five years however, TEVAR, in addition to medical treatment was associated with improved aorta-specific survival and delayed disease progression. (27,28) Results of the ongoing Acute Dissection: Stent graft or Best Medical Therapy (ADSORB study) which aim to compare best medical management with stent graft in acute uncomplicated patients with TBAD presenting less than 14 days after onset of symptoms will provide further insight. (29)

## 2.6 Prognosis

The prognosis of untreated TAAD is extremely poor, with a mortality of 1% per hour. Fifty per cent of all patients are dead within the first 48 hours, and 75-90% within the first week. (21,30,31)

Medically managed TAAD carries a mortality of 30-50% at 48 hours but of those who survive, the trajectory is different, with 1-year mortality rate of 12%. (31) In contrast, surgical mortality is between 15-20%, although this is lower at approximately 10-12% in high volume aortic centres.

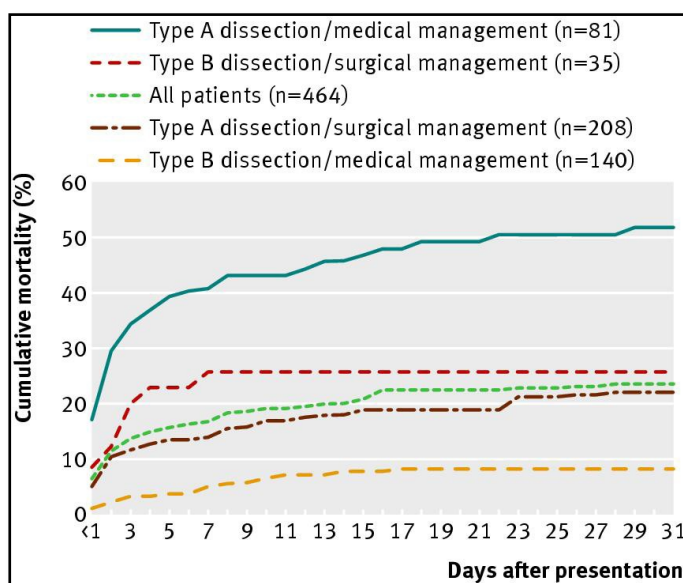
Acute TBAD may be complicated by visceral or limb ischaemia or aortic rupture. Mortality rates in this setting are much higher.

In-hospital mortality rates according to the type of dissection and the relevant management are given in Table 1 and are illustrated by Kaplan Meier curves in Figure 10. Figure 11 depicts the longer-term mortality rates for Type A and TBAD and Figure 12 compares the five-year survival for TBAD when managed conservatively versus endovascular intervention.

Of note, up to 1-in-4 patients with Type B aortic dissection surviving hospital discharge are dead at 3 years. Factors responsible for this poor prognosis need to be sought and understood in order to improve management and as a result, the survival rates. (25,31,32)

TABLE 1 MORTALITY RATES FOR AORTIC DISSECTION BY TYPE AND MANAGEMENT

		Mortality rates by management %									
		Untreated	Medical				Open surgery				TEVAR
		1 week	48h	1y	3y	30d	1y	3y	5y	30d	1y
	<b>Type A</b>	50-91	50	12	32	15-20	4	10-15	17	-	-
	<b>Acute TBAD</b>										
	Uncomplicated	-	-	-	22	-	-	-	-		-
	Complicated	-	-	-	50	70	-	-	-	7	-
	<b>Chronic TBAD</b>	-	-	-	-	-	21	-	-	-	7

FIGURE 10  
MORTALITYIN-HOSPITAL  
FOR

MEDICALLY MANAGED AND SURGICALLY MANAGED AORTIC DISSECTION. MEDICALLY MANAGED TAAD HAS THE WORST IN HOSPITAL MORTALITY AT OVER 50% AT 30 DAYS.(15)

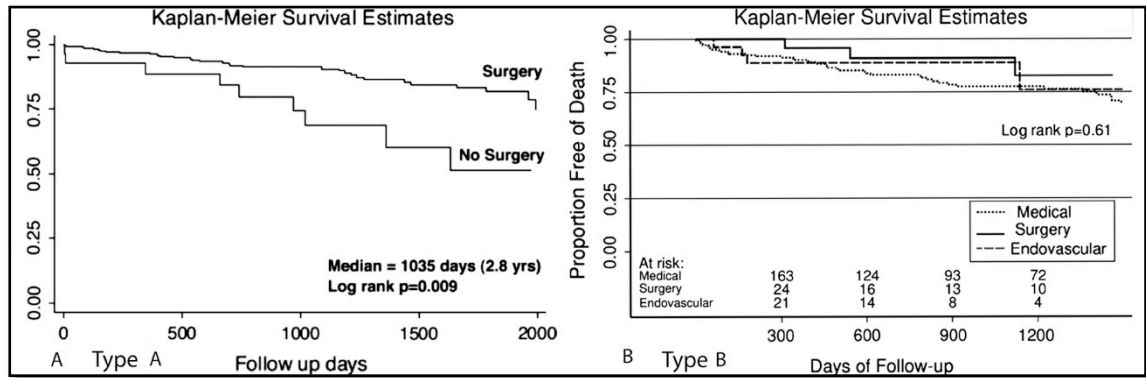


FIGURE 11 A UNADJUSTED KAPLAN-MEIER SURVIVAL CURVE STRATIFIED BY IN-HOSPITAL MANAGEMENT FROM DATE OF HOSPITAL DISCHARGE IN PATIENTS WITH TAAD DISSECTION. (31)  
B. UNADJUSTED KAPLAN-MEIER SURVIVAL CURVE STRATIFIED BY IN-HOSPITAL MANAGEMENT OF PATIENTS WITH ACUTE TBAD WHO SURVIVE TO HOSPITAL DISCHARGE (32)

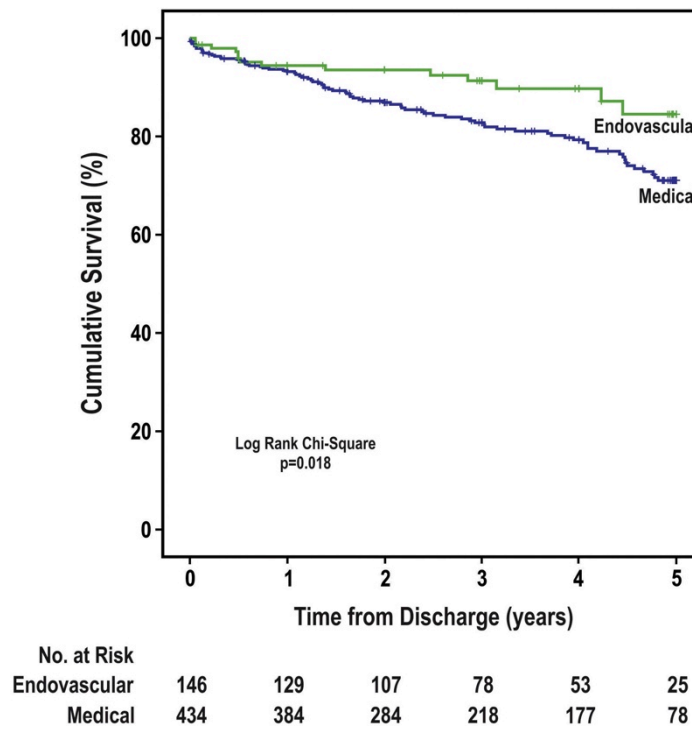


FIGURE 12 FIVE-YEAR SURVIVAL RATES FOR MEDICALLY TREATED TBAD VERSUS ENDOVASCULAR THERAPY. (25)

## 2.7 Fate of the false lumen

Failure to seal the false lumen successfully, either during surgery by failing to exclude the primary tear or by thrombosis over time in medically treated cases leads to on-going aortic expansion and potentially further complications. Several studies have indicated the importance of the fate of the false lumen in aortic dissection (33-39). **Although blood pressure has been implicated in false lumen expansion, no study to date has investigated this accurately.**

## 2.8 Follow-up

Patients with chronic stable and repaired aortic dissection require careful and regular follow up in view of potential late complications including continued aortic dilatation and re-dissection, in particular, in the case of the untreated distal aorta. Risk factors for these potential complications include untreated hypertension, a non-resected entry tear, a large initial aortic diameter, a patent false lumen and Marfan pathology. (34) Patients treated with endografts must also be monitored for potential future endoleaks.

Based on local clinical protocols which may vary from unit to unit, patients are usually followed up with imaging at 3-month intervals in the first year, careful monitoring of their blood pressure at every visit and titration of their anti-hypertensive medication. Imaging of the aorta is necessary to monitor anatomical changes and magnetic resonance imaging (MRI) seems the best option given the avoidance of ionising radiation. Unfortunately, not all centres have access to MRI scanners and imaging with CT seems to be the commonest modality in use at present (26). Although phase-contrast MRI (PC-MRI) can provide blood velocity data, no modality has as of yet, provided other important physiological haemodynamic parameters such as pressure or wall shear stress.

## 2.9 Clinical issues

Aortic dissection represents a complex disease with a multifactorial aetiology and a variable prognosis. Although considerable work has been done and continues to be undertaken into this life threatening disorder, the mainstay of treatment and follow-up has not changed dramatically. This is reflected in the overall prognosis and outcomes from this challenging disease. Although dissection itself adds a separate dimension, the complexity of the aorta as an organ should not be forgotten. The movement of the aorta with respect to the cardiac cycle, the changes in diameter, area and other quantifiable dimensions is remarkable. The addition of such forces upon a fragile intimal flap must have a significant impact. (40,41)

Although tear morphology is important in predicting prognosis and steering clinical management, it is in fact the resulting haemodynamics that determine the pathophysiology of dissection. (42,43) Several studies have demonstrated the importance of geometric considerations such as tear location, number and size in determining outcomes in this patient group. Weiss et al postulated that adverse haemodynamics, in particular, pressure gradients were responsible for higher rates of complicated dissections in patients with tears that were located on the concavity of the aortic arch (43). Other studies have demonstrated that larger tears lead to true lumen collapse and visceral ischaemia (44). Large tears can lead to pressure equalisation between the true and false lumens and the absence of exit tears can lead to a pressurized false lumen, which will be vulnerable to expansion. (39)

The aim of any surgical intervention is to seal the false lumen and promote thrombosis. However, in cases where only partial thrombosis follows from an inadequate or incomplete surgical intervention, there is considerable risk of false lumen pressurization. Tsai et al. demonstrated that partial thrombosis occurs in up to a third of patients following TBAD and this is directly associated with a 2.7 fold increase in mortality compared to a patent false lumen. The hypothesis for this phenomenon is shown in Figure 13. (39)

From these and other observations, it is likely that mechanical and haemodynamic conditions play a significant role in the propagation of aortic dissection. Currently, the only possible



method of determining false lumen pressure is invasively, with the use of a pressure catheter but the invasive nature of this procedure does not lend it self to routine use. In addition to pressure, wall shear stress (WSS) (which is intimately related to blood velocity) plays a significant role in aortic dissection. WSS is related to blood velocity and lower WSS leads to thrombosis. PC-MRI allows for measurement of blood velocity, although this is a time-averaged representation, therefore being susceptible to errors such as Maxwell terms, and eddy currents (45).

At present, we lack sophisticated non-invasive methods that allow a detailed study of this dynamic disease. Computational modelling, imaging and simulation methods may allow for a comprehensive understanding of the complex flow and haemodynamic patterns that are seen in aortic dissection, on a case-by-case, individualised basis. (46) This will in turn allow for customised follow-up and management pathways for this complex sub-group of patients with the overall aim of improving outcomes.

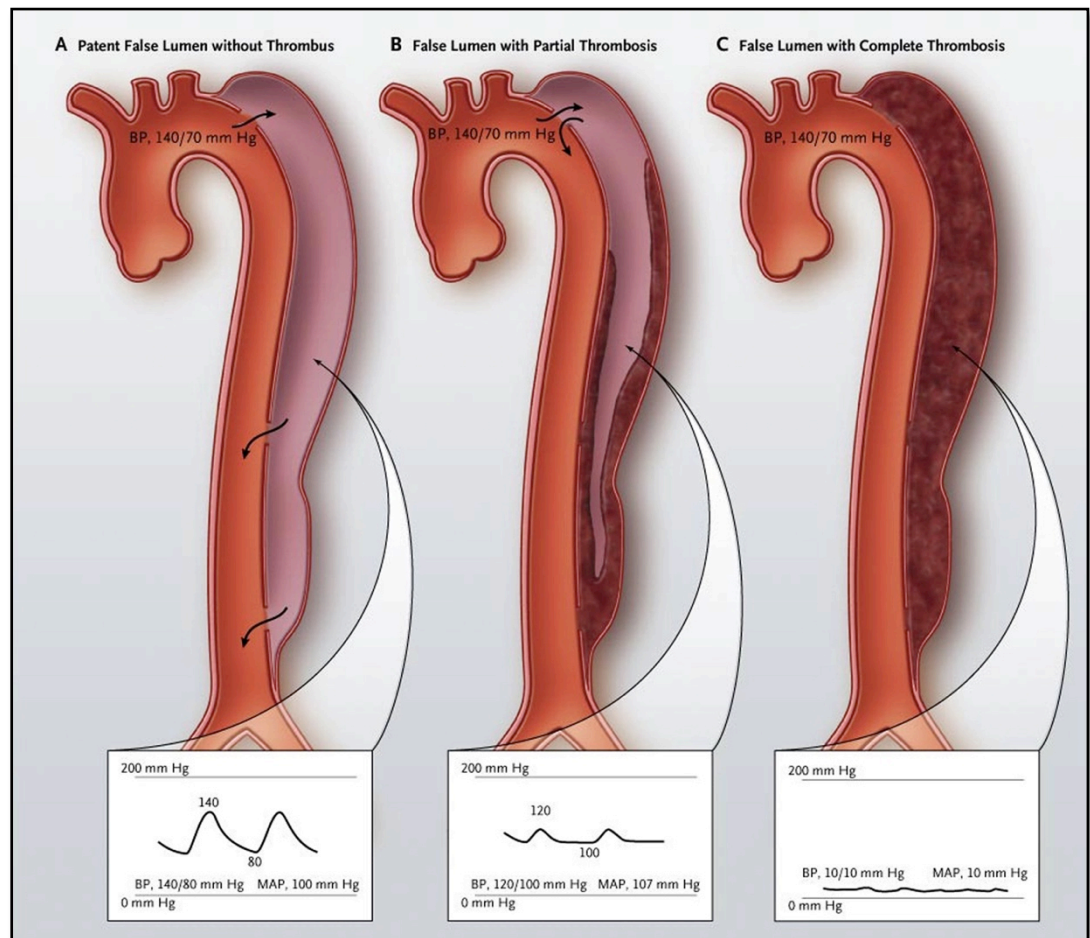


FIGURE 13 A PROPOSED MODEL OF THE PHYSIOLOGICAL CONSEQUENCES OF FALSE-LUMEN PATENCY OR THROMBOSIS, BASED ON HEMODYNAMIC STUDIES IN EX VIVO MODELS AND IN PATIENTS WITH TYPE B AORTIC DISSECTION.

- A. TBAD WITH PATENT PROXIMAL AND PATENT DISTAL RE-ENTRY TEARS IN THE ABSENCE OF THROMBUS. THE BLOOD-PRESSURE TRACING SHOWS SYSTOLIC, DIASTOLIC, AND MEAN ARTERIAL PRESSURES IN THE FALSE LUMEN SIMILAR TO THE PRESSURES IN THE TRUE LUMEN.
- B. TBAD WITH A PATENT ENTRY TEAR AND PARTIAL THROMBOSIS THAT OCCUPIES THE INNER CIRCUMFERENCE OF THE FALSE LUMEN AND OBSTRUCTS THE RE-ENTRY TEARS, FORMING A BLIND SAC. THE BLOOD-PRESSURE TRACING SHOWS DIASTOLIC AND MEAN ARTERIAL PRESSURES IN THE FALSE LUMEN THAT EXCEED THE PRESSURES SEEN IN A, WITH IDENTICAL PRESSURES IN THE TRUE LUMEN.
- C. TBAD WITH A FALSE LUMEN FILLED WITH THROMBUS AND NO LONGER COMMUNICATING WITH THE TRUE LUMEN. THE PRESSURE WITHIN THE FALSE LUMEN IS LIKELY TO BE LOW AND NON-PULSATILE.

BP = BLOOD PRESSURE, MAP= MEAN ARTERIAL PRESSURE(39).

# Chapter 3

## 3.1 Imaging Modalities in Aortic Dissection

### 3.1.1 Challenges

Imaging of the aorta has many challenges. The morphology of the aorta is complex, with the ascending aorta not being a truly vertical structure, thereby making it difficult to obtain accurate images. The normal aorta is dilated at the level of the sinuses and then has an indentation or waist that is approximately within 2-3mm of the annular size at the sinotubular junction. During imaging, identification of this waist or a loss of waist is important as this is an indication of future aortic related issues.

The aortic arch is sharply curved giving an oblong contour on axial images and this can give misleading dimensions. The descending aorta at the level of the 12<sup>th</sup> thoracic vertebra becomes the abdominal aorta and in the elderly can curve quite acutely, again giving rise to non-circular images on axial planes. Figure 14 shows the normal CT appearances of the ascending aorta, with important landmarks used in clinical reporting. Note is made of the natural waist at the sinotubular junction.



FIGURE 14 CT IMAGE OF A NORMAL AORTA IN A 54 YEAR OLD MAN. THE DIFFERENT LINES REPRESENT THE LANDMARKS USED IN REPORTING A CLINICAL SCAN. BLACK SOLID LINE= AORTIC ROOT, WHITE SOLID LINE= SINUSES OF VALSALVA, BLACK DASHED LINE= SINOTUBULAR JUNCTION. WHITE DASHED LINE= MID ASCENDING AORTA. BLACK DOTTED LINE= DISTAL ASCENDING AORTA. (47)

The risk of contrast-induced nephropathy is not to be underestimated when considering CT examination and neither is that of exposure to significant radiation. (48,49)

Whilst MRI does not pose the same risk of radiation, the risk of gadolinium induced nephrogenic systemic fibrosis (NSF) in renal failure patients does exist. Additionally the lack of general availability in community hospitals does limit the use of this technique for routine clinical diagnosis. (50)

Trans-thoracic (TTE) and TOE may not always be readily available in all settings. Certainly a negative TTE does not exclude a diagnosis of dissection, and although TOE is far superior in its diagnostic accuracy, it requires an experienced operator and oesophageal intubation in a potentially unstable patient.

### 3.1.2 Computed Tomography

Prompt and accurate diagnosis of the morphology and nature of the dissection and its associated complications is essential to allow for optimal management at a specialist centre.

CT is the first line imaging modality in patients with a high probability of the acute aortic syndrome due to its fast acquisition speed, high spatial resolution. The IRAD registry reported its use in 74% of patients. (15) Unenhanced images are performed to provide information on mediastinal haemorrhage, intramural haematoma, pericardial effusions and impending rupture. (51). A multidetector CT (MDCT) allows for the simultaneous acquisition of data by various detector rows, unlike helical CT where only one detector is used allowing for a proportional decrease in scanner time, improved vascular opacification, with less contrast media, less aortic motion, and fewer breathing artefacts. Electrocardiography-gated (ECG) CT angiography is especially useful for avoiding motion artefacts that might prevent accurate assessment of the aortic root and the ascending aorta, particularly in aortic dissection with involvement of the coronary ostia. (52) ECG can be performed either retrospectively or prospectively. In prospective gating, images are usually acquired during late diastole, whereas in retrospective gating, images are acquired throughout the cardiac cycle. As a result, retrospective gating provides more comprehensive data than prospective gating, albeit at the expense of increased radiation exposure. (53)

CT performs well as far as providing important information for the treating physician, including the tear location and extent of involvement in particular, of the ascending aorta (Figure 15). (54) In addition, information about the branching vessels and their relationship to the true and false lumen are important especially for endovascular repair as is the involvement of the aortic arch and root if open surgery is being planned. Other important information includes the presence of a pericardial effusion, which may be an indicator of impending aortic rupture, involvement of the coronary ostia and visceral arterial involvement.

Although a quick and accurate examination, CT is nonetheless associated with contrast induced nephropathy in those with renal impairment and carries a real radiation risk in young

patients and those who require repeated follow-up examinations after the initial diagnostic scan.(48,49)

With respect to follow up of patients with chronic dissection where intervention may be indicated for size criteria, the presence of substantial inter observer variability in aortic measurements is recognised. Studies have shown that there can be up to 2.8mm +/- 4.4mm difference in maximum aortic diameter measured between experienced radiologists, when using standardized protocols. This can be much higher at 4.0+/- 5.1mm when non-standardized methods are used. (55) Although the introduction of standardised protocols for measurement, such as using fine callipers and measuring the largest diameter perpendicular to the aneurysm centreline decrease this variability, it is never truly eliminated. This is important to bear in mind when repeated scans in the same patient are undertaken and where size changes can mean the difference between intervention and conservative management.

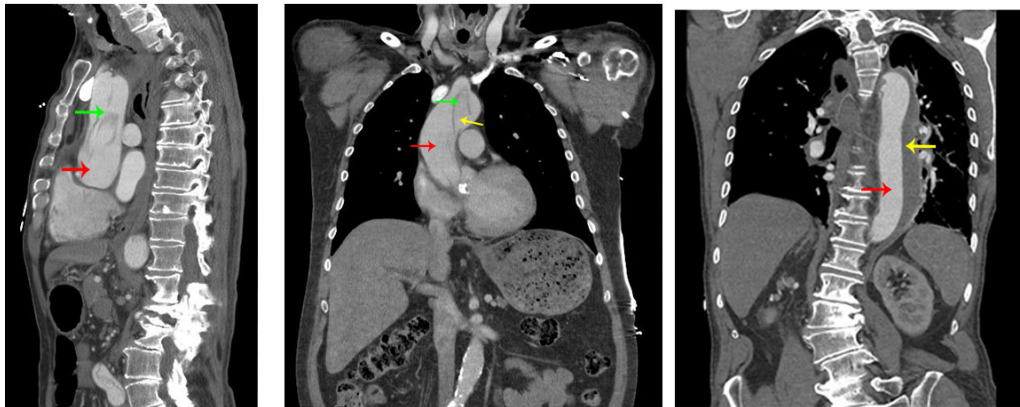


FIGURE 15 CT IMAGES FROM A PATIENT WITH ACUTE TAAD. THE RED ARROW INDICATES THE POSITION OF THE TRUE LUMEN, THE YELLOW ARROW INDICATES THE POSITION OF THE FALSE LUMEN AND THE GREEN ARROW SHOWS THE POSITION OF THE INTIMAL FLAP.

### 3.1.3 Magnetic Resonance Imaging

MRI is a highly sensitive and specific, non-invasive imaging modality. Unlike CT, MRI does not expose patients to ionizing radiation or potentially nephrotoxic iodinated contrast agents, making it an attractive option for patients who require repeated imaging. (56-58) There exists the risk of nephrogenic systemic fibrosis with gadolinium use in those with pre-existing renal impairment but this is rare. (50) Specific to the acute aortic syndrome, MRI is useful for detection of aortic valve and coronary artery involvement. Furthermore, MRI does not require contrast agents to visualize vessel anatomy including the vessel wall and intimal tears.

MRI can provide morphological evaluation such as information on vessel wall, diameter lumen patency, wall characteristics, and relations to other anatomical structures. Additionally, and unlike CT, MRI can provide functional evaluation such as blood flow, velocity. (59)

There are many different magnetic resonance angiography (MRA) techniques, which can include bright blood imaging, with or without contrast, and black blood imaging. The use of gadolinium based contrast agents (GBCA) has expanded the utility of MRA in aortic diseases. Contrast-enhanced MRA (CE-MRA) commonly uses a 3D gradient echo (3D-GRE), allowing thin contiguous image slices to be obtained during a single breath-hold. After the intravenous injection of a bolus of GBCA, there is a T1-shortening of blood so that the blood appears bright regardless of flow patterns or velocities. The image quality of CE-MRA depends on the intra-arterial concentration of the GBCA. It follows therefore that the image timing following contrast injection is crucial. (60) Nonetheless, the timing of image acquisition is less critical than for CT as gadolinium has a wider window of visibility than iodine.

Black blood imaging is particularly useful in aortic dissection, in which a signal void is created by flowing blood and the vessel wall and intimal flap are depicted with positive contrast. (Figure 16, Figure 17) This can delineate tear and intimal anatomy in dissection. (61,62) Black-blood techniques are used in combination with other imaging sequences most often CE-MRA and /or non-contrast enhanced “bright-blood” techniques.



FIGURE 16 CE-MRA IN A PATIENT WITH CHRONIC TBAD. RED ARROW SHOWS THE POSITION OF THE TRUE LUMEN, GREEN ARROW SHOWS THE INTIMAL FLAP, YELLOW ARROW SHOWS THE FALSE LUMEN AND BLUE ARROW THE AREA OF THROMBUS.



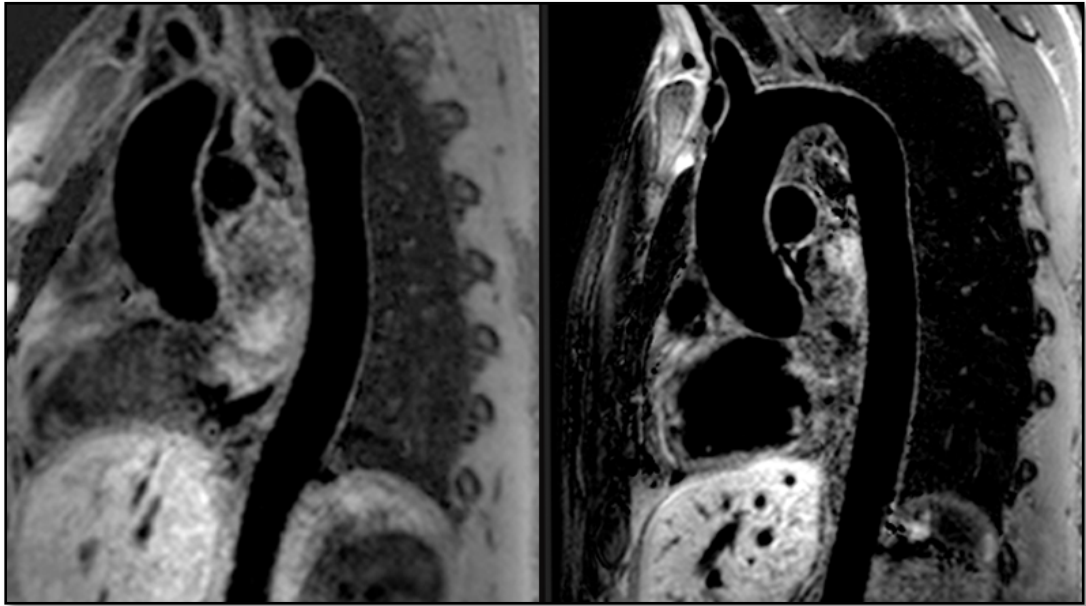


FIGURE 17 WITH BLACK BLOOD MRI TECHNIQUES THE VESSEL WALL APPEARS BRIGHT AND BLOOD BLACK. THIS ALLOWS FOR CLEARER VISUALIZATION OF VESSEL WALL PATHOLOGY. THESE IMAGES ARE FROM HEALTHY VOLUNTEERS.

Usually, slow blood flow is the main challenge of black blood techniques as acquiring diagnostic images with sufficient blood signal suppression is required. Standard black-blood methods consist of a T1-weighted (2D) spin echo sequence acquired with multiple two-dimensional slices to cover the whole aorta in an axial or sagittal view (63). To minimize image artefacts from respiratory motion, images are typically acquired during breath-holds. Although this technique allows for high in-plane spatial resolution in the order of  $1\text{-}2\text{ mm}^2$ , the slice thickness is typically in the order of  $6\text{-}10\text{ mm}$ , which may prohibit the visualization of small tears in the intimal flap in the case of aortic dissection.

Further disadvantages of this approach are slice-to-slice mis-registration due to poor reproducibility of breath-hold positions and image artefacts due to slow-flowing or stagnant blood. To address these limitations three-dimensional (3D) bright blood dynamic contrast enhanced MR angiography of the aorta can be performed, which allows for isotropic resolution and insensitivity to respiratory motion (if performed during a breath-hold) and blood flow artefacts. However, this technique provides bright blood contrast with only

intermediate spatial resolution (2-4 mm<sup>3</sup> isotropic voxel size) and requires the administration of potentially nephrotoxic contrast agents, which may be contraindicated in patients with poor renal function. To overcome the limitations of the 2D black-blood and 3D bright-blood approaches for imaging aortic dissection, 3D black-blood vessel wall imaging methods have been developed using T<sub>2</sub>-prepared Inversion Recovery (T<sub>2</sub>IR) or alternatively T<sub>2</sub>-prepared Phase Sensitive Inversion Recovery sequences (T<sub>2</sub>PSIR). (63,64)

### ***3.1.3.1 Sequences for black blood imaging for vessel wall analysis***

The pulse sequence diagram of the T<sub>2</sub>PSIR and T<sub>2</sub>IR pulse sequences used are shown in Figure 18. T<sub>2</sub>IR has previously been used for flow-independent peripheral angiography. However, a similar sequence design can be utilized to generate black-blood vessel wall images.(65)

In both approaches, an inversion pulse is performed to null signal from blood to generate black-blood contrast. To improve contrast between blood and vessel wall, a T<sub>2</sub> preparation pulse is performed prior to the inversion pulse (64). The T<sub>2</sub> preparation effectively eliminates a large portion of the longitudinal magnetization (M<sub>z</sub>) from the vessel wall, which has a short T<sub>2</sub> relaxation time while retaining the M<sub>z</sub> from blood, which has a long T<sub>2</sub>, thereby minimizing the effect of the subsequent inversion pulse on the vessel wall signal. In this sense, the recovery of the vessel wall M<sub>z</sub> is accelerated compared to the blood M<sub>z</sub>, which starts with a larger negative magnetization immediately after the inversion pulse.

In a conventional inversion recovery sequence using magnitude reconstruction the polarity of M<sub>z</sub> is unknown, which may lead to reduced contrast between the vessel wall and blood if the inversion time (TI) between the inversion pulse and image acquisition is not carefully optimized. Phase sensitive inversion recovery can be used to improve robustness and to limit the adverse effects of suboptimal TI as this method can be used to restore the M<sub>z</sub> polarity

during image reconstruction and generate optimal contrast between tissues. (66,67) This is achieved by introducing a second image acquisition in the subsequent cardiac cycle, ( $ACQ_2$  in Figure 18) which is used as a reference image with positive polarity and allows for the determination of polarity in the first acquisition ( $ACQ_1$  in Figure 18). This technique has not been used in aortic dissection before.

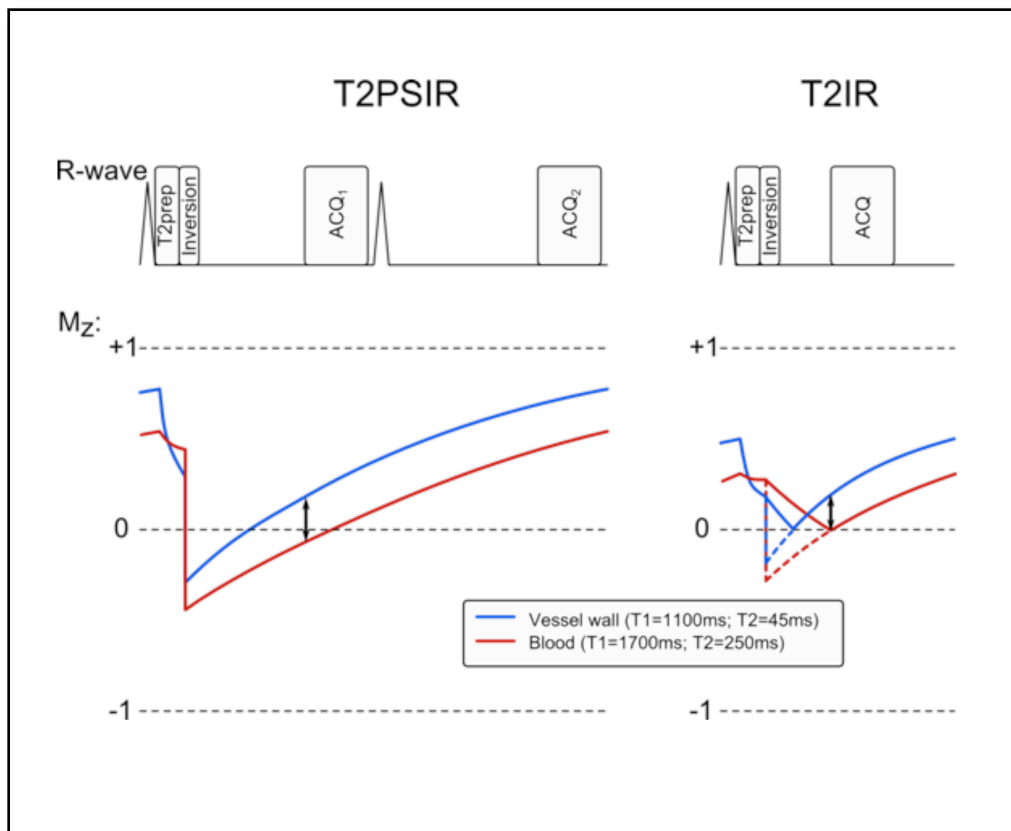


FIGURE 18 T2PSIR AND T2IR SEQUENCES. TO MINIMIZE FLOW ARTEFACTS ORIGINATING FLOWING BLOOD DURING THE PERFORMANCE OF THE T2PREP THIS PRE-PULSE IS PERFORMED IN EARLY SYSTOLE IMMEDIATELY AFTER R-WAVE DETECTION. THE INVERSION TIME IS DETERMINED SUCH THAT BLOOD SIGNAL IS NULLED FOR T2IR WHILE FOR T2PSIR BLOOD SIGNAL CAN BE NULLED FOR A WIDE RANGE OF INVERSION TIMES DUE TO THE PHASE SENSITIVE RECONSTRUCTION.

### ***3.1.3.2 Dual phase MRI imaging***

Image acquisition in MRI is usually performed in the diastolic phase of the cardiac cycle as there is a relatively low flow in this state. However to study aortic motion, data image acquired in both systole and diastole would be ideal as this would allow for an evaluation of aortic motion in the normal and abnormal aorta. This form of imaging would seem potentially more realistic given that the aorta is a complex dynamic entity.

### **3.1.4. Echocardiography**

Echocardiography uses transthoracic or trans-oesophageal probes that emit ultrasound waves directed at cardiac structures. The returning signals are then received by the emitting probes and are then reconstructed to produce images of the heart. Echo probes also perform Doppler which measures the frequency shift of returning ultrasound waves to determine the speed and direction of moving blood in the heart.

TTE is a good clinical tool to measure proximal parts of the ascending aorta, and is useful in the follow up of proximal aortic diseases such as aortic aneurysms. Aortic root diameters are best visualised using the long-axis views and the right parasternal view affords the best estimation of the true ascending aortic size. The aortic arch and supra-aortic vessels are best visualised in the suprasternal view. TTE has a sensitivity of 78-100% for TAADs and 31-55% for TBADs. (57)

Trans-oesophageal echocardiography benefits from the proximity of the oesophagus to the aorta, allowing for high-resolution aortic imaging (Figure 19). Views of the ascending aorta, root and valve are best appreciated in the long axis (120-150°) and short axis views (30-60°) A blind spot due to the overlying trachea and right main bronchus exists around a short segment of the distal ascending aorta making useful interpretation of this region difficult. The descending aorta on the other hand is well visualised from the left subclavian to the coeliac

trunk as is the aortic arch. TOE overall has a positive predictive value of 89% and a negative predictive value of 99% for acute aortic syndrome. (38,68,69)

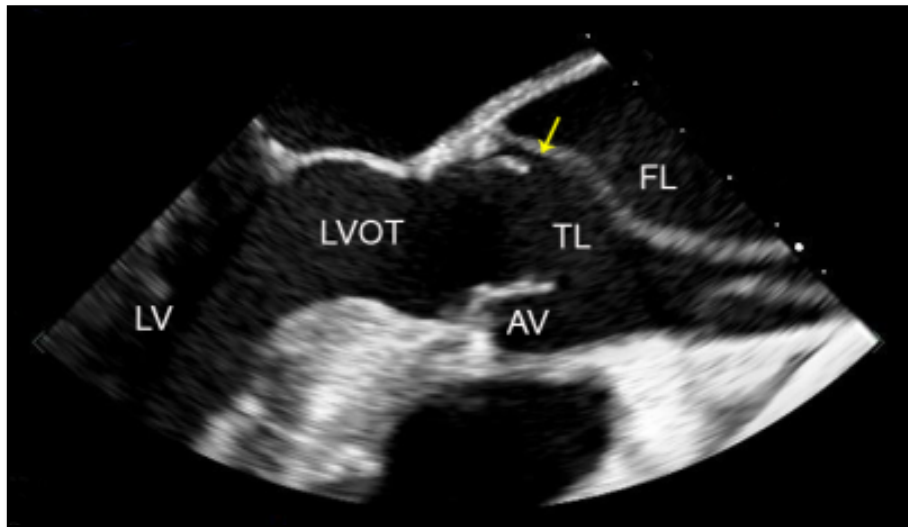


FIGURE 19 TOE LONG AXIS VIEW OF THE AORTIC ROOT SHOWING THE INTIMAL FLAP (YELLOW ARROW) AND TRUE AND FALSE LUMENS (TL, FL). LVOT = LEFT VENTRICULAR OUTFLOW TRACT, LV= LEFT VENTRICLE.

# Chapter 4

## 4.1 Computational Fluid Dynamics and Simulation

With the advent of sophisticated 3-D imaging modalities, in particular, MRI, computational methods have moved forward from initial applications in idealised vascular models to patient specific anatomically and physiologically appropriate models. The use of image based modelling tools to investigate cardiovascular disease, in particular in the carotid, coronary and cerebral circulations dates back to the 1990s. (70-74) Since then patient specific applications have been developed for example, to predict the risk of rupture in aortic aneurysms. (75)

The workflow needed to develop a patient specific model begins with the construction of an anatomically accurate geometry from imaging data, which can be in the form of CT, MRI or even ultrasonography. Next, physiological data such blood velocity and pressure are obtained from ultrasound, PC-MRI or invasive pressure monitoring, for example during a cardiac catheter. Boundary conditions both upstream and downstream are then applied, to represent the heart pump and the distal systemic circulation. Next, a mesh generator is used to discretize the constructed geometry and finally, the incompressible Navier-Stokes equations relating to blood flow are solved. The end result is physiological information relating to a patient, and includes important data as related to cardiovascular system such as blood pressure and wall shear stress, Figure 20.

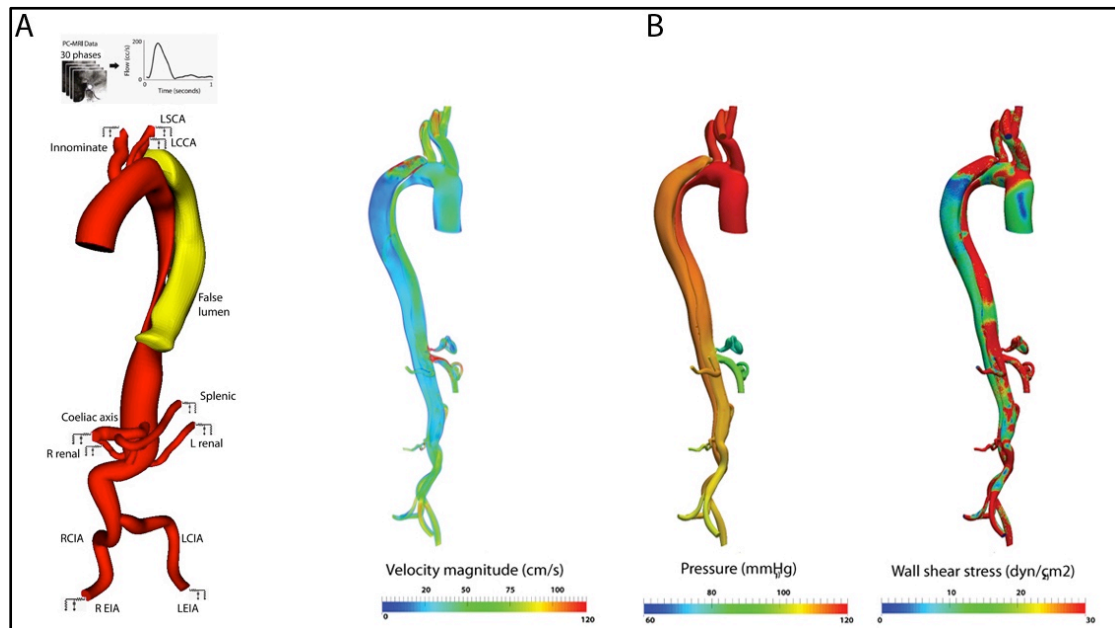


FIGURE 20 A. PATIENT-SPECIFIC ASCENDING AORTIC FLOW WAVEFORM MEASURED BY PC-MRI IS MAPPED TO THE INFLOW FACE OF THE CAD MODEL. A 3-ELEMENT WINDKESSEL MODEL WITH A PROXIMAL RESISTANCE ( $R_p$ ), CAPACITANCE ( $C$ ), DISTAL RESISTANCE ( $R_d$ ) BOUNDARY CONDITION IS USED TO REPRESENT THE RESISTANCE AND COMPLIANCE OF THE VASCULATURE DOWNSTREAM OF EACH OUTLET. B. HAEMODYNAMIC RESULTS FROM CFD IN A PATIENT WITH AORTIC DISSECTION. FIGURES REPRESENT EARLY SYSTOLE MAPS OF BLOOD VELOCITY (LEFT) BLOOD PRESSURE (CENTRE) AND WALL SHEAR STRESS (RIGHT).

#### 4.1.1 CFD in dissection studies

Several studies have investigated blood flow analysis in complex aortic geometries including aortic dissection and coarctation of the aorta. These have all shown the utility of CFD to investigate intra-aortic haemodynamic techniques in what may otherwise be an extremely challenging case.

Karmonik et al have carried out several studies investigating the complex intra-aortic haemodynamics in aortic dissection. These include understanding the effects of occluded and patent intimal tears, haemodynamic changes in the aorta pre and post TEVAR and a comparison of aortic haemodynamics in a healthy and dissected aorta. (76-78). Rudenick et al investigated the agreement of haemodynamics between a computational model of a dissected aorta with that of an idealised model. These showed good agreement. (79) The

main limiting factors in the majority of these studies have been the assumptions made to determine inflow and outflow boundary conditions. Many studies use flow data from healthy individuals and apply them to pathologic cases such as dissection, which is not ideal, given the complex anatomical changes and likely resulting haemodynamics in aortic dissection. (80,81)

Although this limitation itself underpins the technical and practical difficulties in obtaining real time pressure and flow data from this select group of patients, it highlights the potential inaccuracies in the final model and resulting simulations developed. Patients with acute or chronic aortic dissection represent abnormal aortic haemodynamics and likely abnormal vascular structure throughout the body. In a bid to control hypertension, itself a driving force increasing wall shear stress and thereby propagating the intimal tear distally or proximally, beta-blockers are routinely prescribed to these patients in the acute setting and other agents such as aldosterone II antagonist in the chronic patient. These itself cause significant changes to the aortic haemodynamics, reducing wall shear stress and additionally cardiac workload. It is therefore quite apparent that applying normal human flow data to these complex patients will overestimate flow conditions. Additionally, some studies have applied pressure data from normal subjects or assumed zero pressure conditions, which again represent the same afore mentioned problems.

To this end, Dillon-Murphy et al have shown the application of patient specific flow data from 2D PC-MRI to inform an accurate model of aortic dissection and used tuned lumped-parameter Windkessel models to represent accurately the resistance and compliance of the peripheral vasculature. (82) This study showed local areas of increased blood velocity, pressure and wall shear stress around the area of the entry tear. Additionally, an increase in cardiac workload with the onset of dissection was seen, up to a factor of 14% when compared to a normal aorta.

This study also highlighted the difficulties in accurately identifying secondary tears from CT data which itself can be of limited quality. The investigators went on to study the impact of



fewer tears compared to many tears in a dissected aorta and showed that the presence of many tears resulted in an equalisation of pressures between the true and false lumens.

# Chapter 5

## Aims

This work is structured around the following aims:

1. Investigate the potential utility of non-invasive haemodynamics (such as blood velocity, pressure, and pulse pressure) derived via image-based modelling and compare this to invasive pressure readings taken at the time of TEVAR in recruited patients with chronic TBAD.
2. To use this novel non-invasive method of evaluating false lumen haemodynamics to follow-up patients and determine if indeed abnormal false lumen haemodynamics contribute to aortic growth and therefore poorer outcomes.
3. To investigate the efficacy and utility of two black blood (vessel wall) MRI sequences to image the aortic wall, with the aim of detailed visualisation of the dissected intimal flap and tear location.
4. To study the variation in aortic motion during the cardiac cycle using dual phase MRI imaging and to use this method to study the variation in aortic motion and of the intimal flap in aortic dissection.

# Chapter 6

## General Materials and Methods

### 6.1. Overview

This study was divided into four parts.

#### 6.1.1 Validation study

The first part was a validation study whereby invasive pressure recordings taken at the time of TEVAR were compared to non-invasive pressure estimates from preoperative imaging (PC-MRI) and simulation models. All adult patients (18-80 years) admitted with a diagnosis of Type B (acute and chronic) aortic dissection and surgically repaired TAAD with a residual, untreated Type B component were candidates for this study. Patients with chronic renal failure and those with other contraindications to MRI scanning were excluded.

Patients with acute TBAD were approached on the wards and a patient information leaflet pertaining to the study was provided (Appendix 1). This explained the course of the investigation and allocation into the invasive arm if surgical intervention was contemplated and the non-invasive arm if conservative management was planned. In both circumstances a detailed pre-intervention (if any was planned) MRI scan was performed if the patient's clinical condition was deemed stable.

Chronic stable patients who were already in a clinical follow up program were contacted by means of an invitation letter and were given details and methods of indicating interest in participation. A total of 4 patients were recruited into this arm of the study.

### **6.1.2 Follow-up study**

In the second part of the study involving chronic stable patients, false lumen haemodynamics were assessed entirely non-invasively using MRI and simulation. A total of four patients were recruited into this arm, three with a one-year follow up. The last patient was recruited late into the study and only underwent a single scan. All patients were recruited following an invitation letter and all patients provided written consent to participate in the study.

### **6.1.3 Black blood study**

A third study was conducted to evaluate the utility of new black blood sequences in imaging of aortic dissection, to help delineate tear anatomy and morphology. Eleven healthy volunteers and two patients with a Type B component in a previously repaired TAAD setting were included. All subjects provided written consent for this study.

### **6.1.4 Dual phase study**

In the fourth and final part, a dual phase MRI study with imaging acquisition in systole and diastole was conducted to investigate aortic motion and strain throughout the cardiac cycle. Here 5 healthy volunteers and 2 patients with a residual Type B component were included. All subjects provided written consent for this study.

## **6.2 Ethical approval**

Ethical approval from the local Research and Ethical Committee (REC) was confirmed to be in place prior to the commencement of the study. This was to cover the non-invasive and invasive elements of the work. Based on this, between May 2013 and June 2013, three patients undergoing TEVAR for symptomatic or rapidly enlarging chronic TBAD had invasive pressure recordings taken at the time of their procedure.

Subsequent review of the ethics, post data collection indicated that the ethics approval in place was insufficient for the nature of the invasive investigation. Despite detailed clinical consent as well as that specifically for invasive pressure readings being sought from the patients, based on College recommendations this data was not given permission for use in this research study.

Following on from this, a new application was made to the local REC and full ethical approval was granted in February 2014, for both prospective and retrospective data collection, for the invasive and non-invasive elements of the study. (REC reference: 14/LO/0286, London Bromley). However, based on the College's review, the previously acquired invasive data was not permitted to be included.

Additionally, subsequent changes in local surgical practice also meant that no TEVARs were undertaken for chronic TBAD between January 2014 and January 2015 (unless in a clinically urgent scenario, whereby recruitment was not deemed suitable as MRI scans of these patients could not be acquired safely). This meant that no further recruitment to the invasive study was possible. Ethical approval for the volunteer studies as well as for the subsequent patient imaging studies was in place and all participants gave written consent.

# Chapter 7

## 7.1 General Computational Fluid Dynamics Methods

### 7.1.1 CRIMSON

Creation of patient specific models using patient imaging data was performed using the in house CRIMSON software. CRIMSON (Cardiovascular Integrated Modelling and Simulation) is powerful, all-encompassing image-based blood flow simulation software capable of rapid and accurate segmentation of complex geometries, allowing generation of parametric models, surface and volume meshes, and specification of boundary conditions and output of files necessary for fluid flow simulation using the CRIMSON flow solver.

The flow solver uses Windkessel outflow conditions coupled to each of the outlet faces of the aortic model. These Windkessel models require the specification of proximal and distal vascular resistance parameters ( $R_p$  and  $R_d$ , respectively) as well as a vascular compliance parameter ( $C$ ) that represents the characteristics of the distal arterial bed not physically included in the 3D aortic model. These parameters are tuned to match patient pressure and flow data.

CRIMSON was developed in the Figueroa Lab (Biomedical Engineering, at King's College London) and has its foundations in the highly versatile MITK platform (Medical Imaging Interaction Toolkit [www.MITK.org](http://www.MITK.org)). Many of the original features of MITK have been preserved whilst others have been adjusted to provide a user-friendly method for 2D and 3D vessel segmentation.

To create a geometric computer aided design model (CAD), the 2D segmentation methods introduced by Wang et al was utilized. (83) Technical details follow.

#### ***7.1.1.1 Path lines***

In this multi-step method, paths are defined through an approximate centreline of the blood vessel of interest. Each branching vessel has its own path line, although at bifurcations, one of the smaller vessels (e.g. external iliac) has a path extending from the parent (aorta) vessel (Figure 21). To develop a path line the selected image and vessel of interest are highlighted. Next path points are plotted in a 3D window, using the sagittal, coronal and axial image slices.

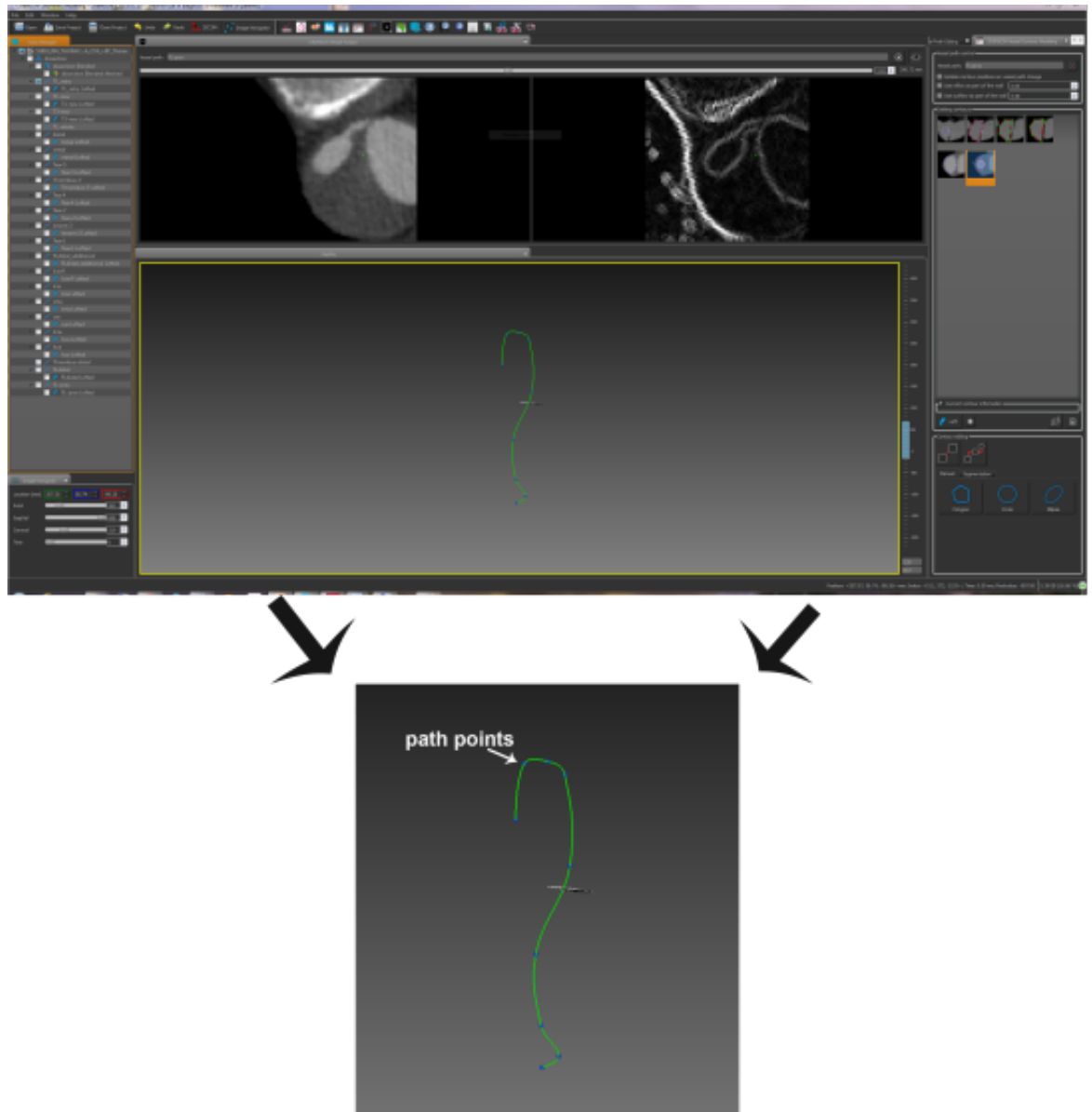


FIGURE 21 PATHLINE CREATION FROM PATH POINTS USING IMAGE DATA IN CRIMSON



### ***7.1.1.2 Contouring***

By creating a vessel path, “reslicing” of the image data is possible. The reslice plane displays the image data on the plane perpendicular to each point of the vessel path. As the vessel path roughly approximates the vessel centreline, the reslice plane provides a reasonable cross-section of the vessel wall. Contours describing the boundary of the vessel wall and are created on the reslice plane at a number of locations along the vessel path (Figure 22). Fewer contours result in a smoother appearance of the resulting model. Care has to be taken at furcating points of vessels and in the case of dissection, the true and false lumens to ensure that contours do not intersect. This leads to ‘bleeding in’ of vessels and a model that cannot be used.

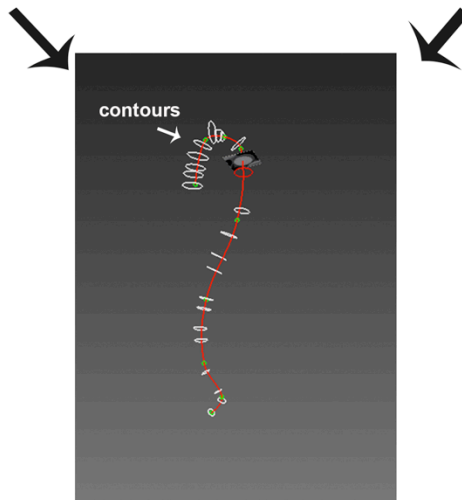
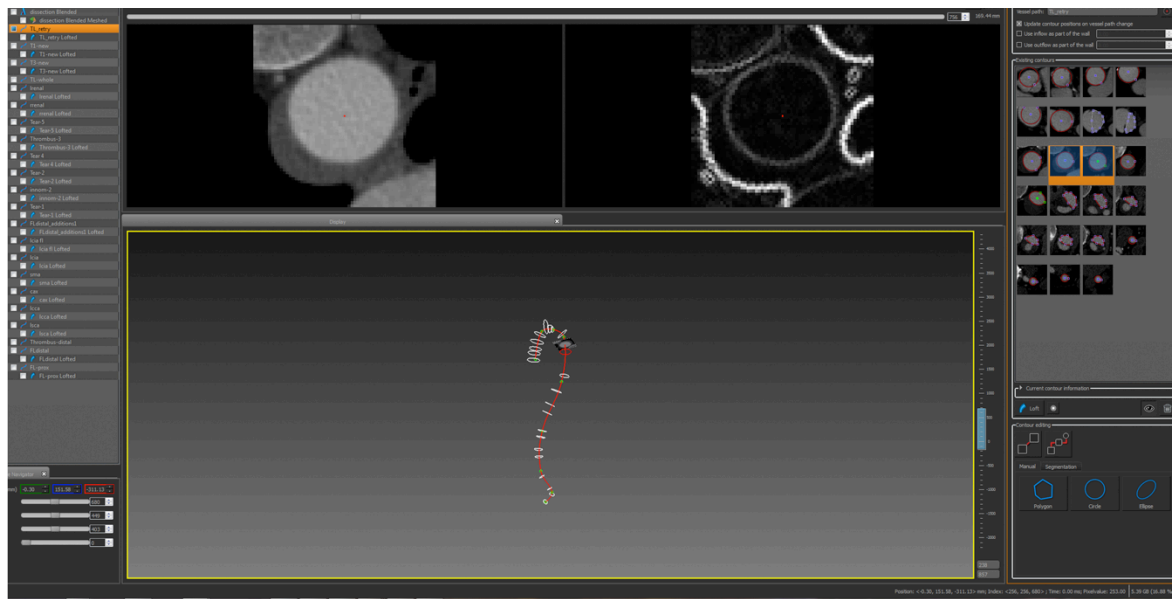


FIGURE 22 CONTOURING OPERATION ALONG THE VESSEL PATHLINE

### ***7.1.1.3 Lofting and Blending***

CRIMSON uses the (2D) contours to generate an analytical surface representation of the vessels by creating lofted B-spline surfaces between contours. Blending and union (lofting) operations are the final step to the creation of a 3D CAD representation of the patient's aorta and main branches. Here a Boolean union operation is performed, merging the B-spline representations of the different branches into a single 3D CAD model. Sharp edges between any intersecting branches can be removed via a blending operation whereby a fillet of a given radius is introduced at each intersection (Figure 23).

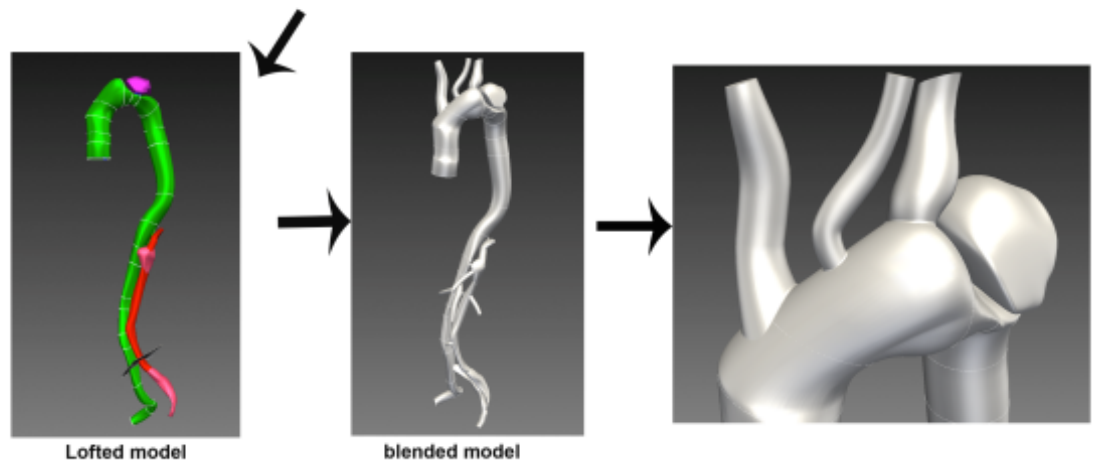
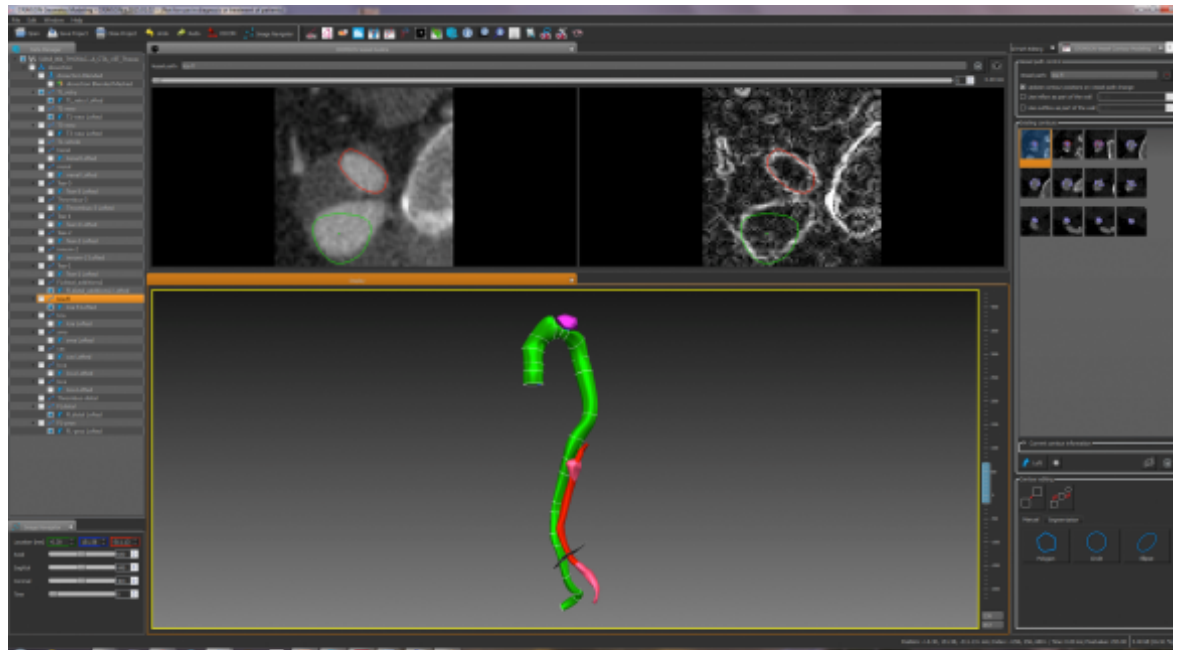


FIGURE 23 LOFTING AND BLENDING OPERATIONS

#### ***7.1.1.4 Meshing operation***

Once a finite element mesh (e.g., discretisation of the geometry of the aorta in small pieces suitable for computational analysis) is generated, CRIMSON uses the MeshSim libraries (<http://www.simmetrix.com/products/meshsim/MeshSim.html>) to mesh the model with linear tetrahedral elements. Due to the no-slip condition (i.e. relative zero velocity between a viscous fluid, in this case blood, and the solid it interacts with, in this case the vessel wall at the fluid-solid interface) the region close to the vessel wall is typically the region with the highest velocity gradients in the domain. Therefore, it is desirable to refine the mesh close to the vessel walls. This may be done with the use of boundary layers.

Another useful tool in the meshing operation is curvature refinement, which increases the surface mesh in regions of high curvature such as small vessels or branching points. Here complex flow profiles may be better captured. For the purposes of this work a mesh size of 1.0mm was used, with curvature refinement, giving an approximate mesh made of 1.4 million elements. Figure 24 shows the meshed model.

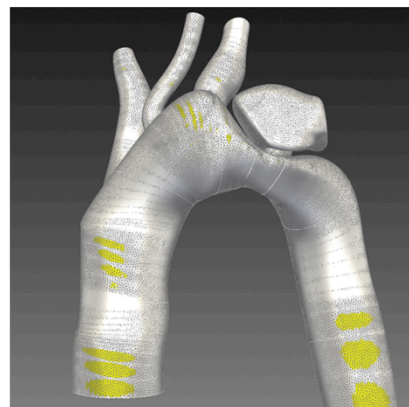
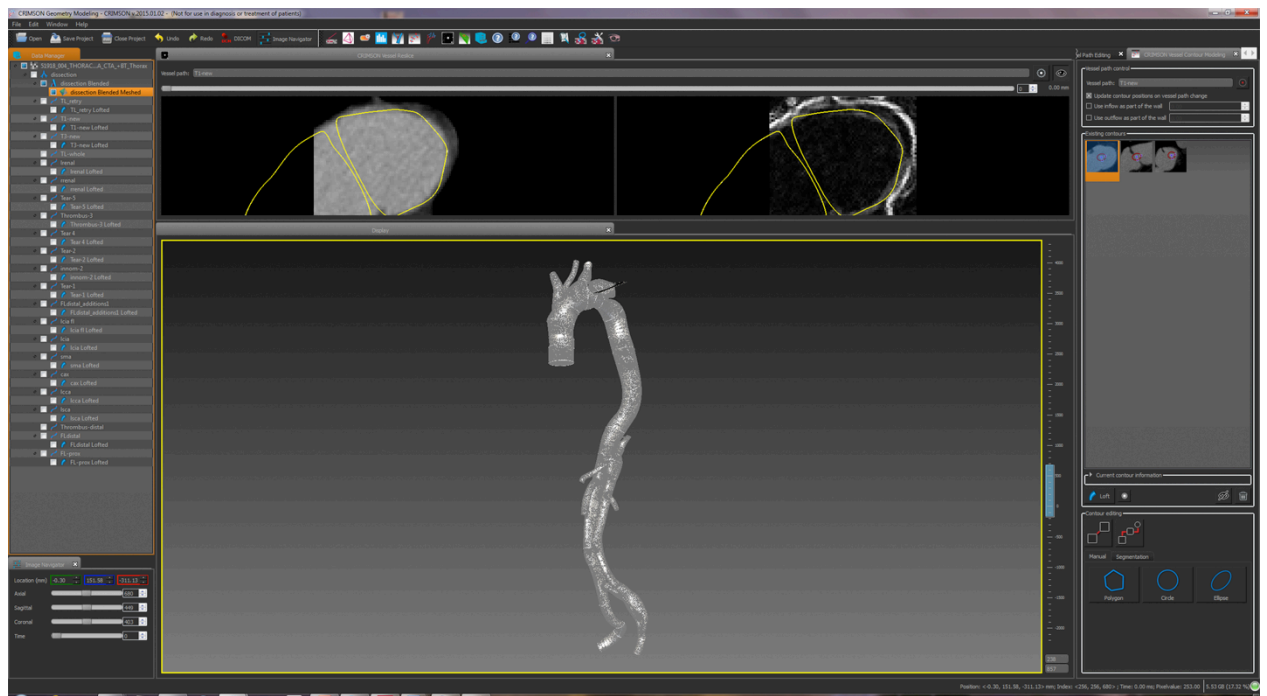


FIGURE 24 MESHING OPERATION

### **7.1.2 Simulation**

Computational fluid dynamics (CFD) analyses are performed on a 640-core SGI UV 1000 super-computer with 4TB of RAM. Both meshing and CFD analysis tasks are carried out using the Crimson flowsolver code. The high-performance computer system is located at Guy's campus, King's College London. CFD results provide detailed information on spatial and temporal haemodynamic quantities such as blood velocity, blood pressure, and wall shear stress.

# Chapter 8

## 8.1 Validation study Methods

### 8.1.1 Equipment details

Investigation of invasive intra-aortic (true and false lumen) haemodynamics was performed using a Certus PressureWire (St. Jude, MN, USA) (Figure 25). This is a strengthened 0.014" wire with high-fidelity sensor technology which allows for simultaneous measurement of intravascular pressure, temperature and thermodilution (84). A hydrophilic coating enhances manoeuvrability and device compatibility.

The sensor element of the wire is located 3 cm proximal to the tip and three electrical cables run from the sensor to the proximal end of the wire.

In conjunction with the RadiAnalyzer monitor (St. Jude, MN, USA) Figure 26, accurate ( $\pm 1$  mmHg plus  $\pm 1\%$  of a reading) reading of intravascular pressure can be made and recordings taken for further analysis using the RadiView software (St. Jude, MN, USA).

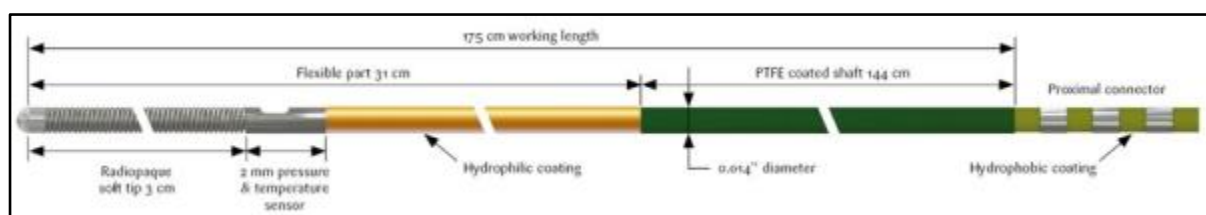


FIGURE 25 A CLOSE-UP VIEW OF CERTUS PRESSUREWIRE (84)



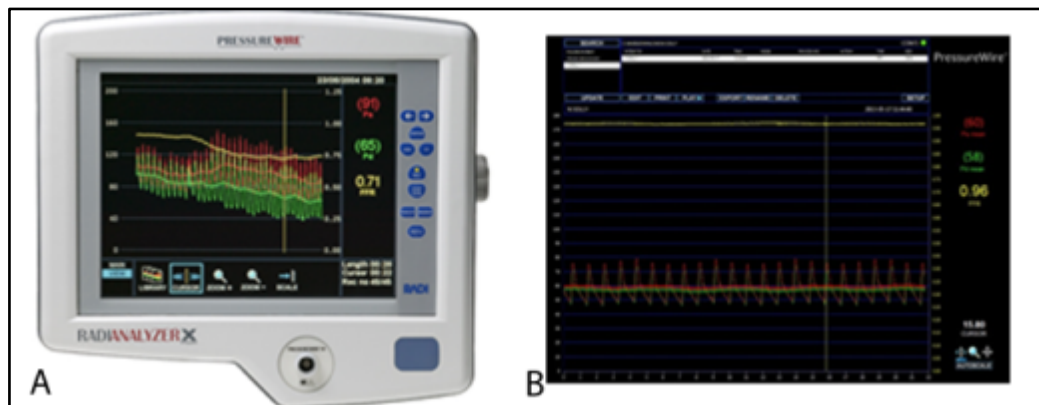


FIGURE 26 A SNAPSHOT OF THE RADIAnalyzer MONITOR (A) AND SCREEN RECORDINGS DURING A TEVAR CASE (B) ARE SHOWN. RED TRACE = AORTIC PRESSURE, GREEN TRACE = FALSE LUMEN PRESSURE (84)

### 8.1.2 Set up for pressure wire recording study

All TEVAR procedures were performed under general anaesthesia with endotracheal intubation and ventilation, in the hybrid-operating suite at St. Thomas's Hospital. This suite is equipped with state of the art interventional and open surgical facilities (Figure 27). Access to the femoral arteries was agreed upon preoperatively by the surgeons and interventional radiologists, as dictated by the anatomy and extent of the dissection. Prior to percutaneous vascular access, the pressure wire recording system and additional adjuncts were set-up. This setup enables simultaneous recording of aortic pressure and true or false lumen pressure once calibration has been performed (aortic pressure is monitored by a pig-tail catheter). An 8Fr sheath was usually used to access the chosen femoral artery and a pig-tail catheter passed up into the true lumen under fluoroscopy. Measurements of the non-diseased (ascending) aortic pressure were recorded by the pigtail and used as reference for calibration of the pressure wire.

Using a Y-connector, (SuperKetch, Minavasys, France) the pressure wire was inserted into the femoral artery and into the true or false lumen, under fluoroscopy. Pressure wire

recordings in each lumen were then taken for 10 seconds at each location, at 3-5 centimetre intervals. In all, the additional pressure measurements add a maximum of 5 minutes to the operative procedure. Details of each TEVAR procedure, including patient details and recording were made on a pre- assembled proforma ( ).

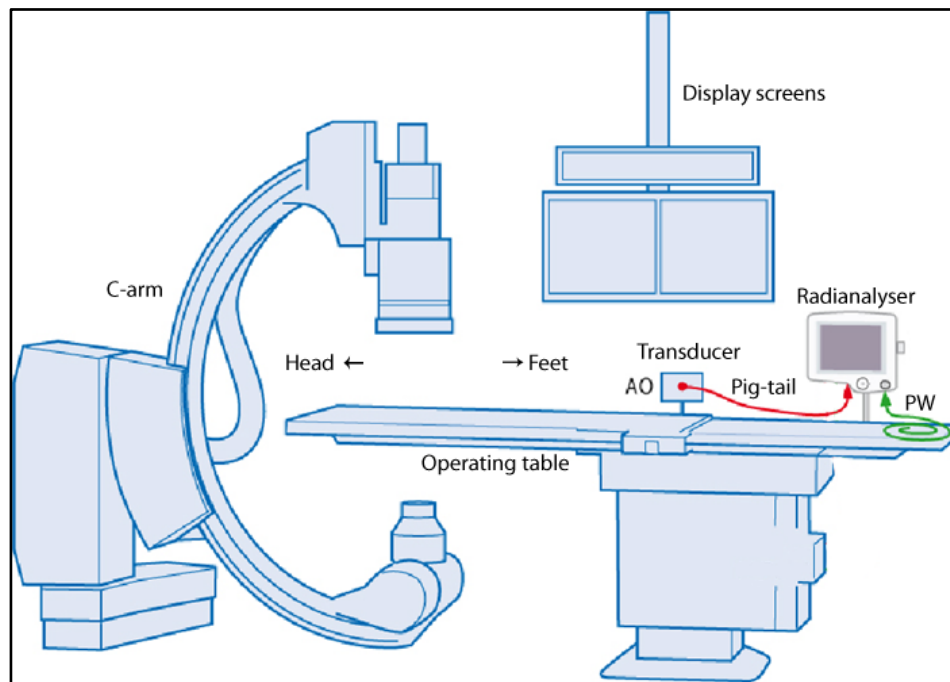


FIGURE 27 SET UP IN THE HYBRID THEATRE. WITH THE C-ARM IN POSITION, THE RADIANALYZER IS ATTACHED TO THE OPERATING TABLE. BOTH THE PRESSUREWIRE (PW, GREEN) AND THE PIGTAIL (AO, RED) ARE CONNECTED TO THE TRANSDUCER AT THE HEIGHT OF THE PATIENT'S RIGHT ATRIUM.



# Chapter 9

## 9.1 Follow up study: Imaging methods

Two patients who had undergone TAAD repair were invited for follow up scanning at a one-year interval. Patients were scanned in the Achieva 3T scanner (Philips Healthcare, Best, The Netherlands) with a 32-element coil at the Rayne Institute, King's College London at St. Thomas' Hospital. All images were reconstructed on the Philips scanner console using standard commercially available software. Details of image sequences have previously been described. (45)

Sequences used to generate images included:

- a. Anatomy images: Isotropic 3D images of the aorta were acquired at least 10 minutes after the administration of contrast, (Multi-hance, Bracco spa, Milan, Italy) given at a dose of 0.2ml/kg, undiluted, to allow time for the contrast agent to fill the false lumen. Data were acquired with a respiratory navigator and ECG triggering to reduce respiratory and cardiac motion artefacts, respectively. All data were acquired in a single respiratory phase (5-mm gating window at end-expiration) and a single cardiac phase (mid-diastole, acquisition time 94ms). A k-space segmented inversion recovery prepared steady-state free precession sequence was used (field of view [FOV], 400 253 156mm<sup>3</sup>; acquired voxel size, 1.5mm<sup>3</sup>; flip angle, 20°; inversion time, 350ms; repetition time [TR]/echo time [TE], 4.0/1.3ms; 22 k-space lines per cardiac cycle). Timing of the data acquisition from the R-peak (trigger delay) was determined from a 2-chamber view. The anatomy images were used to position 2D PC-MRI slices perpendicular to the aorta.

- b. 2D PC-MRI: Through-plane flow encoded images were acquired perpendicular to the aorta at three positions: the ascending aorta 15mm above the sinotubular junction, the arch of the aorta to capture the origin of the head and neck vessels and the descending thoracic aortic at the level of the diaphragm (including the true and false lumen). Data were acquired in free-breathing with ECG-gating, and data were retrospectively assigned to 25 cardiac phases (FOV, 300 300 mm<sup>2</sup>, slice thickness, 10 mm; acquired voxel size, 1.9 mm<sup>2</sup> ; flip angle, 10°; velocity encoding, 150-200 cm/s; TR/TE, 5.2/2.9ms; temporal resolution, 34ms; number of signal averages, 2. The velocity encoding was set at 150 cm/s, and after the 2D PC-MRI acquisition was complete, the reconstructed images were checked immediately for aliasing. The velocity encoding was increased to 200cm/s or above if these were present, with data acquired again until a velocity encoding that correctly encoded for the peak velocity was achieved. These data were used to set up boundary conditions for the computational simulations and to verify the CFD solution.

All MRI data was post processed using GTFlow Cardiovascular MRI Image analysis software (GTFlow 1.5.10, Gyrotools, Switzerland for flow analyses and Centricity PACS, GE-Healthcare, UK workstation for anatomy data).

# Chapter 10

## 10.1 Black blood study of aortic wall morphology

T2 prepared inversion recovery and T2 prepared phase-sensitive inversion sequences allow the aortic lumen to appear dark and the aortic wall bright. This provides detailed vessel wall anatomy, which may help characterize the shape of the flap and potentially identify connecting tears between true and false lumen. This study focussed on investigating the utility of these two sequences, in particular the quality of images acquired and their potential use in dissection patients.

### 10.1.1 In-vivo experiments

Eleven healthy volunteers and two patients with known chronic TBAD following repair of the Type A component underwent a three-dimensional anatomy scan. Two patients were part of a surveillance programme with CT scans at yearly intervals to detect changes in the morphology of the aorta. The study was approved by the local ethics committee and all participants provided written consent.

All images were acquired on an Achieva 3T scanner (Philips Healthcare, Best, The Netherlands) at the Rayne Institute, King's College London at St Thomas' Hospital. with a thirty two-element cardiac coil and reconstructed on the scanner console using commercially available software. A  $T_2$  prepared Look-Locker scan was acquired in a sagittal orientation through the aorta with inversion pulses and imaging in every cardiac cycle to determine the optimal inversion time to null signal from blood for the  $T_2$ IR scan (85). As  $T_2$ PSIR is insensitive to deviations from the optimal inversion time for blood signal nulling the same inversion time for this scan.  $T_2$ IR and  $T_2$ PSIR sequences were acquired in all healthy volunteers in a randomized order. Two patients with aortic dissection were scanned with the  $T_2$ PSIR sequence only.

The T<sub>2</sub>prep module used an echo time of 40ms with two B1-insensitive adiabatic refocusing pulses for both T<sub>2</sub>IR and T<sub>2</sub>PSIR as shown in Figure 29a. (65,86) The T<sub>2</sub>IR and T<sub>2</sub>PSIR prepulses were combined with a spoiled gradient echo sequence, acquired in a sagittal orientation using ECG-triggering and with the following imaging parameters: field-of-view = 380 (foot-head) × 260 (anterior-posterior) × 50 (left-right) mm, spatial resolution = 1.3 mm<sup>3</sup> isotropic, SENSE = 2 (anterior-posterior). The acquisition window was set to 170ms to minimize cardiac motion artefacts. A pencil beam navigator positioned on the right hemidiaphragm was used to suppress respiratory motion artefacts with a gating window of 5 mm. For the T<sub>2</sub>PSIR approach, the gating was based on the navigator information of the first acquisition (Figure 29 ACQ1) and not the reference acquisition (Figure 29 ACQ2).

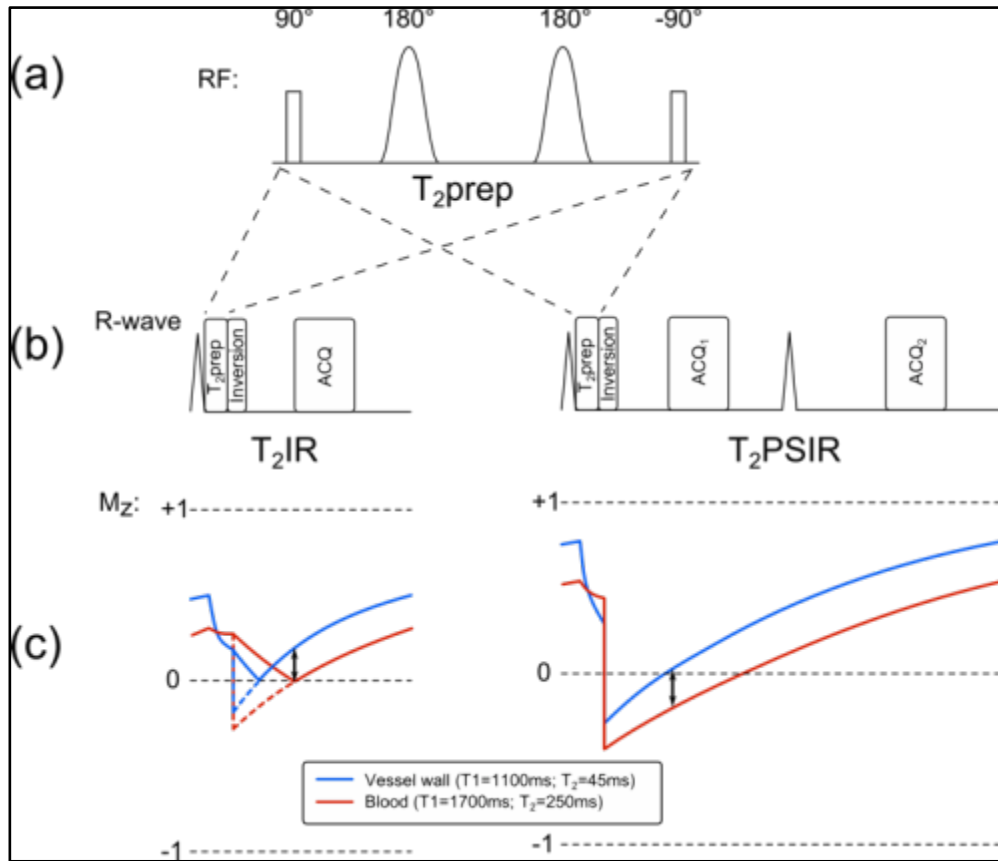


FIGURE 29 T<sub>2</sub>PSIR AND T<sub>2</sub>IR SEQUENCES. T<sub>2</sub>PSIR AND T<sub>2</sub>IR SEQUENCES (B). IN BOTH SEQUENCES AN INVERSION PULSE IS PERFORMED TO NULL THE SIGNAL FROM BLOOD AND A T<sub>2</sub>PREP, USING 2 ADIABATIC REFOCUSING PULSES (A), IS PERFORMED TO IMPROVE THE CONTRAST BETWEEN BLOOD AND VESSEL WALL. IN THE T<sub>2</sub>PSIR SEQUENCE AN ADDITIONAL IMAGE ACQUISITION IS PERFORMED IN THE SUBSEQUENT CARDIAC CYCLE TO CALCULATE THE POLARITY OF THE SIGNAL (C). TO MINIMIZE FLOW ARTEFACTS ORIGINATING FLOWING BLOOD DURING THE PERFORMANCE OF THE T<sub>2</sub>PREP THIS PRE-PULSE IS PERFORMED IN EARLY SYSTOLE IMMEDIATELY AFTER R-WAVE DETECTION. THE INVERSION TIME IS DETERMINED SUCH THAT BLOOD SIGNAL IS NULLED FOR T<sub>2</sub>IR WHILE FOR T<sub>2</sub>PSIR BLOOD SIGNAL CAN BE NULLED FOR A WIDE RANGE OF INVERSION TIMES DUE TO THE PHASE SENSITIVE RECONSTRUCTION.



### 10.1.2 Pilot study: optimizing parameters to ensure flow-independence

Although the inversion pulse is flow-independent, a previous study has demonstrated that the  $T_2$  prepared pulses are to some extent flow-dependent (87). This flow dependency is exacerbated at high fields such as 3T due to increased B1 and B0 inhomogeneities (87). B0 inhomogeneities can be also interpreted as an additional time independent and constant background gradient field,  $G_{bg}$ .

In practice, this means that during the application of the  $T_2$  prepared prepulse in the presence of this background gradient field, the transverse magnetization of flowing blood experiences some de-phasing proportional to the flow velocity. This may result in only partially suppressed blood signal in the  $T_2$ IR and  $T_2$ PSIR images and areas of bright-blood signal (or flow artefacts) in regions with high velocity blood flow.

The flow-dependency of the  $T_2$  prepared pulses may be particularly noticeable if they are performed in a cardiac phase with high velocity flow, such as during peak systole. To investigate the flow-dependence of the  $T_2$  prepared pulses and the subsequent effect on the proposed black-blood scans we performed a pilot study in two healthy subjects (volunteers 10 and 11) where we modified the temporal position of the  $T_2$  preparation (and subsequent inversion pulse) in the cardiac cycle. In this study, a phase-contrast image was first acquired orthogonal to the ascending and descending aorta to measure flow.

From this image we identified a cardiac phase with low flow, in early-systole (0-50 ms after the R-wave) and one with high flow in mid-systole (200-250 ms after the R-wave). We then acquired one scan with the preparation pulses ( $T_2$  preparation and inversion) performed in mid-systole (high flow) and another scan with the preparation pulses performed immediately following the R-wave in early systole (low flow). However, by adjusting the temporal position of the  $T_2$  prepared pulses to early systole, which has less flow, the flow artefacts can be avoided. For the remaining healthy volunteer and patient scans the  $T_2$  prepared and

inversion pulse were performed in early systole immediately following the R-wave with image acquisition in mid-diastole (Figure 30).

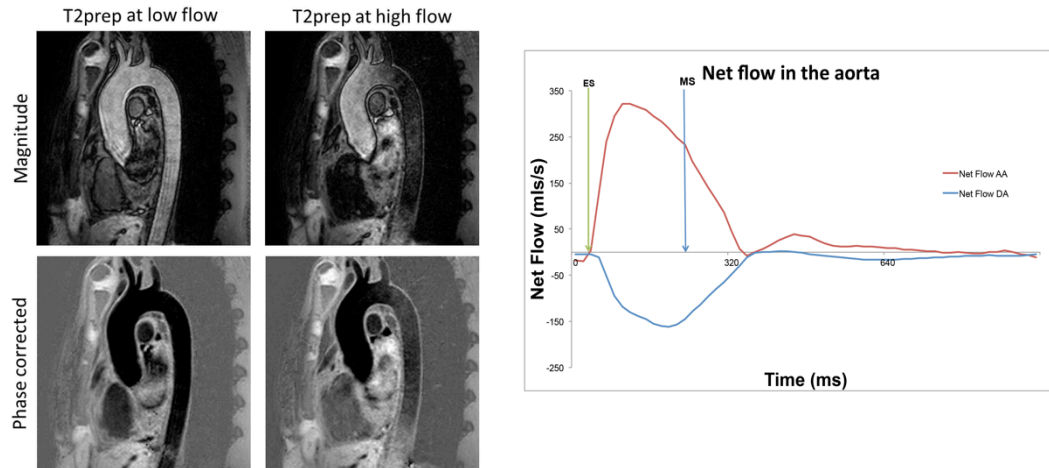


FIGURE 30 IMAGES OBTAINED FROM ONE OF THE TWO PILOT STUDY SUBJECTS DEMONSTRATING FLOW DEPENDENCE OF  $T_2$ PSIR. THE CHART ON THE RIGHT DEMONSTRATES FLOW IN THE ASCENDING (RED, AA) AND DESCENDING AORTA (BLUE, DA), OVER TIME AND THE TIME-POINTS IN THE CARDIAC CYCLE WHEN THE  $T_2$ PREP WERE PERFORMED FOR THE LOW AND HIGH FLOW CONDITIONS. ES= EARLY SYSTOLE, LOW FLOW (0-50MS) MS= MID SYSTOLE, HIGH FLOW (200-250MS).

### 10.1.3 Data analysis and statistics

Comparison between the  $T_2$ IR and  $T_2$ PSIR sequences was based on image quality scores, which included a visual scoring system, apparent contrast-to-noise ratio (aCNR) as well as the sharpness of the images as calculated using dedicated software.(88) The sharpness measurements were performed on a 4-centimetre segment on the vessel wall-lumen interface of the descending aorta. The aCNR was calculated between the aortic vessel wall and aortic luminal blood, with signal noise obtained from a region of air in the lung (avoiding any vasculature). The visual scoring system used ranged from 1-4 where 1 signified poor image quality and 4, excellent image quality (89). Two blinded experts were asked to

compare the two sequences and score them in each volunteer. The scan time for each sequence per patient was also recorded. Statistical analysis was carried out using the Wilcoxon signed-rank test, at  $p < 0.05$  and a kappa statistic to compare subjective agreement between the two raters. For the Wilcoxon test, a W value was calculated, which, if less than the calculated critical value for the sample size, was deemed statistically significant.

# Chapter 11

## 11.1 Dual phase study for aortic motion and strain: imaging methods

### 11.1.1 Study population

Five healthy volunteers and two patients with a TAA repair and a residual Type B component were included in this study. All subjects provided written consent.

### 11.1.2 Image acquisition

Image acquisition in MRI scanning generally occurs in diastole where there is less cardiac and blood motion and therefore fewer artefacts. For the purpose of this study, to evaluate aortic motion and changes during the cardiac cycle, images were obtained in systole and diastole.

All images were acquired on an Achieva 3T scanner (Philips Healthcare, Best, The Netherlands) at the Rayne Institute, King's College London at St. Thomas' Hospital, with a thirty two-element cardiac coil and reconstructed on the scanner console using commercially available software. 3D coronal images were acquired in all subjects.

Imaging parameters at 3T for both sequences include: TR/TE = 5.0/2.3 ms, acquisition duration = 100ms,  $T_2\text{prep}$  echo time = 70ms, FOV =  $264 \times 380 \times 46 \text{ mm}^3$ ,  $\Delta x = 1.6 \times 1.6 \times 1.6 \text{ mm}^3$ ,  $\alpha = 20^\circ$  for the first acquisition and  $5^\circ$  for the PSIR reference acquisition, SENSE factor = 2 (anterior-posterior). A pencil beam navigator was used for respiratory gating, with a 5 mm gating window. A cine phase contrast scan was performed in order to determine the blood flow in the ascending aorta just distal to the aortic valve and to determine the cardiac phase. Data acquisition was performed in systole and diastole in all subjects (n=7).

### 11.1.3 Image segmentation

CRIMSON was used as described before to segment the aorta and identify the points of interest this time using MRI derived images. Pathlines were created from which contours were mapped and a solid volume CAD model was interpolated. The image data and resulting 3D model were compared to resolve any inaccuracies. Initially, diastolic and systolic models for each patient were created and superimposed to show a visual depiction of motion from diastole to systole (Figure 31).

To allow for comparable analysis, dimensions of each contour at each of the desired locations were calculated in CRIMSON for each subject, in diastole and in systole. This provided information circumferential change. Additional methods of comparison included strain calculations.

To determine a longitudinal strain, a centreline was developed in the aorta, without any branching vessels attached. A mesh was created for the aorta and was repeated for each isolated segment of the aorta. CRIMSON was used to calculate the volume for each isolated mesh for each isolated segment of the aorta. The centreline for each segment was calculated by importing the meshed segments into VMTK (vascular modelling tool kit). (90)

The true and false lumen were segmented as 'separate vessels' in the case of aortic dissection.

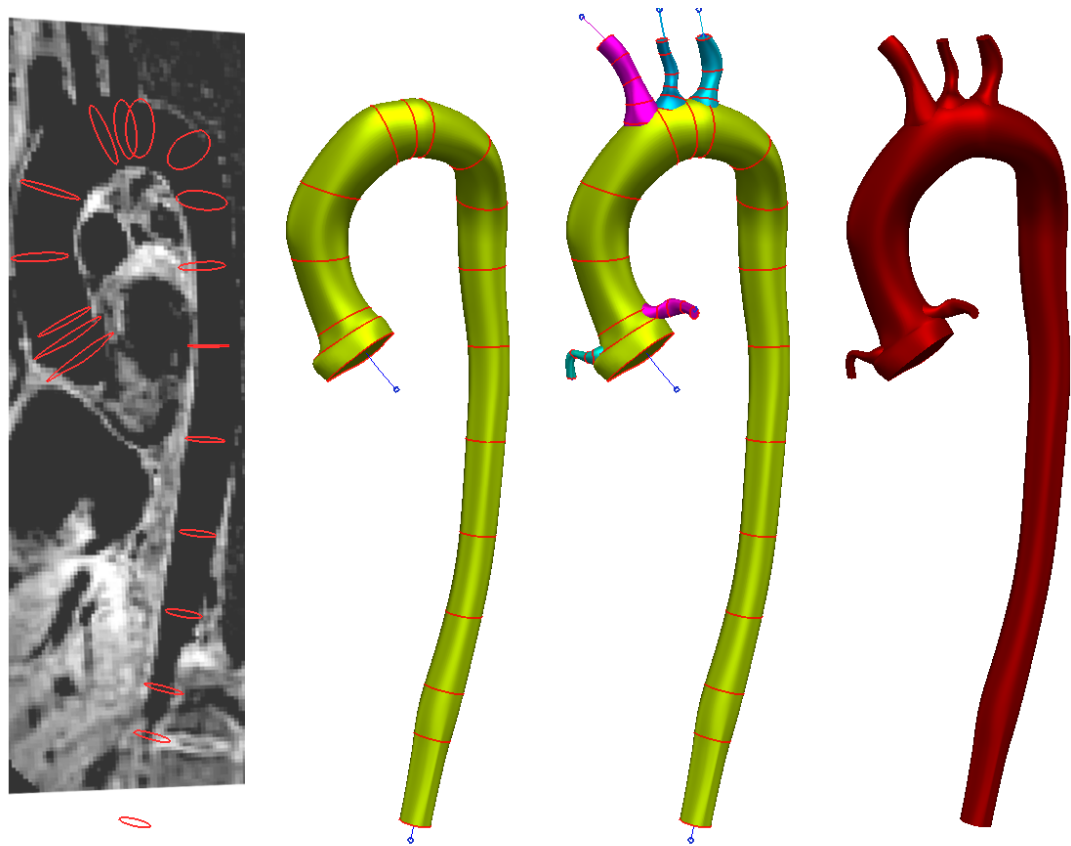


FIGURE 31 IMAGE SEGMENTATION FOR THE DUAL PHASE STUDY.

#### 11.1.4 Image analysis

Initial work on this study lead to the development of segmented models of all subjects in systole and in diastole. It was apparent however, that there were two problems. The first issue related to the use of flow to determine the phase of the cardiac cycle. Initial scans for systole were triggered at a time of maximal flow which corresponded to early systole. Here however, on image analysis there was not much difference in cardiac motion (Figure 32, Figure 33). Image analysis showed a very similar state of the heart and the aorta when imaged in systole or in diastole. This was very early in systole when the motion of the heart resembled very late diastole. All subsequent imaging was done using cine imaging whereby flows across the aortic valve were determined. A flow curve was generated to determine

maximal aortic flow and triggering the scan just after this, therefore in mid-late systole (Figure 34).

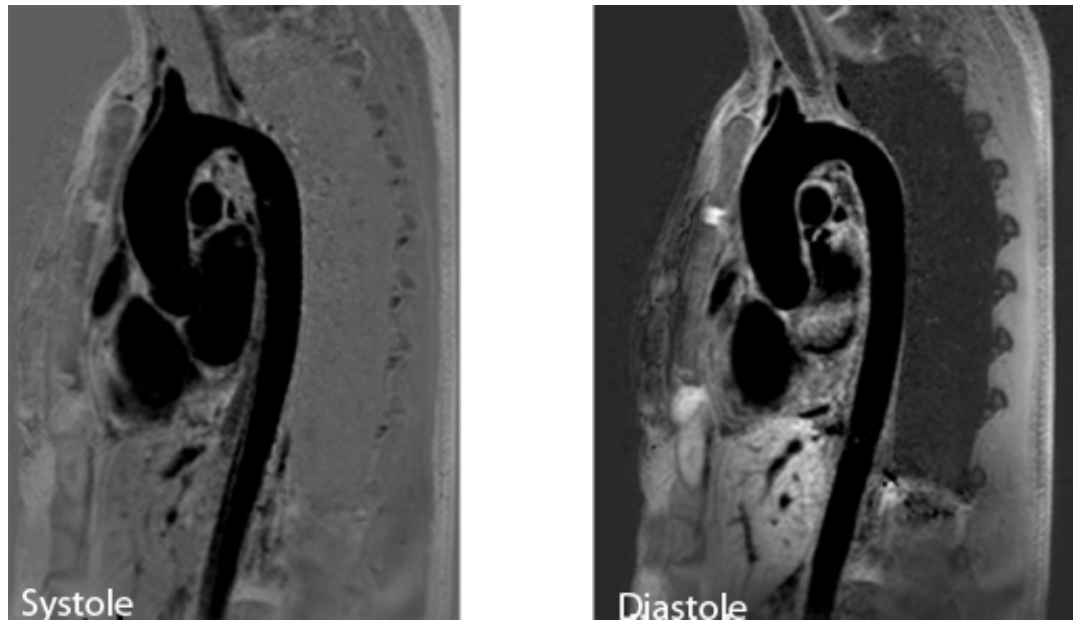


FIGURE 32 SYSTOLIC AND DIASTOLIC IMAGES FROM THE SAME SUBJECT. NOT MUCH DIFFERENCE IN CARDIAC AND AORTIC MOTION WAS VISIBLE BETWEEN THE TWO PHASES.

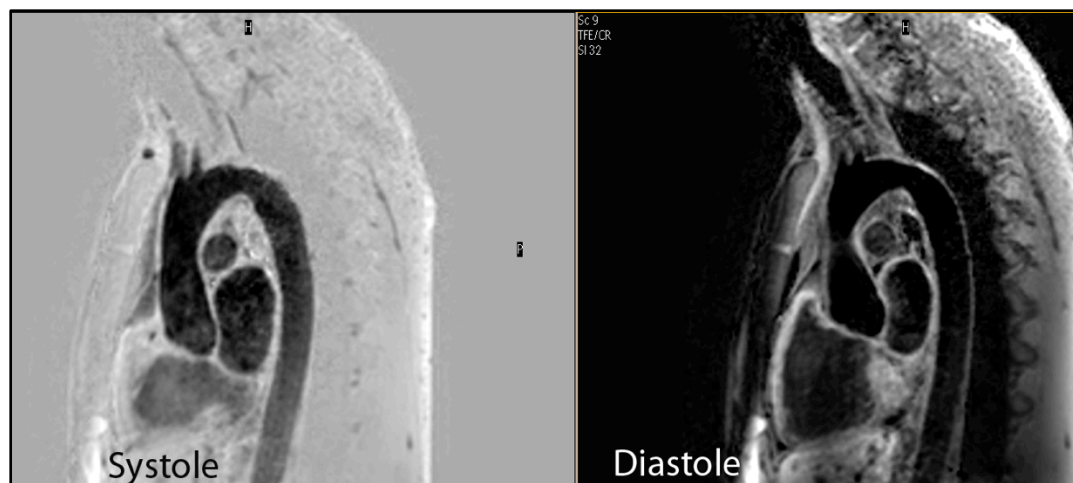


FIGURE 33 CINE TRIGGERED SCANS SHOW A DIFFERENCE IN SYSTOLIC AND DIASTOLIC STATES OF THE HEART.

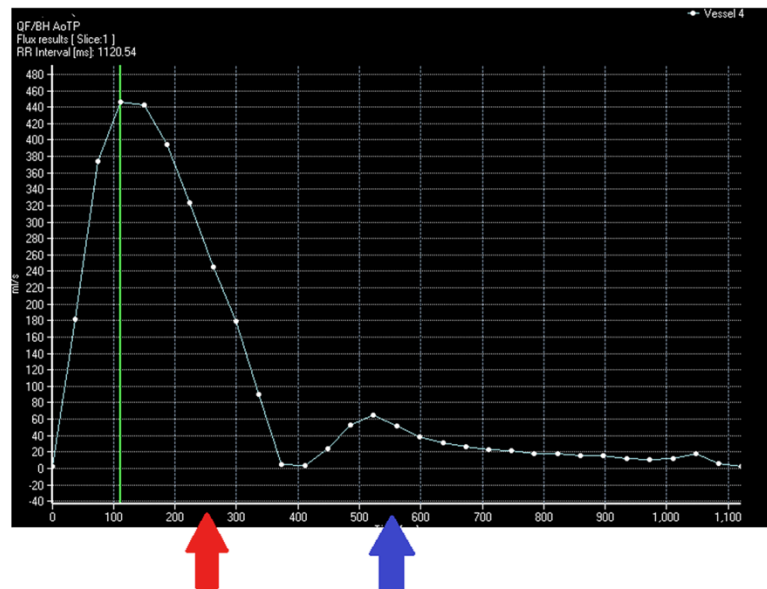
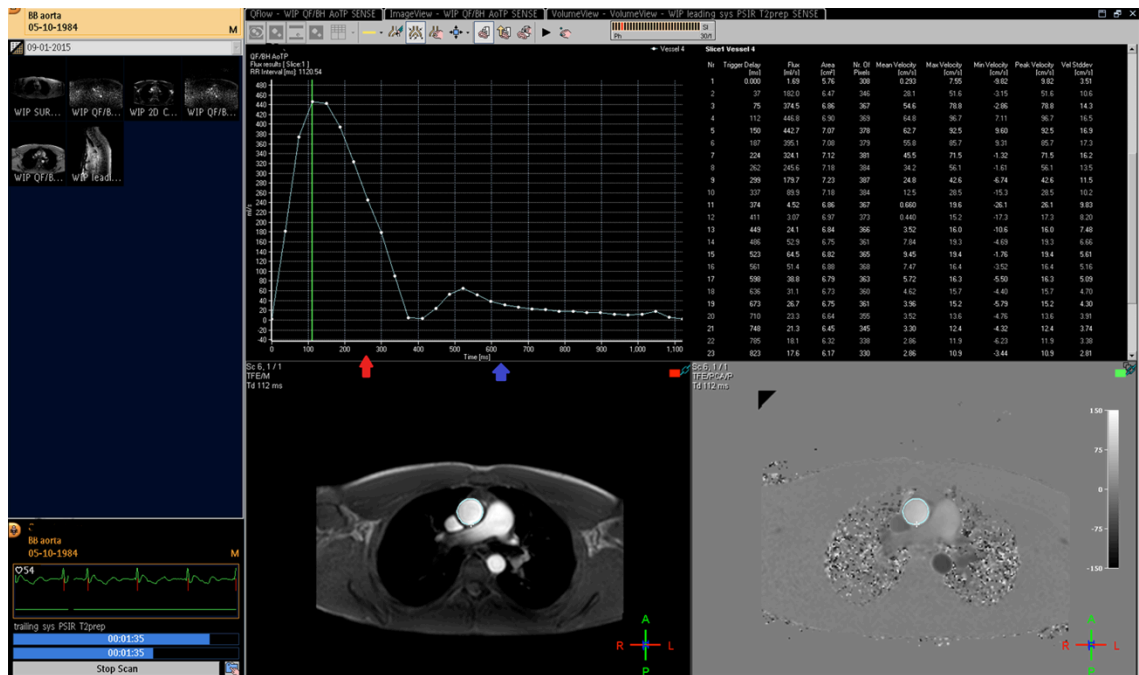


FIGURE 34 AN ALTERNATE STRATEGY OF INCLUDING A CINE IMAGE WITH DYNAMIC CARDIAC IMAGING TO DETERMINE SYSTOLE AND DIASTOLE WAS INCLUDED IN ADDITION TO CALCULATING FLOW IN THE ASCENDING AORTA ABOVE THE LEVEL OF THE AORTIC VALVE WITH PC-MRI. SYSTOLIC IMAGING WAS THEN TRIGGERED AS SHOWN BY THE RED ARROW AND DIASTOLIC BY THE BLUE ARROW.

The second issue with dual phase imaging related to the discrepancy between image datasets, which meant that not all subjects had full image data sets extending into the



abdominal aorta. This meant that for accurate comparison, fixed points that were visible in all subjects were essential rather than arbitrary aortic lengths. Following on from this, four discrete points from the aorta were identified for all subjects in both the systolic and diastolic datasets. These were:

1. distal to the left coronary artery (LCOA),
2. proximal to the innominate artery (P.InoA),
3. distal to the left subclavian artery (LSCA)
4. the 1<sup>st</sup> intercostal artery and
5. the 5<sup>th</sup> intercostal artery (5<sup>th</sup> IcoA).

These were chosen for two reasons. Firstly as these points were easily identifiable on the image data in all subjects and secondly because they allowed the aorta to be divided into specific portions, namely the;

1. ascending aorta (AAo, distal to the left coronary artery and proximal to the P.InoA)
2. The arch (AA, from the P.InoA to distal to the LSCA)
3. The descending aorta (DA distal to the LSCA and to the 5<sup>th</sup> IcoA)

therefore allowing for comparable analysis. (Figure 35)

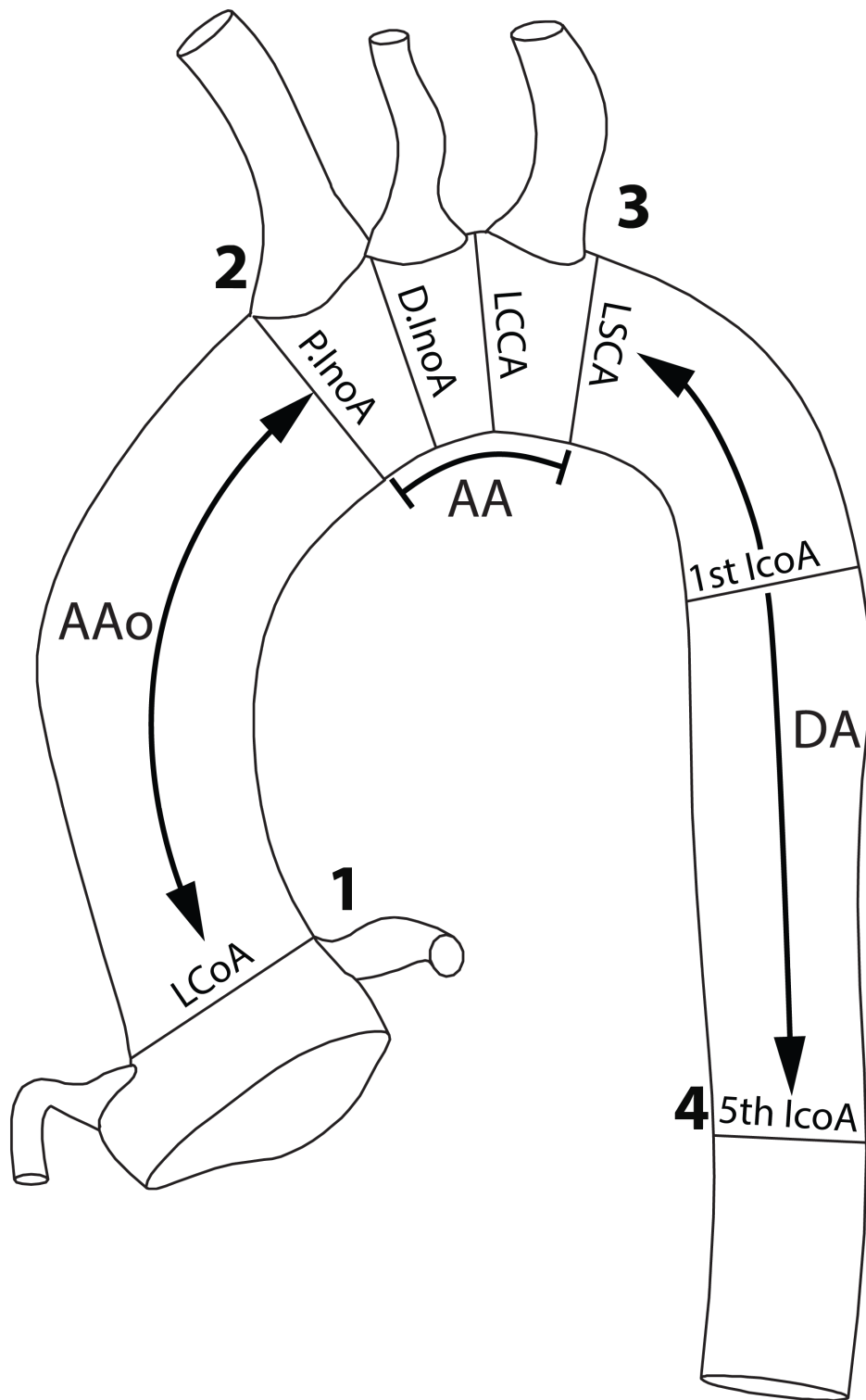


FIGURE 35 REPRESENTATION OF THE AORTA IN THE DUAL PHASE STUDY. THE AORTA WAS DIVIDED INTO SEGMENTS TO ALLOW FOR COMPARATIVE ANALYSIS. THE POINTS 1-4 SERVE TO DISTINGUISH BETWEEN THE ASCENDING AORTA (1-2), ARCH (2-3) AND DESCENDING AORTA (3-4).

### 11.1.5 Analysis of aortic motion and strain

Initial analysis was focused at studying the change in the position of a chosen coronary artery in each subject between systole and diastole. Further analysis investigating longitudinal, circumferential and volumetric changes in the aorta were later included

Strain is defined as the deformation of a material from reference morphology to a new morphology, when experiencing an external force. The Green-Lagrange tensor was used to calculate circumferential ( $E_C$ ) and longitudinal ( $E_L$ ) deformations in length ( $l$ ) and this is independent and suitable for large strains

$$E = \frac{l_s^2 - l_D^2}{2l_D^2}$$

For volumetric strain ( $E_V$ ), the following equation was used,

$$E_V = \frac{\Delta V}{V_D}$$

where  $\Delta V = V_S - V_D$  and  $V_S$  represents the volumetric strain in systole and  $V_D$  the volumetric strain in diastole. The volume for each segment of the aorta was calculated within CRIMSON.

# Chapter 12

## Results

### 12.1 TEVAR Study Results

Three patients underwent TEVAR for on-going dilatation of the thoracic aorta following on from their acute TBAD event. A fourth patient presented with an acute TBAD, in November 2014, and was originally planned to undergo TEVAR. Close monitoring and blood pressure management of this patient led to change in the decision to a conservative strategy.

However, in anticipation of the original plan of TEVAR, the patient was recruited and underwent MRI scanning, and CT image data was acquired to develop a CAD model. Table 2 shows the demographics of the recruited patients. Figure 36 is a CT image library of the 4 TEVAR patients.

TABLE 2 DEMOGRAPHICS OF THE TEVAR POPULATION PATIENTS

Pt Id	Age (y)	Sex	Date	Type of dissection	Reason for TEVAR
1	60	M	April 2013	Acute TBAD	Acute chest and abdominal pain
2	59	M	May 2013	Acute TBAD	Symptomatic and size >5.5cm
3	47	F	Oct 2002	Chronic TBAD	Rapidly increasing size
4	30	M	Aug 2014	Acute TBAD	TEVAR not performed

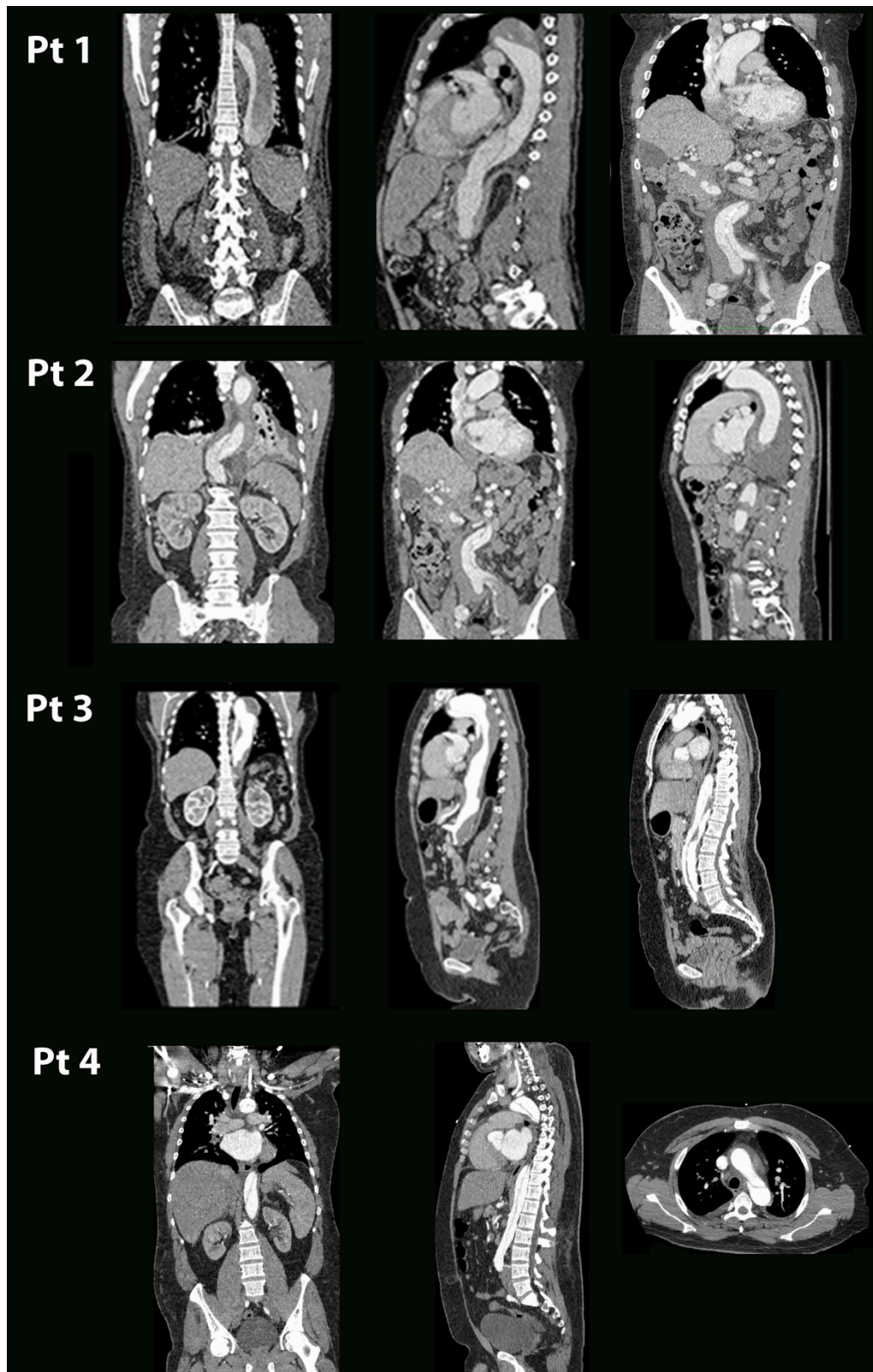


FIGURE 36 CT LIBRARY OF IMAGES FOR ALL TEVAR PATIENTS 1-4,

## **12.1.1 TEVAR- Patient 1**

### ***12.1.1.1 Background***

A 60-year-old gentleman was referred from Exeter University Hospital with a 2-day history of acute dyspnoea and central chest pain. He had a history of hypertension and had undergone a laparotomy for a bleeding gastric ulcer 19 years ago. A CT scan performed at the referring hospital demonstrated a TBAD originating in the descending aorta at the level of the diaphragm. The right renal artery was fed by the false lumen whereas the rest of the visceral vessels originated from the true lumen. In view of on-going abdominal pain and concerns regarding gut malperfusion, the patient was referred to St. Thomas' Hospital. On arrival, intravenous beta-blockade was commenced but despite adequate hypertensive control, the persistence of abdominal symptoms prompted the decision for surgical intervention.

### ***12.1.1.2 Preoperative Imaging***

CT imaging was performed as per clinical routine protocol (Figure 37). MRI using the previously mentioned sequences was performed.

### ***12.1.1.3 Procedure: TEVAR for symptomatic TBAD***

Arterial access was achieved via the right femoral artery, using an 8Fr sheath. A pigtail catheter was inserted into the aorta and calibration with the RadiAnalyzer system was performed. Next, the PressureWire Certus (PW) was calibrated before insertion, as per manufacturer's instructions and inserted within the SuperKetch Y-connector. True lumen and corresponding aortic measurements were taken followed by false lumen and aortic measurements.

#### ***12.1.1.4 Non-invasive haemodynamic study- workflow process leading to simulation***

Using CRIMSON software a CAD model was developed for Patient 1, using anatomic data from a preoperative clinical CT scan (2D PC-MRI data was post processed in GTFlow (Switzerland) to determine a velocity and flow profile for specific regions of the aorta (ascending, arch and descending aorta) using contours to define the vessels of interest The resulting data was input into a spreadsheet to determine a velocity and flow profile for the chosen vessel. (Figure 38)

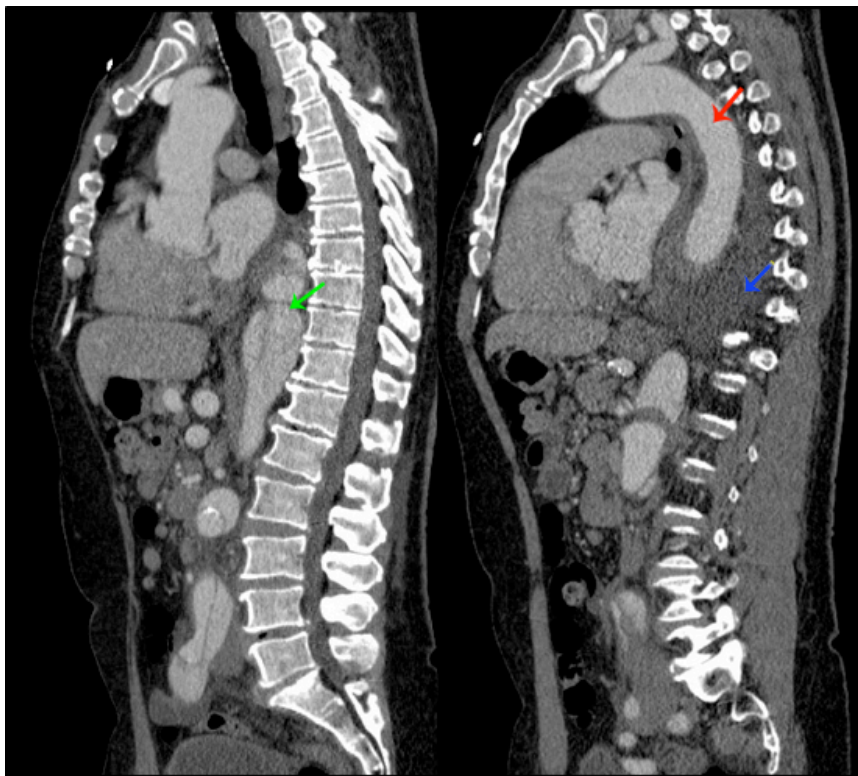


FIGURE 37 PATIENT 1. ACUTE TBAD IMAGES FROM CT SCANS AT PRESENTATION. BLUE ARROW INDICATES THROMBUS FORMATION. RED ARROW INDICATES THE POSITION OF THE TRUE LUMEN. GREEN ARROW INDICATES LOCATION OF INTIMAL TEAR.

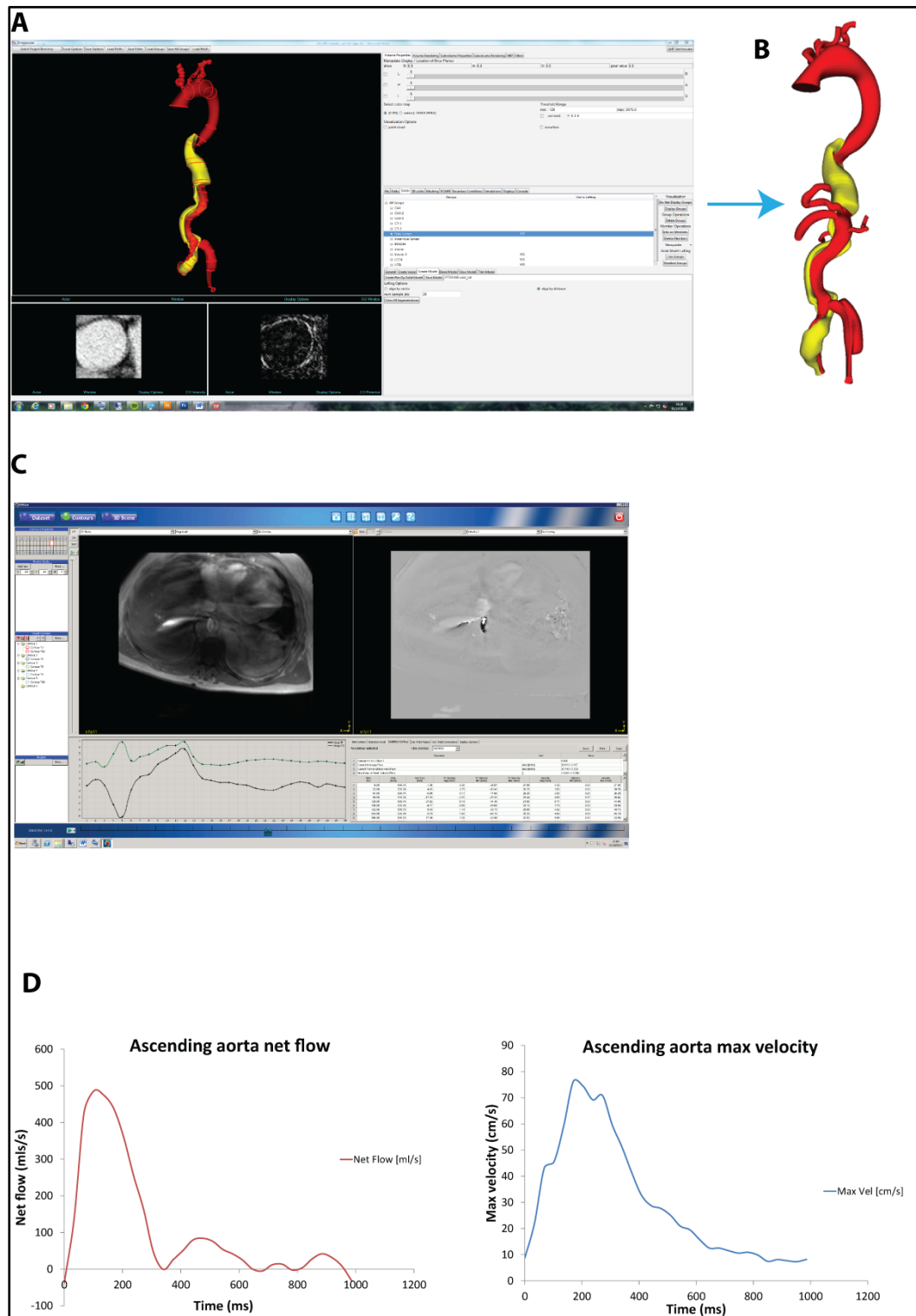


FIGURE 38 WORKFLOW FOR CREATING A 3D CAD MODEL FOR SIMULATION. A. IMAGE DATA IS USED TO CREATE GEOMETRY IN CRIMSON. B. A 3D CAD MODEL IS DEVELOPED. C. FLOW DATA IS ACQUIRED FROM PC-MRI USING GT-FLOW. D. FLOW DATA IS CONVERTED INTO GRAPHICAL FORMAT.



## **12.1.2 TEVAR- Patient 2**

### ***12.1.2.1 Background***

A 59-year-old gentleman was admitted to Woolwich Hospital with a 6-month history of dyspnoea, anorexia and weight loss. There was no history of acute chest or back pain and although he had been diagnosed with hypertension a year previously, he had not received treatment for this. His baseline blood pressure on admission was 180/70mmHg. In view of his symptoms of dyspnoea, he underwent CT scanning which demonstrated a TBAD, immediately distal to the left subclavian artery. The presence of a large descending aortic component prompted transfer to St. Thomas' Hospital for intervention. Preoperative management at St. Thomas' included continuous veno-venous filtration in view of his renal impairment and intravenous beta-blockade combined with GTN to control hypertension.

### ***12.1.2.2 Preoperative imaging***

Preoperative CT scan demonstrated a dissection in the descending aorta distal to the left subclavian artery (Figure 39).

### ***12.1.2.3 Procedure: TEVAR for symptomatic TBAD***

Access was achieved via the right femoral artery, using an 8Fr sheath. A pigtail catheter was inserted into the aorta and calibration with the RadiAnalyzer system was performed. Next, the PW was calibrated before insertion, as per manufacturer's instructions and inserted within the SuperKetch Y-connector. True lumen and corresponding aortic measurements were taken followed by false lumen and aortic measurements.

#### ***12.1.2.4 Non-invasive haemodynamic assessment***

To obtain non-invasive haemodynamics, 2D PC-MRI data was post processed in GT Flow, to obtain velocity profiles at 3 different levels in the aorta, namely the ascending aorta (Ao1), the arch vessels (Ao2) and the descending aorta at the level of the diaphragm (Ao3). These velocity profiles were used to develop the simulation process. Figure 40 shows the workflow process of developing the CAD model in CRIMSON and the use of GTFlow to post-process MRI data to obtain velocity profiles in this instance at the arch outflow level.



FIGURE 39 CT IMAGES OF PATIENT 2. THE RED ARROW SHOWS THE TRUE LUMEN, THE YELLOW ARROW INDICATES THE FALSE LUMEN.

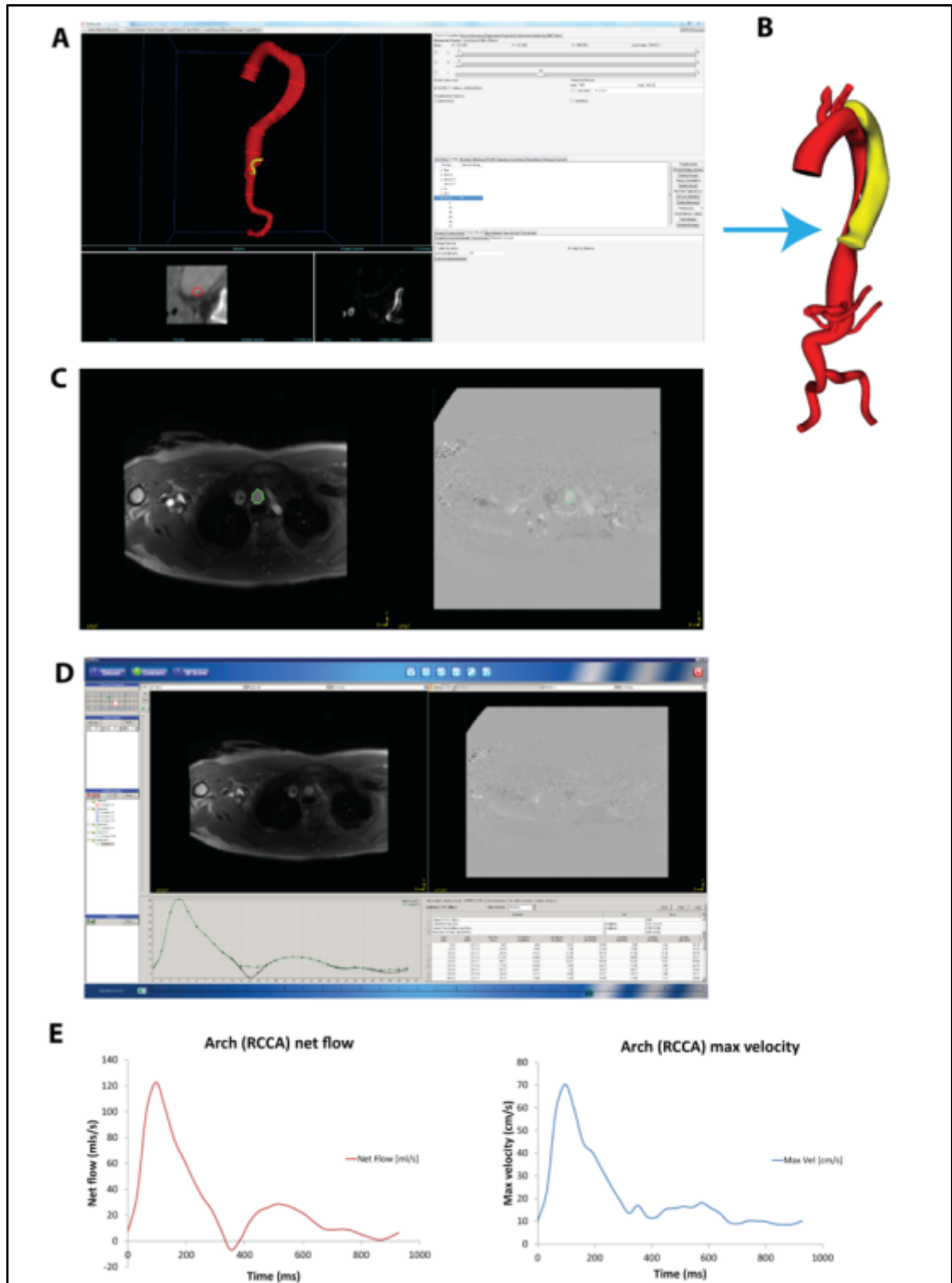


FIGURE 40 WORKFLOW FOR PREPARING A MODEL FOR SIMULATION. A. 3D GEOMETRY FROM IMAGE DATA RESULTS IN B. AN ANATOMICALLY ACCURATE MODEL. C AND D. GT FLOW IS USED TO EXTRACT RELEVANT FLOW DATA AT VARIOUS POINTS IN THE AORTA. E. THE FLOW DATA IS CONVERTED INTO EXCEL READY FOR USE IN SIMULATION.

### **12.1.3 TEVAR Patient 3**

#### ***12.1.3.1 Background***

In December 2002, A 57 year old female presented with acute chest and back pain and an ischaemic right leg. Subsequent investigations demonstrated a TBAD with compromise of the right external iliac artery. In addition, an anatomical anomaly of an aberrant right subclavian artery was detected. A Zilver stent was inserted to allow revascularisation of the right leg, with effective results. In view of the otherwise stable nature of the dissection, the patient was entered into a close monitoring programme with 6 monthly CT evaluation.

In January 2013, however, a rapid increase in the false lumen size was detected compared to previous scans and a decision was made to perform TEVAR preceded by arch debranching to allow for a comfortable proximal landing zone and re-routing of the aberrant right subclavian artery.

#### ***12.1.3.2 Procedure: TEVAR for enlarging aortic diameter***

Arterial access was achieved via the right femoral artery, using an 8Fr sheath. A pigtail catheter was inserted into the aorta and calibration with the RadiAnalyzer system was performed. Next, the PW was calibrated before insertion, as per manufacturer's instructions and inserted within the SuperKetch Y-connector. True lumen and corresponding Figure 41 shows the preoperative CT.

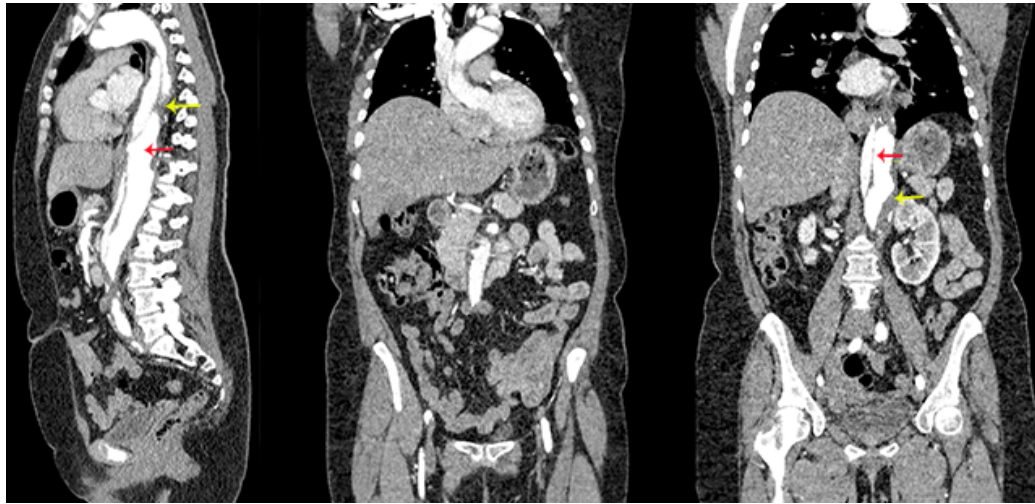


FIGURE 41 PATIENT 3. A: PRE-OPERATIVE CT SCAN WITH RED ARROW HIGHLIGHTING THE TRUE LUMEN AND THE YELLOW ARROW HIGHLIGHTING THE FALSE LUMEN.

## 12.1.4 Patient 4

### 12.1.4.1 Background

A 30 year old gentleman with a history of severe, uncontrollable hypertension presented with acute chest and back pain in September 2014. He was diagnosed with a TBAD on CT scan (Figure 42). His BP at the time of MRI was 208/147mmHg. Anti-impulse therapy was commenced and the symptoms subsided. In view of this he was monitored closely and eventually the decision to manage conservatively with a repeat CT scan in 4 months' time was made. Figure 43 shows the CAD models developed for Patient 4 using CRIMSON. Figure 44 shows the position of the acute intimal tear and corresponding location on CAD model.

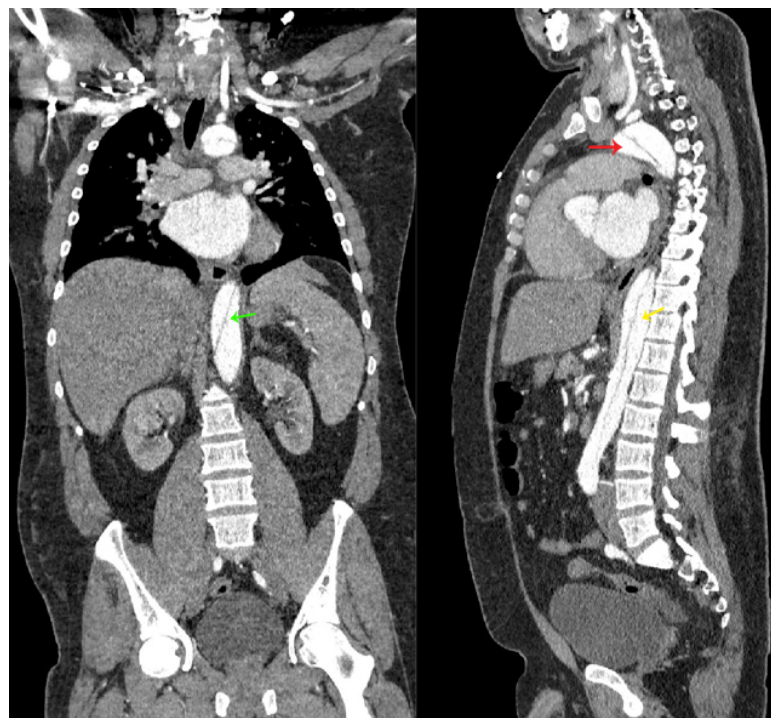


FIGURE 42 CT SCAN IMAGES FROM A 30-YEAR OLD MALE WITH AN ACUTE TBAD. THE GREEN ARROW INDICATES THE POSITION OF THE INTIMAL FLAP. THE YELLOW ARROW INDICATES THE FALSE LUMEN AND THE RED ARROW THE TRUE LUMEN.

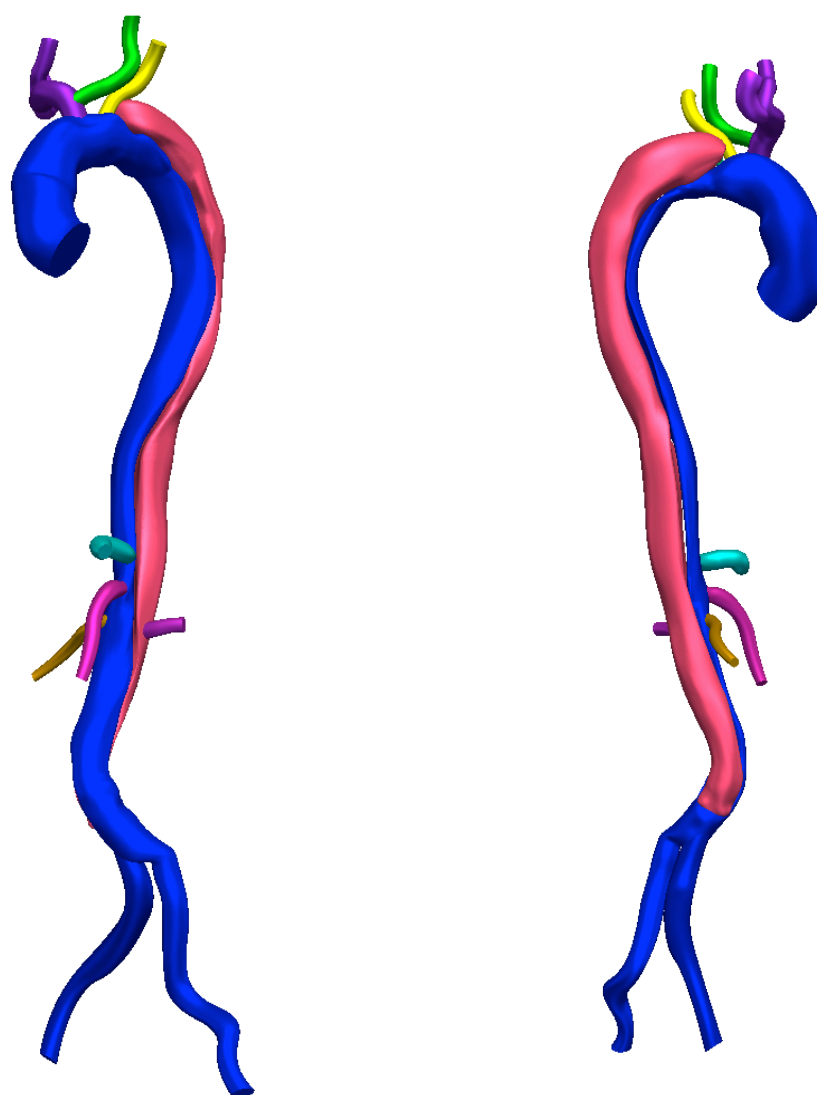
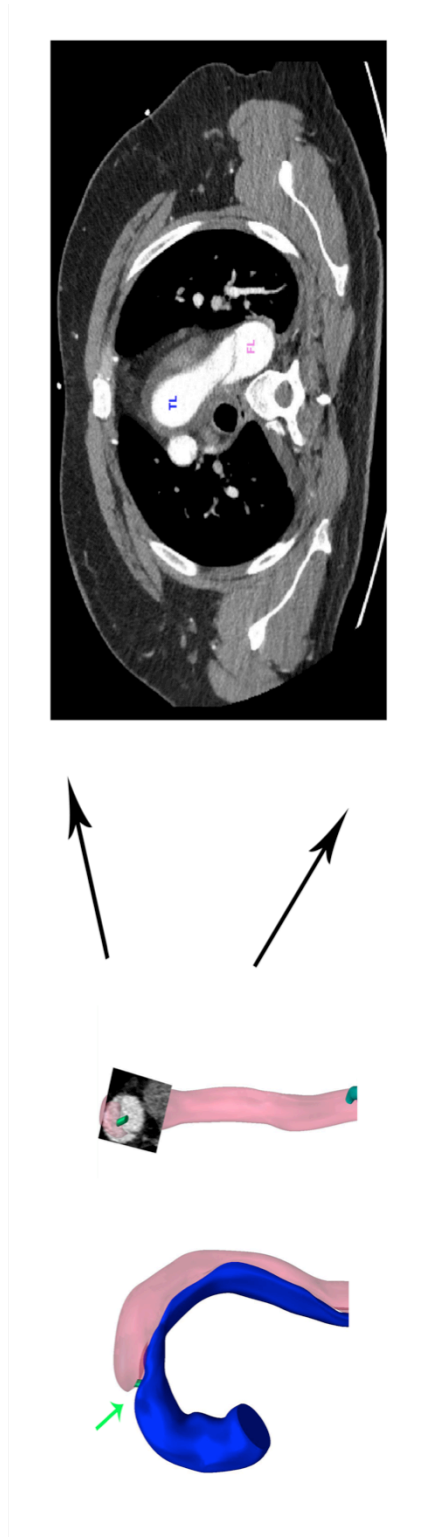


FIGURE 43 A 3D MODEL OF PATIENT 4 SHOWING THE TRUE (BLUE) AND FALSE LUMEN (PINK). NO THROMBUS WAS PRESENT DUE TO THE ACUTE NATURE OF THE DISSECTION.

FIGURE 44 PATIENT 4. 3D MODEL WITH AREA OF TEAR (GREEN ARROW) HIGHLIGHTED AND CORRESPONDING CT IMAGE SHOWING THE SAME.





## 12.2 Recording of pressure wire results

Figure 45 shows an example of results obtained from a pressure wire study during TEVAR for a patient with TBAD. In patients with an acute pathology the false lumen pressure was seen to be larger than in those with a more chronic pathology.

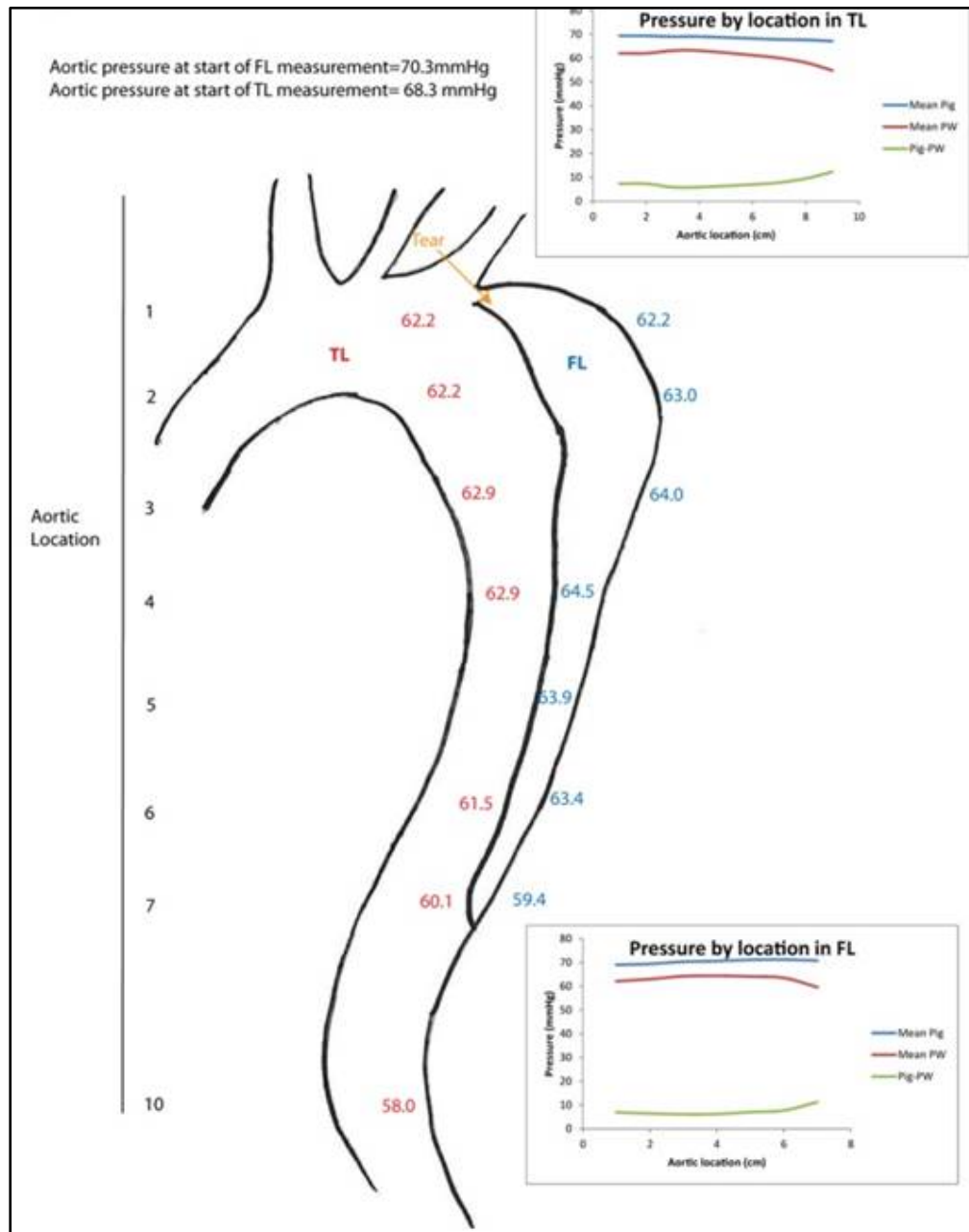


FIGURE 45 PROFORMA FROM AN EXAMPLE OF A HYPOTHETICAL TEVAR CASE SHOWING RECORDING OF INTRA-AORTIC HAEMODYNAMICS. PRESSURE WIRE RESULTS WERE PLOTTED OVER THE AORTIC LENGTH FOR EACH PATIENT.

# Chapter 13

## Results

### 13.1 Follow up study results

Three patients were recruited into the follow up study arm. All had undergone acute repair for TAAD and had a residual Type B component that was being monitored with serial CT scans on an annual basis. Two patients had two scans performed each, one year apart. The final patient was recruited late and therefore had only one scan performed.

The details of all recruited patients are given in Table 3

TABLE 3 FOLLOW UP PATIENTS DEMOGRAPHICS AND SCAN DETAILS

<b>Pt ID</b>	<b>Age (y)</b>	<b>Sex</b>	<b>Dissection</b>	<b>Post-operative result</b>	<b>CT images</b>	<b>MRI scans</b>
1	63	M	A, Sept 2011	Residual Type B	Sept 2011  Aug 2013  Sept 2014	Sept 2013  May 2014
2	30	F	A, Oct 2008	Residual Type B	Oct 2008  Aug 2013  Mar 2014	Aug 2013  Mar 2014
3	56	M	A, Mar 2012	Residual Type B	Mar 2012  July 2013  Aug 2014	Aug 2013  July 2014
4	54	M	A, 2012	Residual Type B	Feb 2012  April 2013  March 2014	May 2014  Dec 2014

### 13.1.1 Follow up patient 1

A 63 year old gentleman with a history of hypertension had an acute TAAD in 2011. He underwent emergency repair of the ascending aorta and made an excellent post-operative recovery. The residual TBAD was noted preoperatively on the CT scan and the patient was eventually discharged home with annual CT scan follow up.

This patient attended for 2 MRI scans one year apart. The sequences performed as described in the general material and methods.

2D PC-MRI data was acquired at each scan session and two CAD models demonstrating the aortic geometry one year apart were developed the CT image data within CRIMSON software. Figure 46 shows the completed CAD model with and without the thrombus lofted in as well as the thrombus as a separate entity. Figure 49 shows the same for the same patient one year later.

In Figure 48 the method of determining thrombus presence is shown using CRIMSON.

Table 4 shows the quantitative morphological changes over the one year period with respect to the volume of the true and false lumens and the thrombus. There has been a decrease in the false lumen volume and an increase in thrombus formation over the course of the year. Figure 49 and Figure 50 show the changes with respect to tear morphology. The main change was the healing of tear at location 4 in 2013. Finally, simulation was performed on these CAD models (without the thrombus lofted in). The results are shown in Figure 51, Figure 52 and Figure 53. Of note, the overall intra-aortic pressure was lower in 2014 than in 2013. Additionally the area of tear 4 had a low velocity and pressure overall at baseline in 2013 and it is not surprising that a year later this tear had healed. Finally, the proximal false lumen showed a high pressure at baseline and although this was lower the following year, it still represented a higher pressure area than the distal false lumen. This could mean that the proximal false lumen is pressurised blind sac.

Finally Figure 54 shows the comparison of PC-MRI derived parameters and those from CFD. Although not a perfect match they do show agreement.

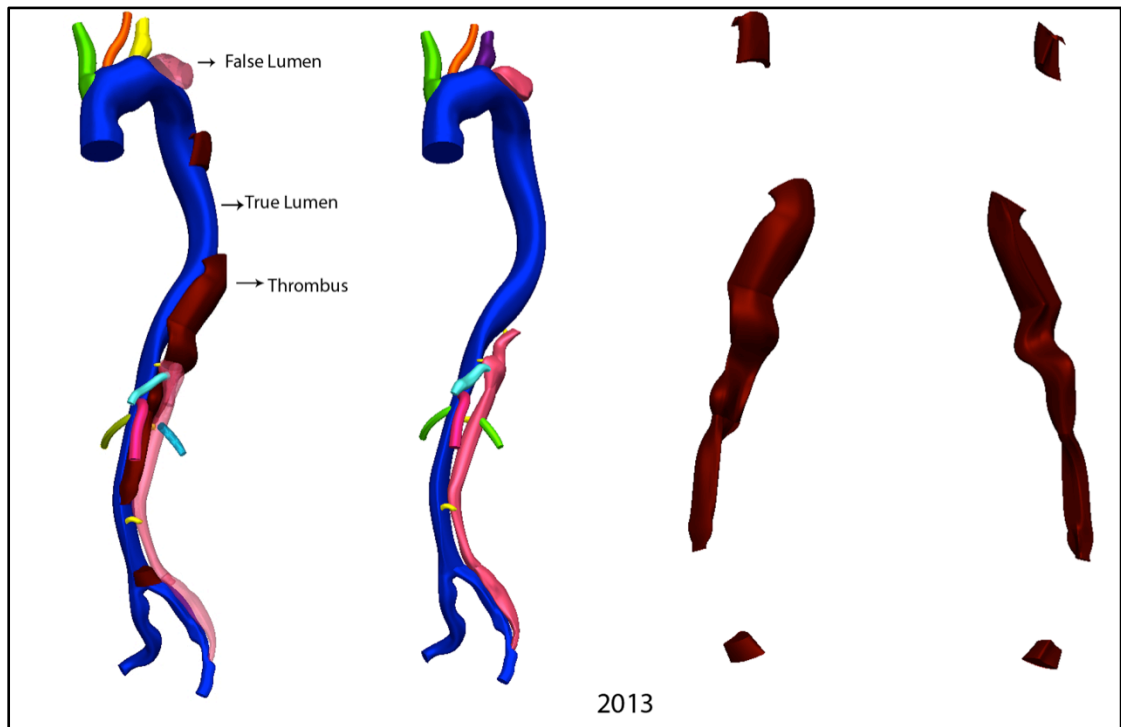


FIGURE 46 PATIENT 1 IN 2013. THE TRUE LUMEN IS SHOWN IN BLUE, FALSE IN PINK AND THROMBUS IN BROWN.

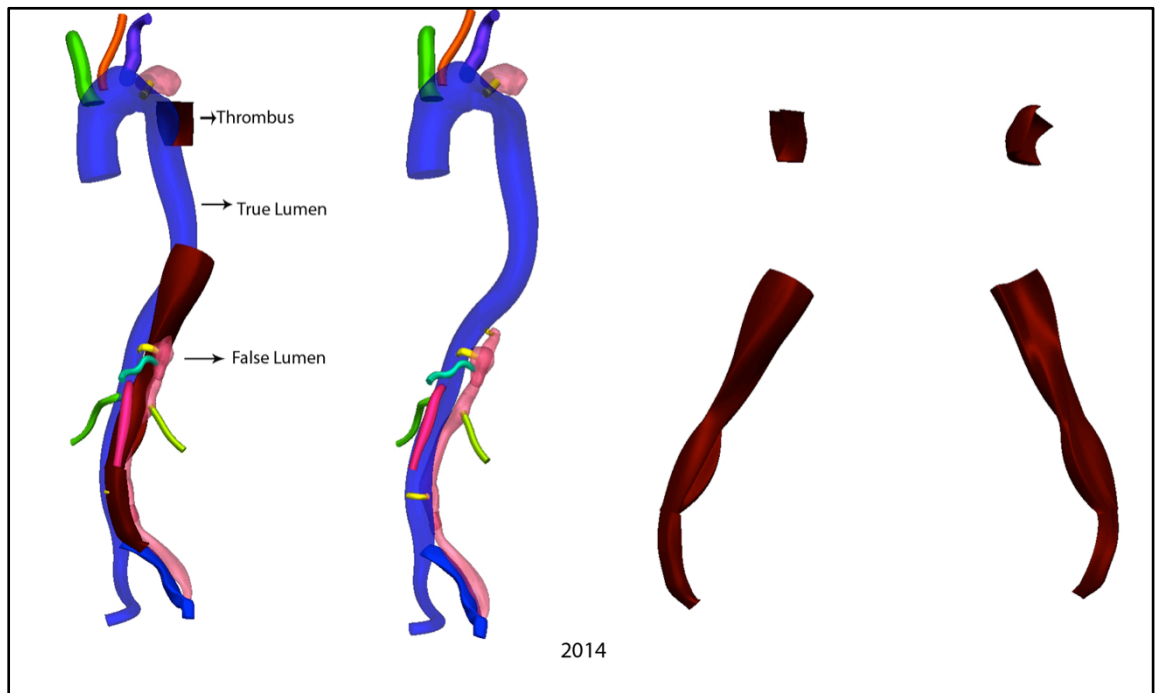


FIGURE 47 PATIENT 1 IN 2014. THE TRUE LUMEN IS SHOWN IN BLUE, FALSE IN PINK AND THROMBUS IN BROWN.

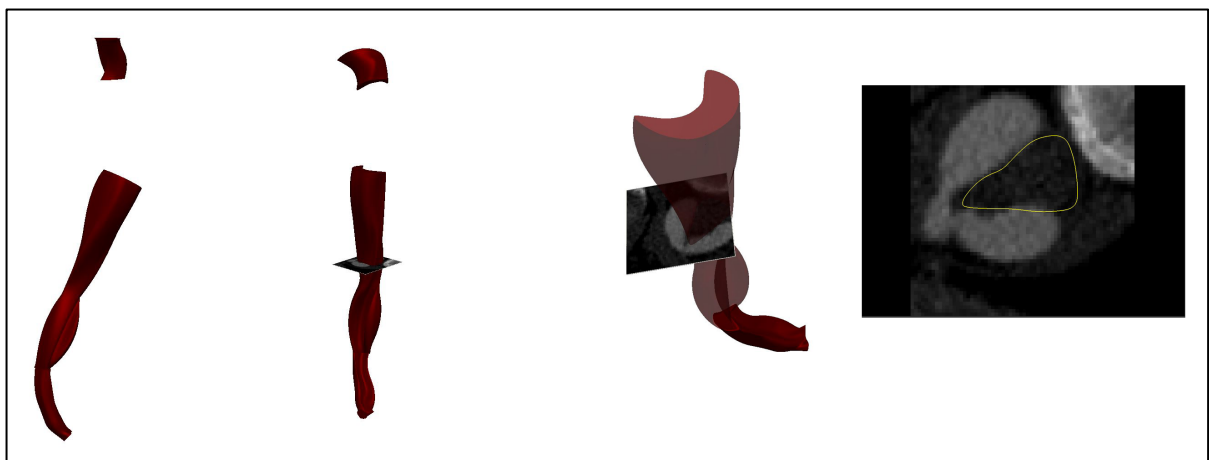


FIGURE 48 PATIENT 1 THROMBUS VOLUME IS 2014 WITH CORRESPONDING CT IMAGE DEPICTING THROMBUS.

TABLE 4 MORPHOLOGICAL CHANGES OVER THE PERIOD OF ONE YEAR FOR PATIENT 1. THE FALSE LUMEN VOLUME HAS DECREASED AND THROMBUS VOLUME HAS INCREASED.

Year	TL (mls)	FL (mls)	Thrombus (mls)
2013	256	50.08	55.2
2014	256	46.38	97.6

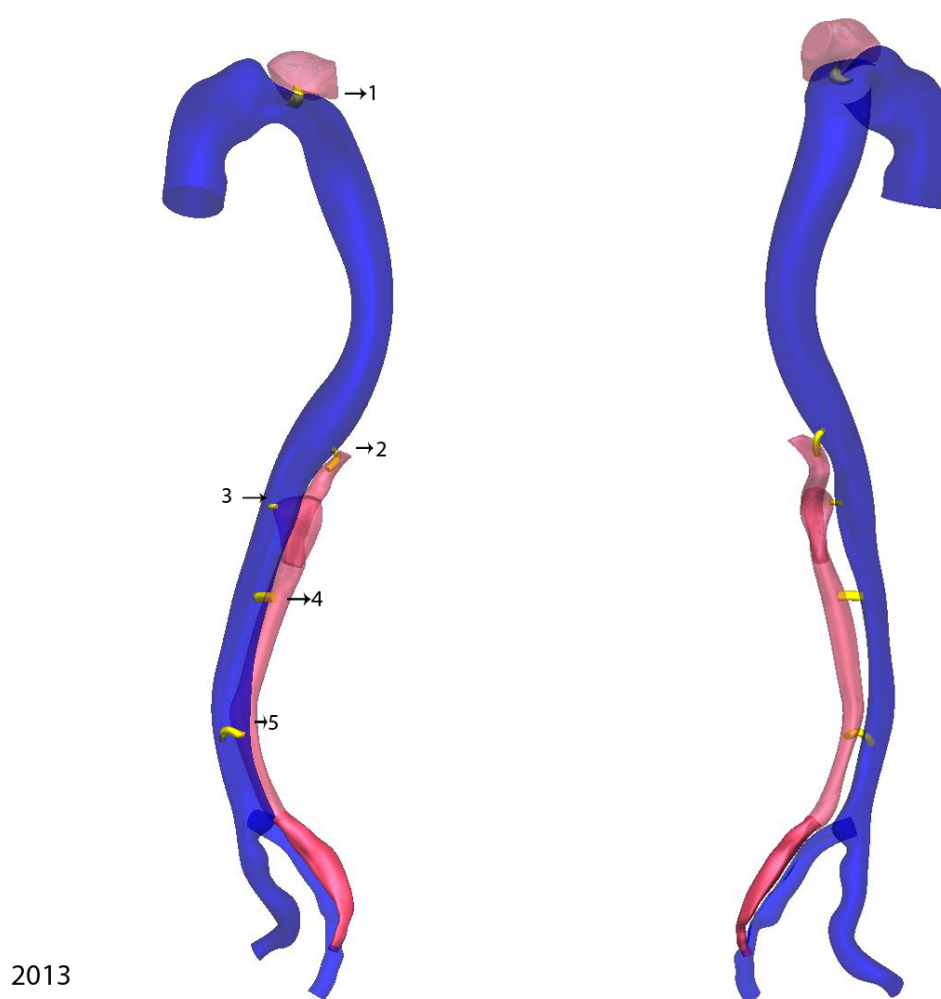


FIGURE 49 CAD MODELS FOR PATIENT 1 IN 2013. THE TEARS ARE MARKED IN YELLOW AND BLACK ARROWS.



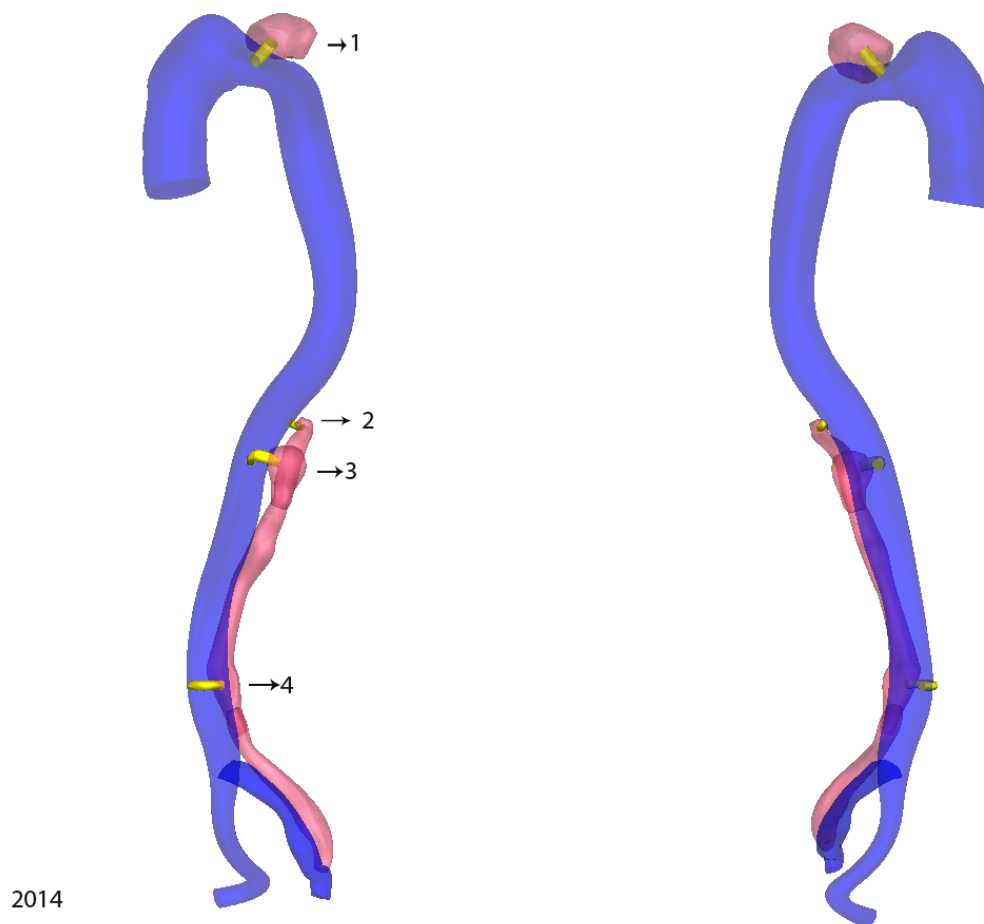


FIGURE 50 CAD MODELS FOR PATIENT 1 IN 2014. THESE MODELS SHOW THE CHANGE IN TEAR MORPHOLOGY AT ONE YEAR POST FOLLOW UP AT LOCATION. TEAR AT LOCATION 4 HAS HEALED.

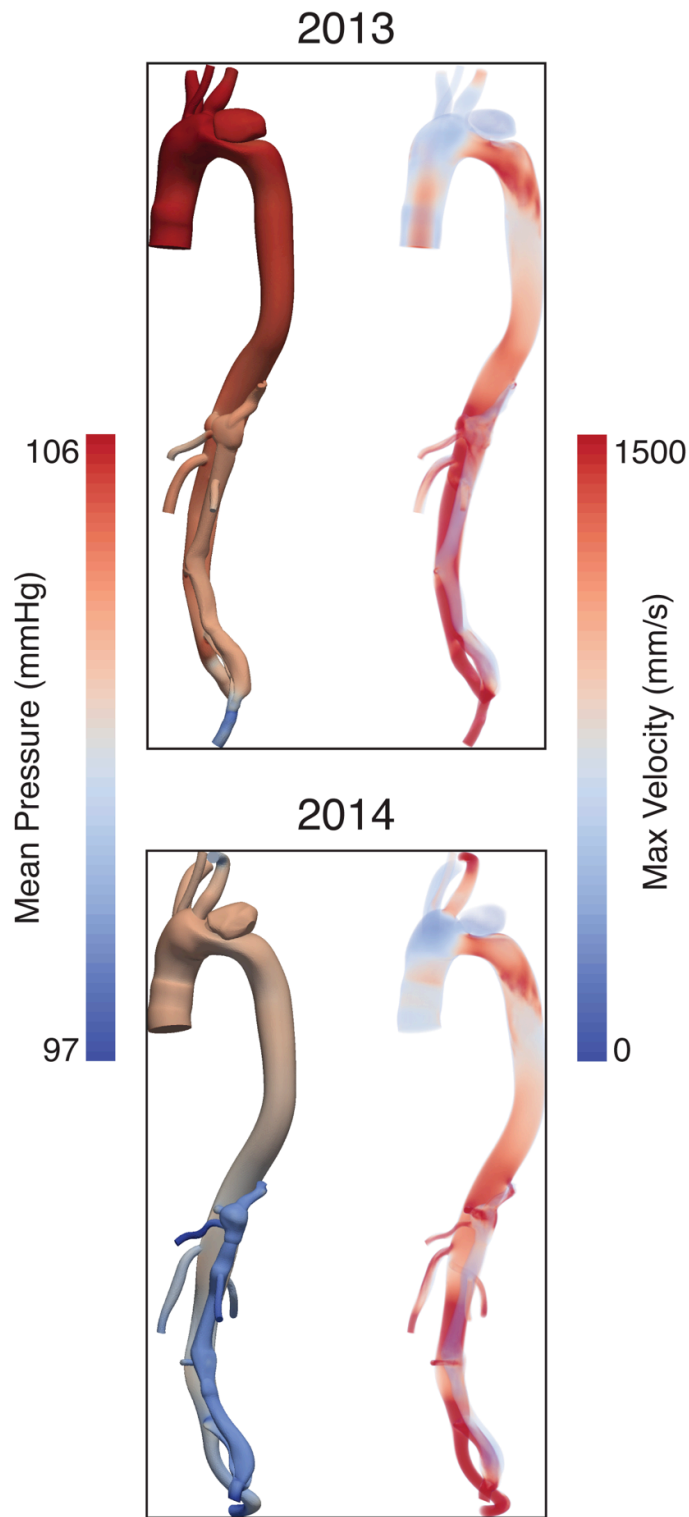


FIGURE 51 SIMULATION RESULTS FROM PATIENT 1. MEAN PRESSURE IS SHOWN ON THE LEFT AND MAXIMUM VELOCITY ON THE RIGHT. TOP: 2013 RESULTS, BOTTOM: 2014 RESULTS. OF IMMEDIATE NOTE IS THE OVERALL LOW MEAN PRESSURE THROUGHOUT THE AORTA AND IN PARTICULAR THE FALSE LUMEN DISTALLY WHEN COMPARED TO THE PREVIOUS YEAR. ADDITIONALLY A LOWER VELOCITY PROFILE IS EVIDENT IN THE AREA OF HEALED TEAR 4.

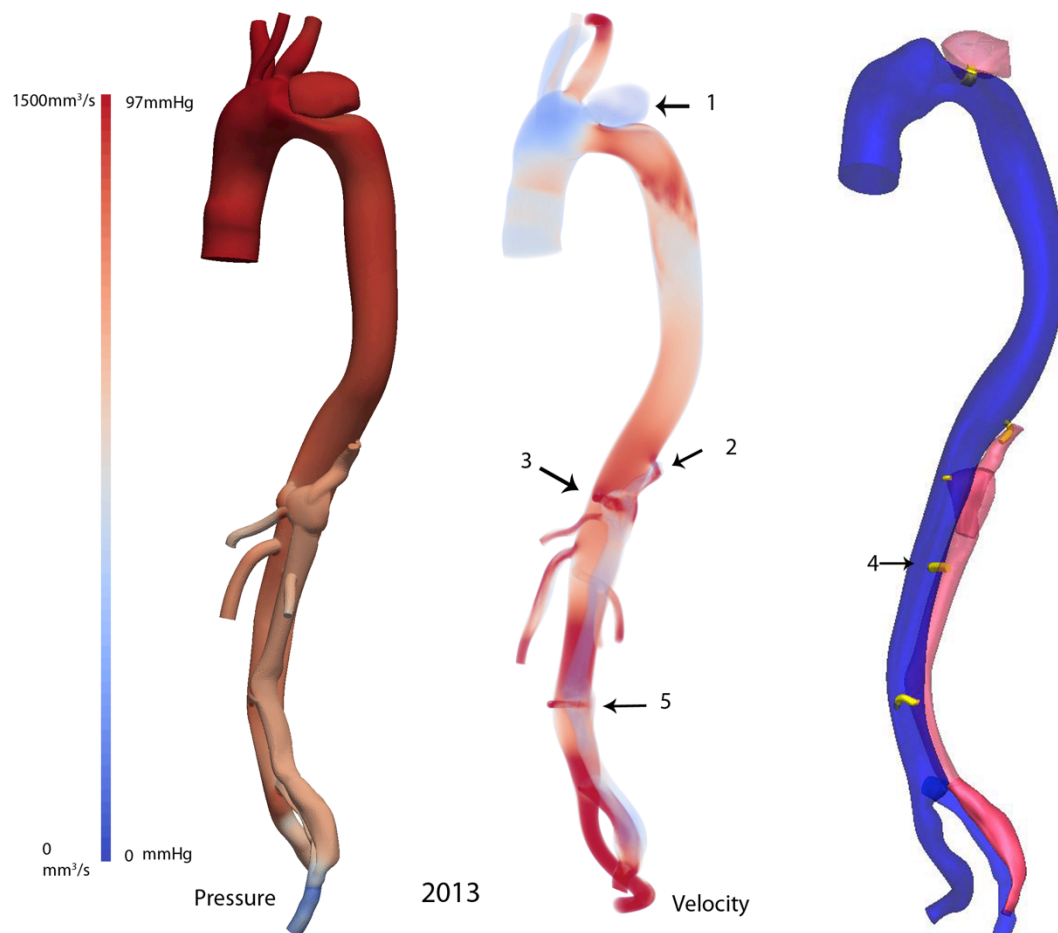


FIGURE 52 SIMULATION RESULTS FOR 2013 LEFT: PRESSURE, CENTRE: VELOCITY AND RIGHT TEAR MORPHOLOGY. OF NOTE: AREA OF TEAR 1 HAS A HIGH PRESSURE BUT LOW VELOCITY POTENTIALLY REPRESENTING A PARTIAL THROMBOSIS OF THE PROXIMAL FALSE LUMEN. TEARS 2,3 AND 5 SHOW A TURBULENT FLOW PATTERN WHEREAS TEAR 4 HAS VERY LOW IF ANY FLOW.

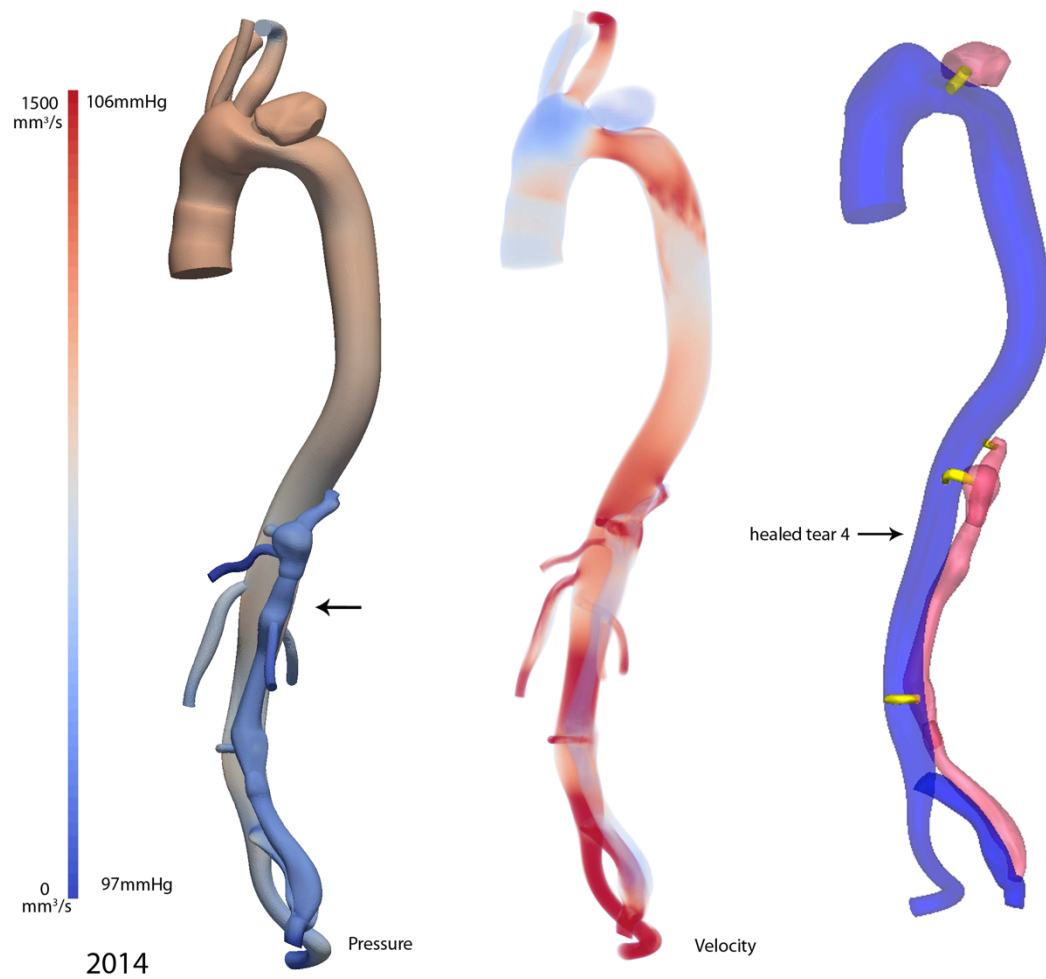


FIGURE 53 SIMULATION RESULTS FOR 2014 LEFT: PRESSURE, CENTRE: VELOCITY AND RIGHT TEAR MORPHOLOGY. OF NOTE: THE OVERALL MEAN PRESSURE SEEMS TO BE LOWER IN 2014. IN PARTICULAR THIS IS TRUE FOR THE DISTAL FALSE LUMEN. TEARS 2,3 AND 5 STILL SHOW A TURBULENT FLOW PATTERN WHEREAS TEAR 4 HAS NOW HEALED FULLY AND IS NOT SEEN IN THE CAD IMAGE ON THE RIGHT.

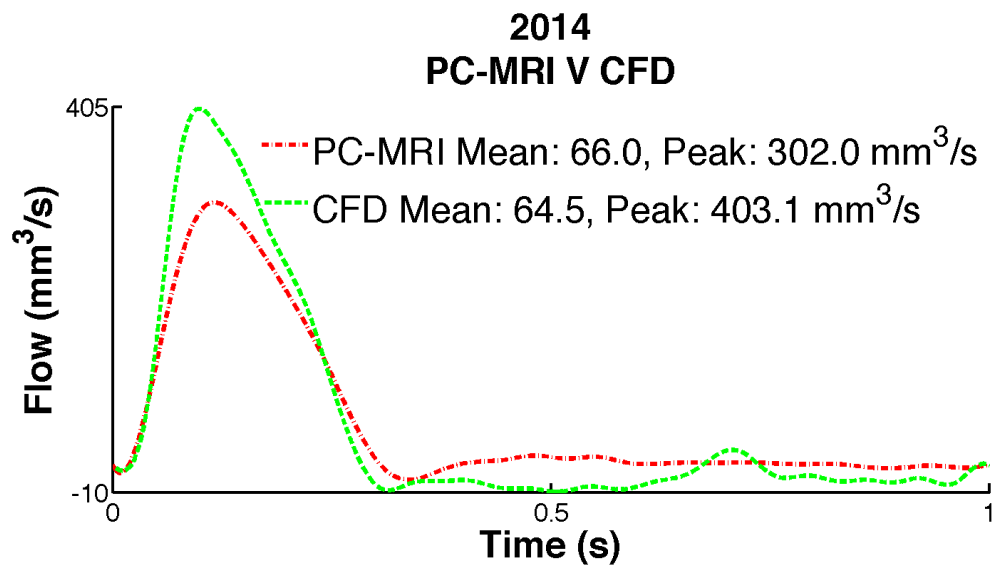
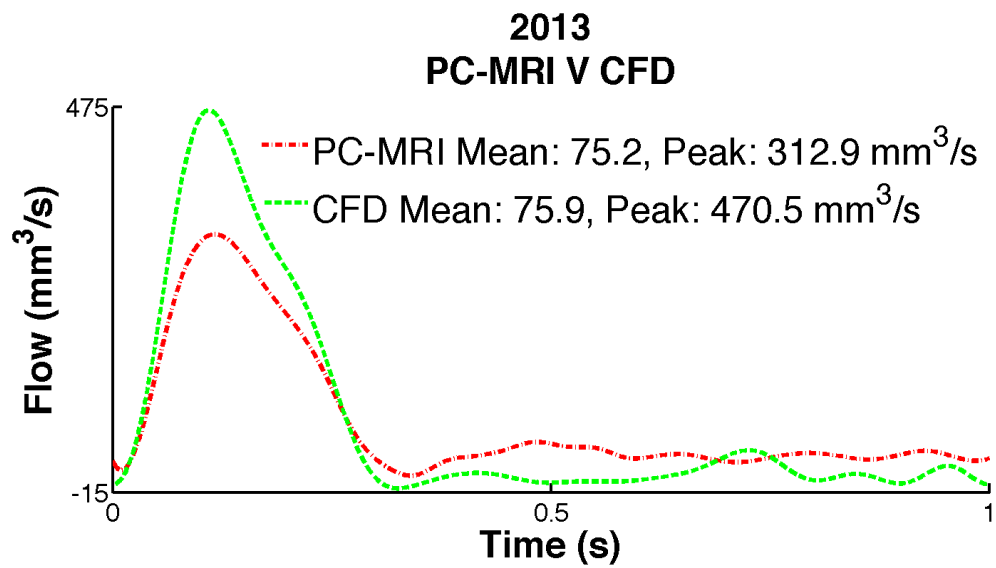


FIGURE 54 AGREEMENT BETWEEN PC-MRI AND CFD SIMULATION FLOW RESULTS FOR PATIENT 1. TOP: 2013 RESULTS. BOTTOM: 2014 RESULTS.

### 13.1.2 Follow up patient 2

In 2008, A 30 year old pregnant female at 35 weeks gestation presented to the A&E department with acute chest pain. She was diagnosed with an acute TAAD by MRI scanning and underwent emergency C-section followed by repair of the ascending aorta. She made an excellent recovery and was discharged home within the week, with regular post-operative follow up arranged. Although she presented back to the A&E up to 4 times in the next year with acute chest pain, and underwent repeated CT scanning, no abnormality was found.

This patient underwent two MRI scans one year apart and data from these along with her annual CT scans was used to develop CAD models. Simulation was not possible due to time and expense constraints. shows the completed CAD models for patient 2 and Figure 56 shows the identification of tears (yellow) and the true and false lumen geometry as seen in CRIMSON. The main point noted in these models was the lack of any thrombus despite the age of the dissection and the number of tears identified (9 tears).

Table 5 shows the volume of true and false lumens and the combined tear volume in each of the models. The combined tear volume seems to have increased slightly and that of the true lumen decreased slightly. The false lumen volume has increased marginally. Figure 57 and Figure 58 show the tear location and the true and false lumen without other branching vessels.

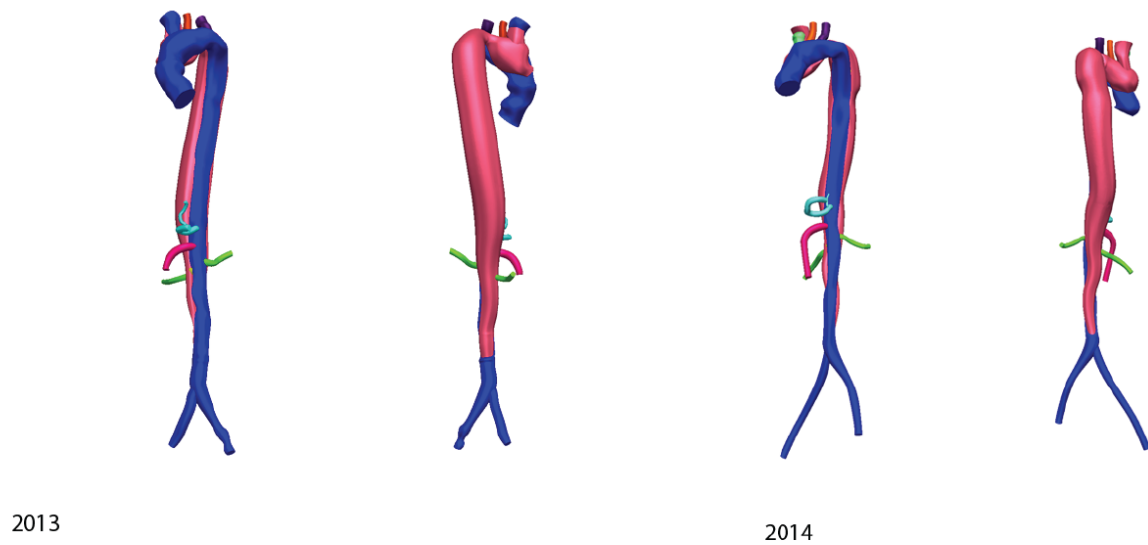


FIGURE 55 PATIENT 2. CAD MODELS OF AORTIC DISSECTION OVER THE PERIOD OF ONE YEAR. THE FALSE LUMEN IS WIDELY PATENT WITH NOT MUCH CHANGE IN SIZE OVER THE YEAR AND NO HEALING OF TEARS.

TABLE 5 VOLUME OF TRUE & FALSE LUMENS AND TEARS

Year	TL volume (mls)	FL volume (mls)	Combined tear volume (mls)
2013	104	215	1.48
2014	90	217	1.61

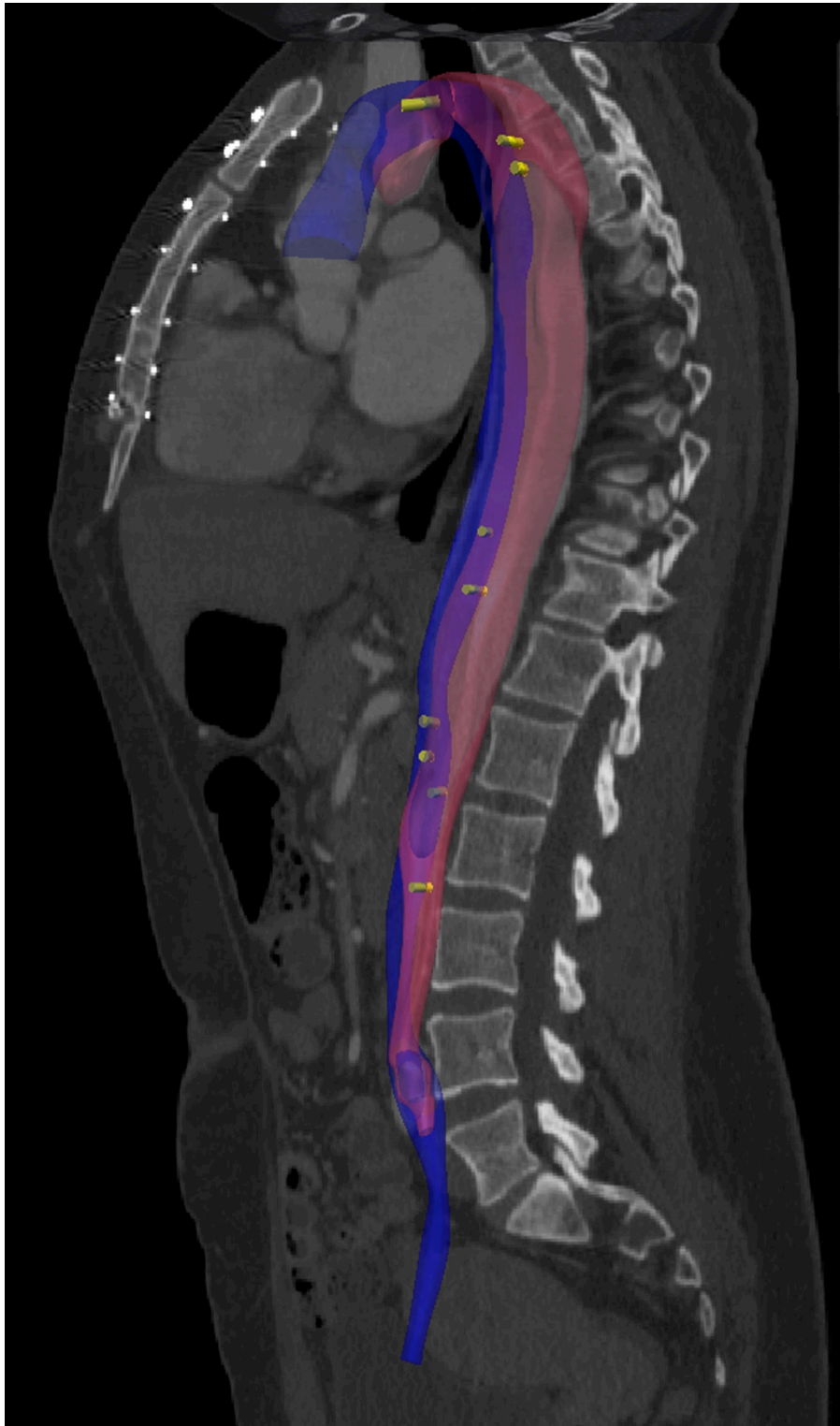
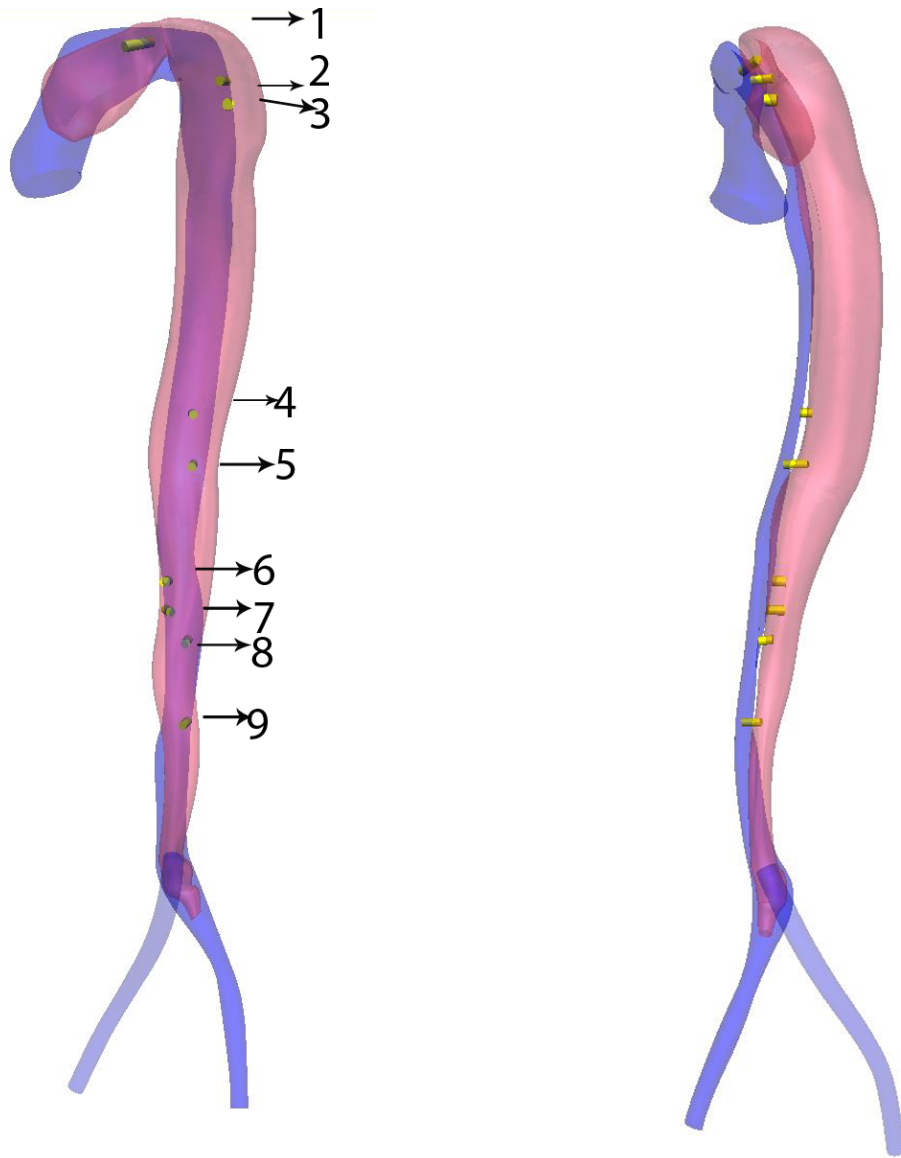


FIGURE 56 PATIENT 2. CAD MODEL DEVELOPMENT IN CRIMSON. TRUE LUMEN IS SHOWN IN BLUE, FALSE IN PINK. TEARS ARE SHOWN IN YELLOW.





2013

FIGURE 57 TEAR MORPHOLOGY FOR PATIENT 2. NINE TEARS WERE FOUND AND NO THROMBUS HAD DEVELOPED SINCE THE ORIGINAL ACUTE DISSECTION 5 YEARS AGO.

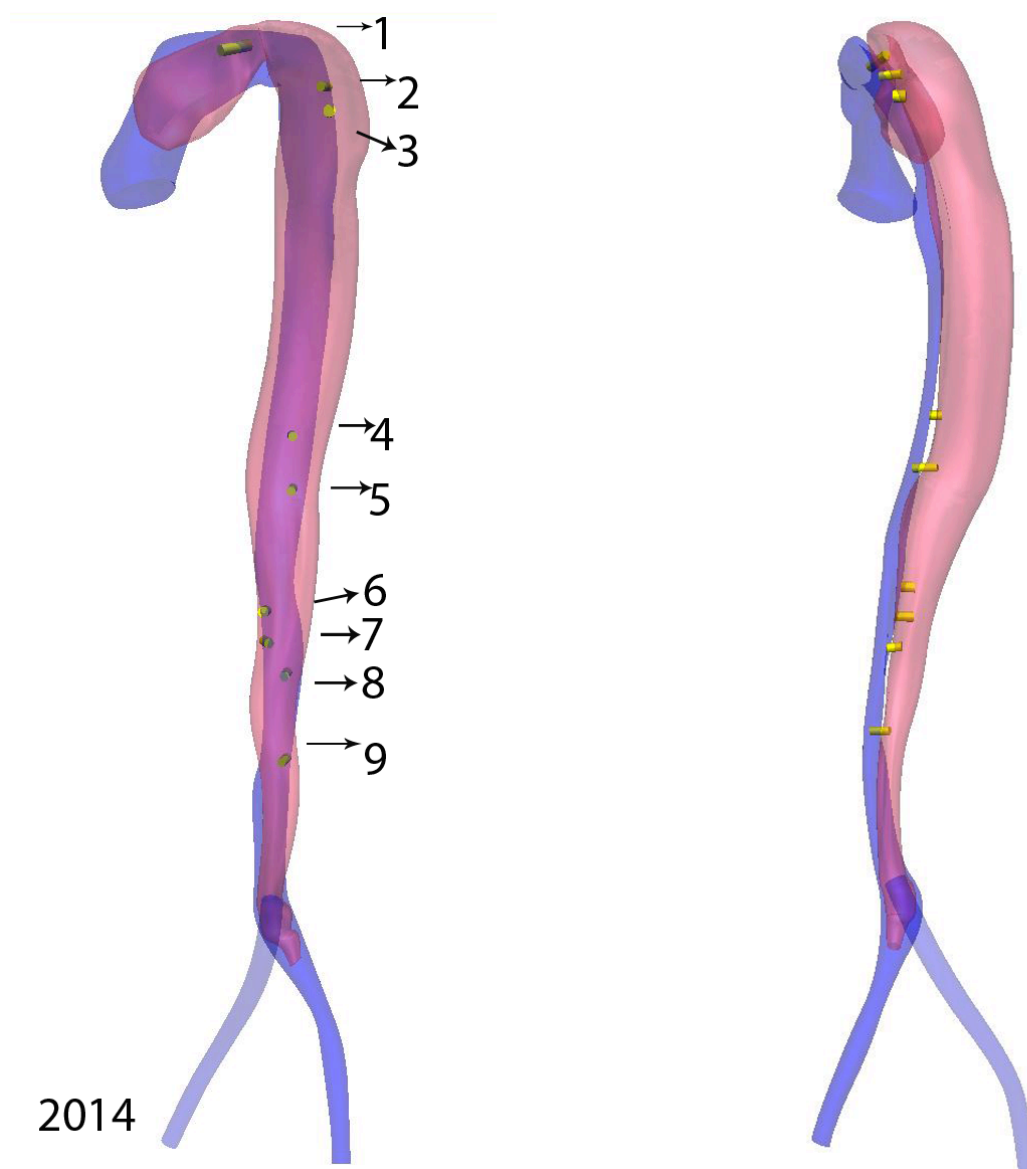


FIGURE 58 TEAR MORPHOLOGY FOR PATIENT 2. ALL 9 TEARS WERE FULLY PATENT ONE YEAR ON, WITH NO THROMBUS FORMATION.

### **13.1.3 Follow up patient 3**

The third patient was a 56 year old gentleman who presented with acute chest and back pain in 2012. Subsequent CT scanning revealed a complex acute TAAD extending into the head and neck vessels and down into the femorals. The patient underwent repair of the ascending aorta and was eventually discharged. He represented with transient ischaemic attacks but these subsided. Follow up imaging was performed on an annual basis. For this patient 2 follow up MRI scans approximately a year apart and in close proximity to the clinically requested CT scans were performed. Although simulation data has not yet been completed, the preliminary flow analysis and CAD models were developed for the baseline scan (Figure 59). This patient had an extremely complex dissection geometry making it difficult to develop accurate CAD models.

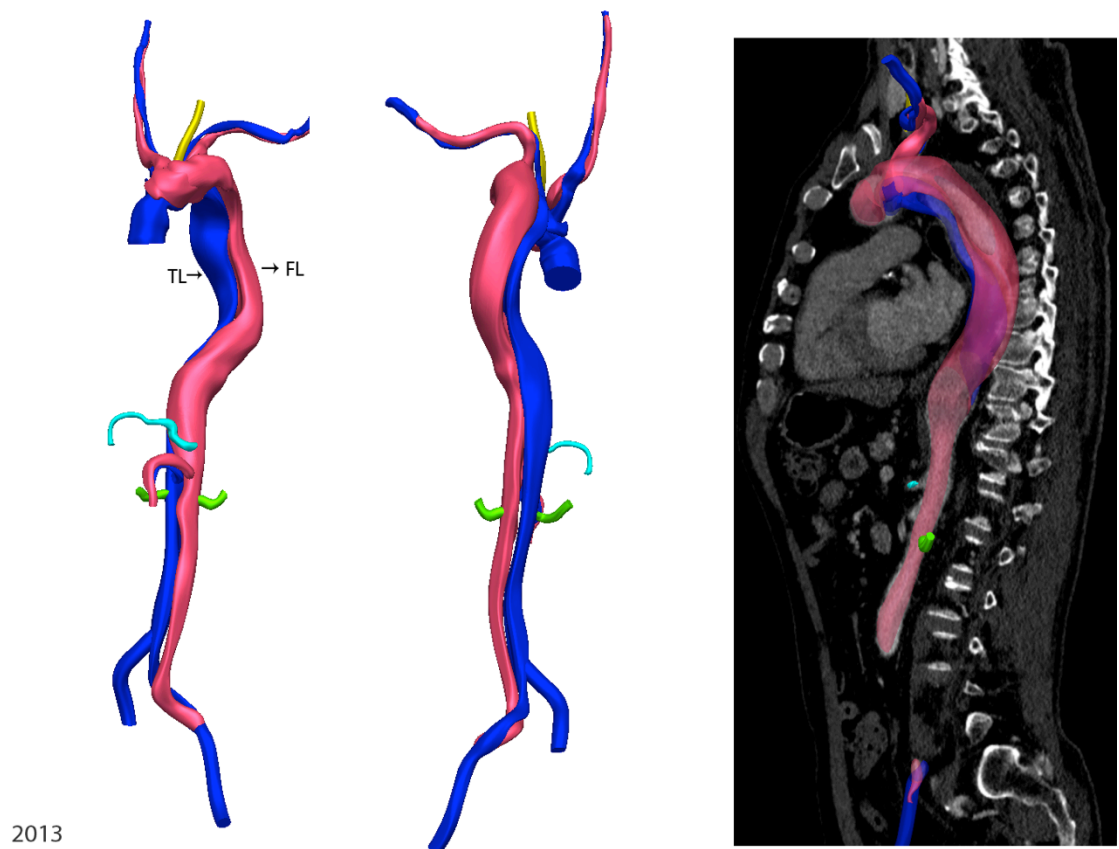


FIGURE 59 BASELINE CAD MODEL FOR PATIENT 3 AND CORRESPONDING CT SCAN. THIS WAS A COMPLEX DISSECTION EXTENDING INTO THE ARCH AND THE SUPERIOR MESENTERIC ARTERY. ACCURATE REALIZATION OF THE GEOMETRY WAS DIFFICULT AND A BLENDED MODEL WAS NOT DEVELOPED.

### **13.1.4 Follow up patient 4**

In 2012, a 54 year old gentleman presented with acute chest pain and ECG findings consistent with a non-ST elevation MI. He underwent primary percutaneous intervention to the circumflex coronary artery. At this procedure an iatrogenic TAAD occurred. The patient therefore underwent emergency surgery to repair the ascending aorta.

A CAD model was developed from the primary CT scan following on from the iatrogenic dissection and subsequent MRI scans performed in May and December of 2014. Unfortunately due to late recruitment as a result of patient unavailability no further CT scans were possible to acquire during the study period.

Nonetheless, a CAD model was developed with the intention of processing for simulation. Figure 60 shows the CAD models without and with the thrombus lofted in Figure 61 shows the identification of tears using CRIMSON. The reslice plane is seen to be moving down the aorta locating the various tears.

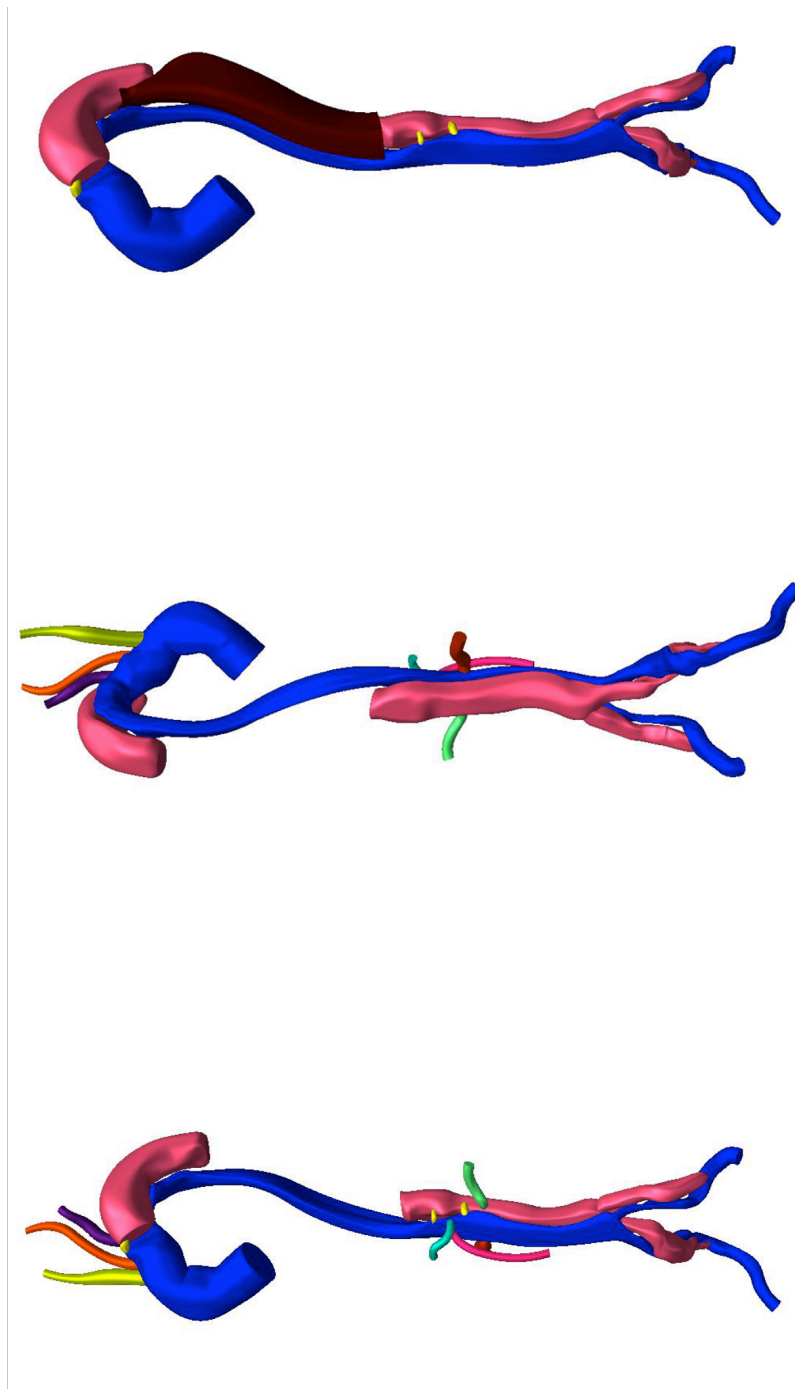


FIGURE 60 PATIENT 4. CAD MODEL OF AORTIC DISSECTION. THE PICTURE ON THE TOP SHOWS THE THROMBUS LOFTED IN (BROWN)

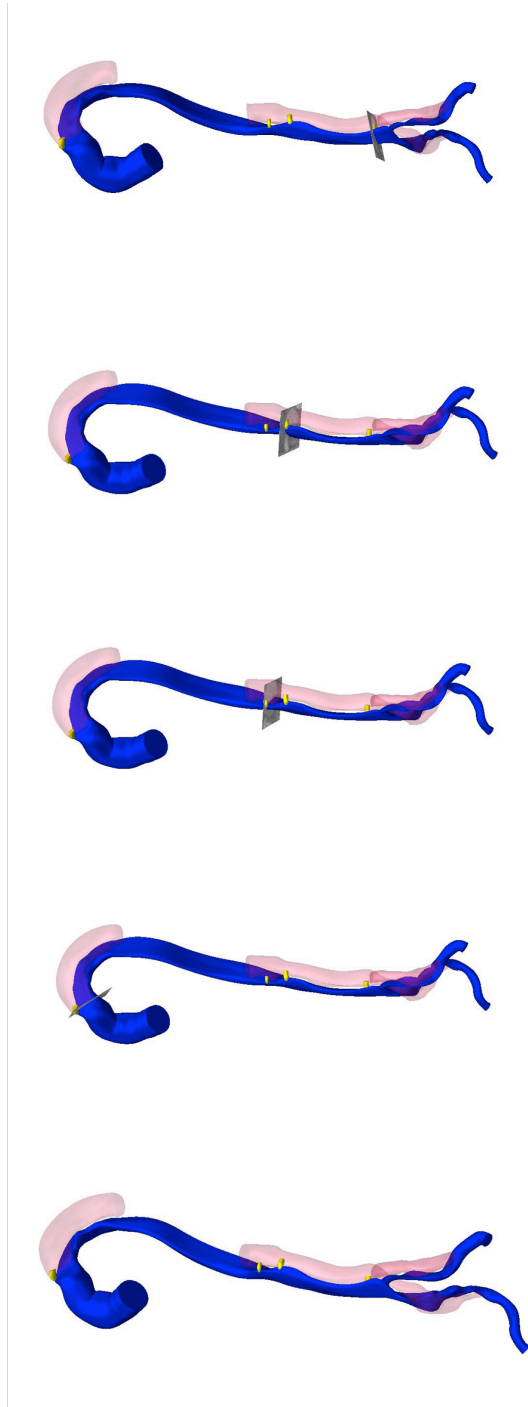


FIGURE 61 PATIENT 4. CAD MODELS SHOWING LOCATION OF TEARS (YELLOW). THERE WERE FOUR TEARS IN TOTAL.

# Chapter 14

## Results

### 14.1 Black blood study results

Three-dimensional T<sub>2</sub>IR and T<sub>2</sub>PSIR vessel wall images were successfully obtained in all 11 volunteers and two patients. Demographics of the subjects are shown in Table 6.

Representative images from three healthy volunteers, reformatted to visualize the ascending and descending aorta using the two sequences are shown in Figure 62. Visual scores by two independent raters are shown in Table 7.

The W values calculated by the Wilcoxon signed rank test for comparison for aCNR, scan time and sharpness between the two sequences at  $p < 0.05$  were zero, which were deemed statistically significant.

These results indicate that the T<sub>2</sub>PSIR sequence, although longer in duration (T<sub>2</sub>PSIR 703.7s  $\pm$  210s vs. 443.2s  $\pm$  251 s for T<sub>2</sub>IR, median 1.9 times longer), provided better quality, with improved objective and subjective image quality as ascertained by the sharpness and aCNR when compared to the T<sub>2</sub>IR sequence.

The visual score results were cross tabulated and the calculated kappa statistic for inter-rater agreement for both sequences was high, indicating good agreement between the experts, for both sequences in all volunteers. Additionally it was seen that the T<sub>2</sub>PSIR sequence performed better on the visual score across all except two subjects where it scored the same as the T<sub>2</sub>IR sequence. Figure 63 shows the images acquired using the T<sub>2</sub>PSIR sequence in two patients with a chronic TBAD, who have previously had a TAAD repair. The intimal flap is clearly visualized in both patients. Corresponding CT images are shown for visual comparison.



TABLE 6 DEMOGRAPHICS OF STUDY SUBJECTS. V= HEALTHY VOLUNTEER, P= PATIENT

Subject	Age (y)	Sex	Age Of dissection (months)	Comorbidity	Complications
V1	37	M	-	-	-
V2	38	M	-	-	-
V3	32	M	-	-	-
V4	28	M	-	-	-
V5	33	F	-	-	-
V6	34	M	-	-	-
V7	30	M	-	-	-
V8	32	M	-	-	-
V9	27	M	-	-	-
V10	25	F	-	-	-
V11	26	F	-	-	-
P1	57	M	27 months	Hypertension	Transient ischemic attack
P2	65	M	34 months	Hypertension	None

TABLE 7 VISUAL SCORE RESULTS FOR EACH OF THE SEQUENCES

Visual Score T <sub>2</sub> IR				
Rater 1	Rater 2			
VS	VS			
	1	2	3	4
1	6	2	0	0
2	0	3	0	0
3	0	0	0	0
4	0	0	0	0
Visual Score T <sub>2</sub> PSIR				
Rater 1	Rater 2			
VS	VS			
	1	2	3	4
1	1	0	0	0
2	0	2	1	0
3	0	0	3	1
4	0	0	0	3

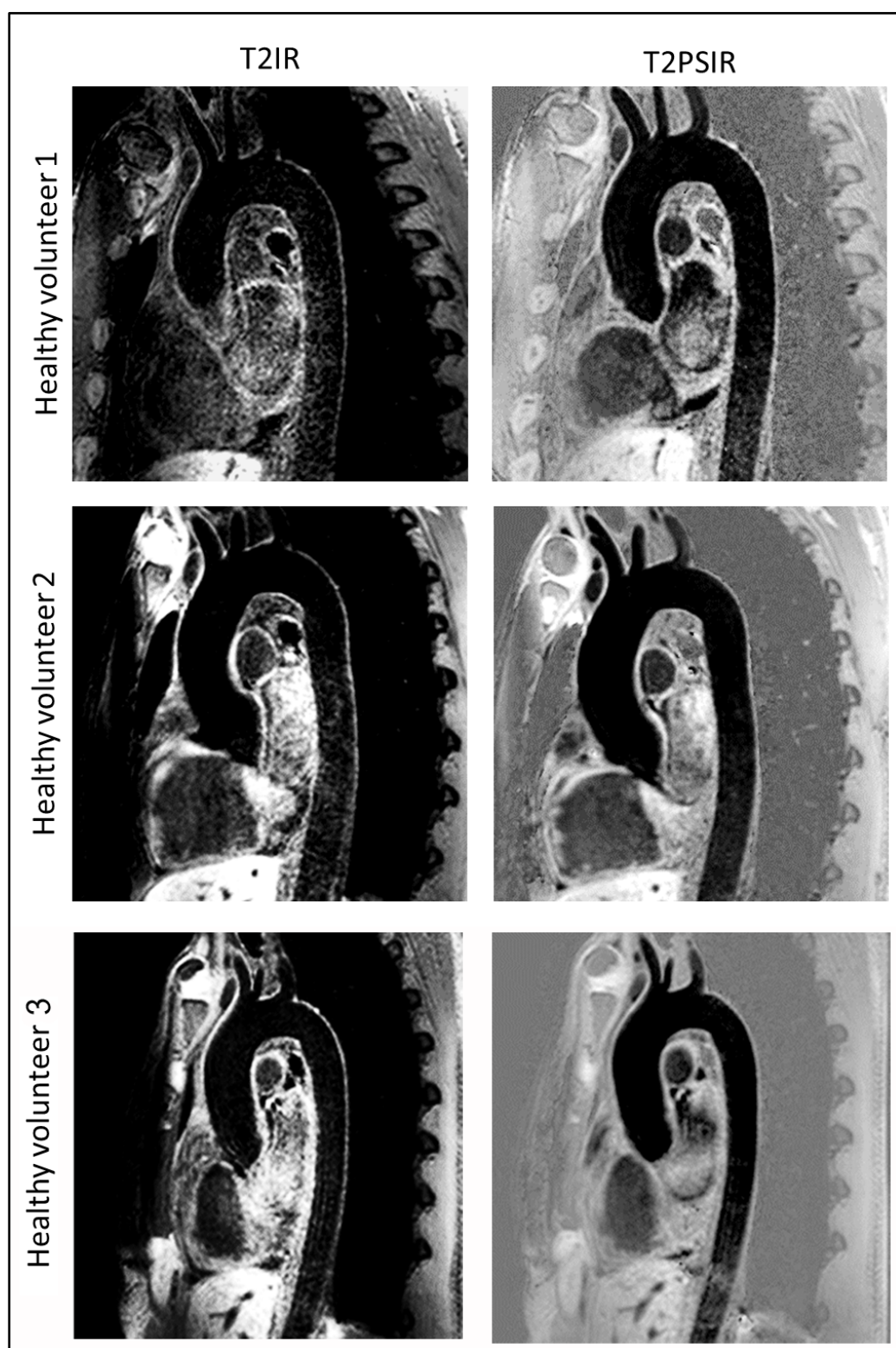


FIGURE 62 REFORMATTED IMAGES FROM THREE HEALTHY VOLUNTEERS USING  $T_2$ IR AND  $T_2$ PSIR. A CLEARER IMAGE WITH BETTER VESSEL WALL VISUALIZATION IS OBTAINED WHEN USING THE  $T_2$ PSIR SEQUENCE.

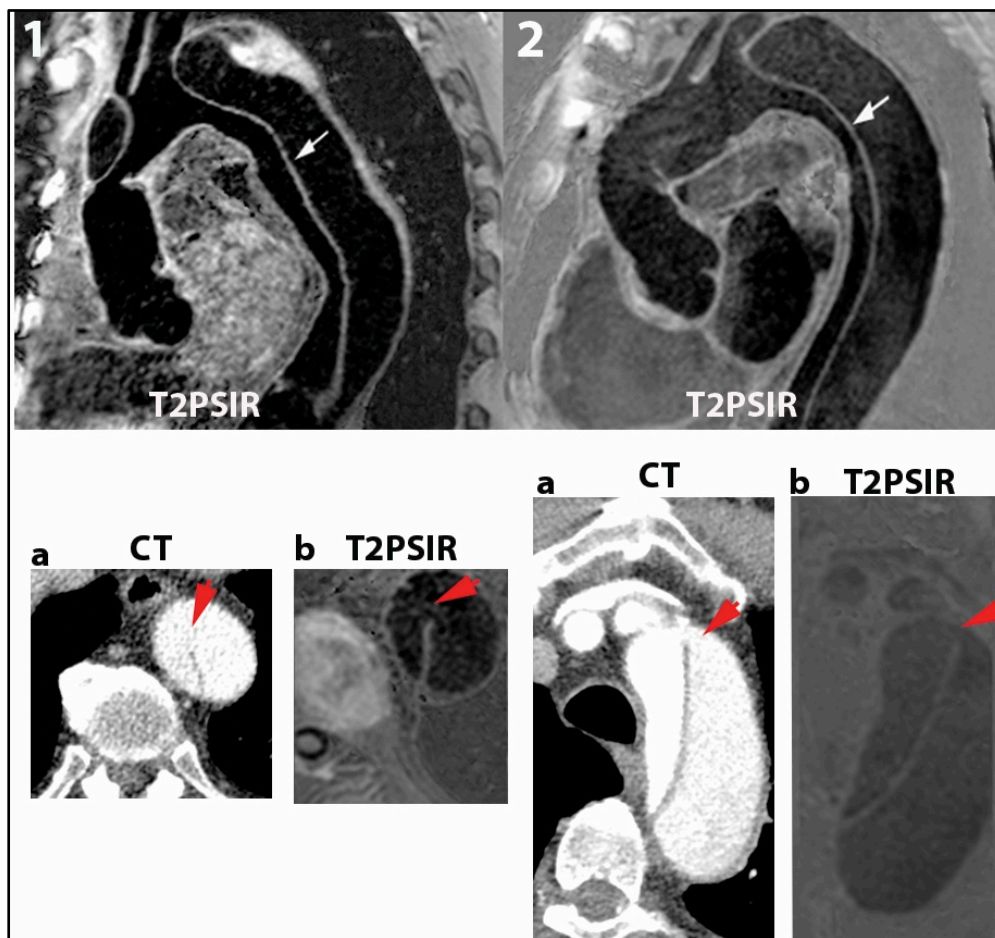


FIGURE 63 SAGITTAL SECTION IMAGES SHOWING  $T_2$ PSIR SEQUENCES PERFORMED IN TWO PATIENTS WITH CHRONIC TBAD. THE WHITE ARROWS SHOW THE POSITION OF THE INTIMAL FLAP, WHICH IS CLEARLY VISUALIZED. CROSS-SECTIONS OF EACH PATIENT'S A) CT SCAN AND B) MRI ( $T_2$ PSIR) SEQUENCE ARE SHOWN BELOW THE SAGITTAL IMAGES. THE RED ARROWS INDICATE THE POSITION OF THE INTIMAL TEAR IN EACH OF THE IMAGING MODALITIES.

# Chapter 15

## Results

### 15.1 Dual Phase results

Five healthy volunteers and two patients with repaired TAAD were recruited into the dual phase study. Demographics of the study subjects are shown in Table 8.

TABLE 8 STUDY POPULATION DEMOGRAPHICS. V=VOLUNTEER, P=PATIENT

Subject	Age (y)	Sex	Smoker	History
V1	32	F	N	-
V2	30	M	N	-
V3	29	M	N	-
V4	24	M	Y	-
V5	23	F	Y	-
P1	50		Y	TAAD with residual Type B component
P2	42		Y	TAAD with residual Type B component. Connective tissue disorder

All subjects were successfully scanned in systole and in diastole and dual phase models were created in CRIMSON for each subject. Figure 64 shows the dual phase model for one healthy volunteer (V1). For all volunteers, the aorta root moved inferiorly during systole. The motion of the left coronary artery was mapped in each healthy volunteer by picking the first coordinate in the pathline for the left coronary artery in each of the models (Figure 65). The left coronary artery was chosen as it was visible in all scans between and across the volunteers. Table 9 shows these results. In this method, the average travel for the left coronary artery in systole was 6.5mm in the horizontal direction, 4.2mm in the inferior

direction and 7.9mm in the z axis. The net motion therefore for the left coronary artery was 11.7mm.

The mean circumferential, longitudinal and volumetric strain for each volunteer was also calculated as described previously. Additionally the circumference for each chosen point was determined in CRIMSON. The change in circumference gave an indication of the change in size of the true and false lumen during the cardiac cycle.

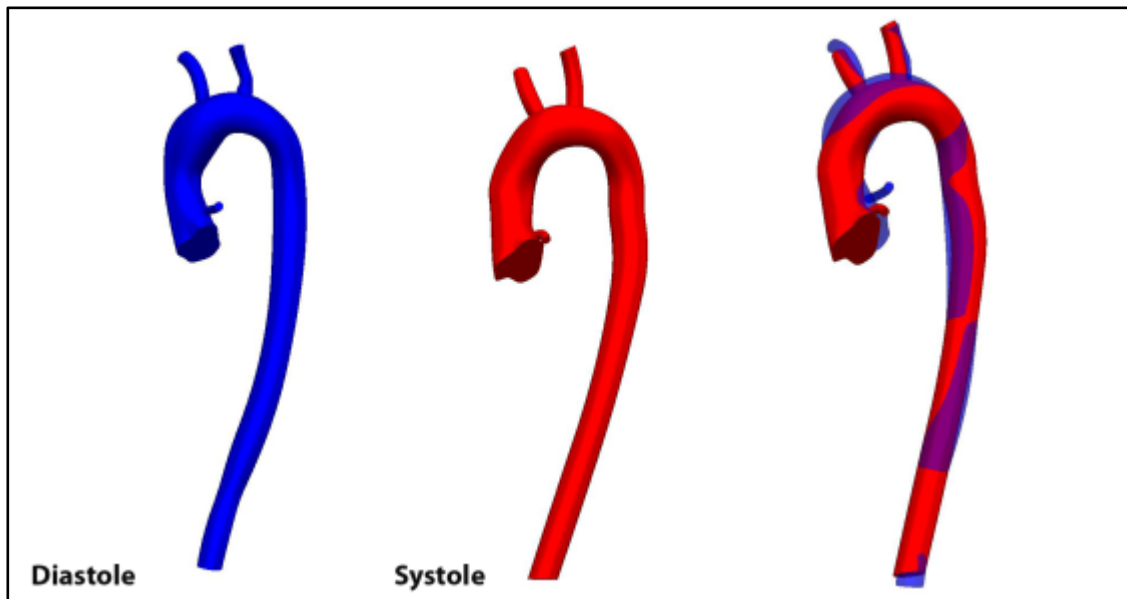


FIGURE 64 DUAL PHASE MODELS. BLUE DIASTOLE, RED, SYSTOLE. THE SUPERIMPOSED IMAGE ON THE FAR RIGHT SHOWS THE CHANGES IN AORTIC MOTION WITH THE CARDIAC CYCLE. THE AORTIC ROOT IS SEEN TO BE TRAVELLING IN THE INFERIOR-LATERAL DIRECTION DURING SYSTOLE. THIS IS DUE TO THE FORCE OF CARDIAC CONTRACTION AND TWISTING MOTION OF THE HEART.

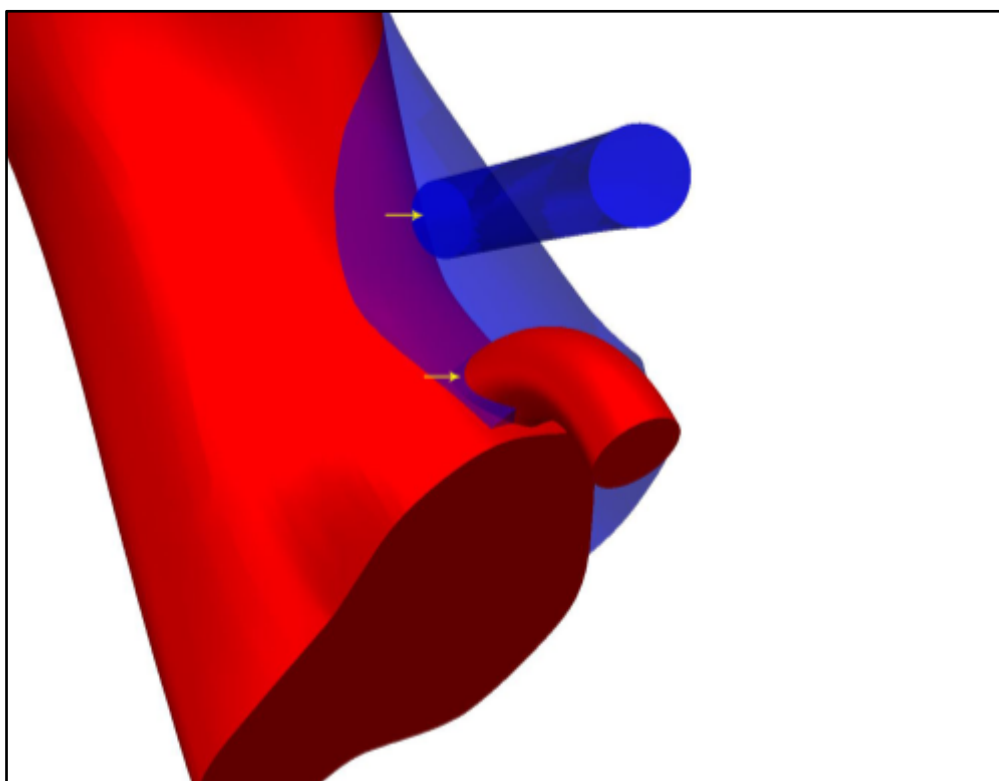


FIGURE 65 ENLARGED VERSION OF THE AORTIC ROOT OF A VOLUNTEER. HERE THE MOTION OF THE LEFT CORONARY ARTERY IS VISUALIZED AND HIGHLIGHTED BY THE YELLOW ARROWS. QUANTIFICATION OF THIS IN THE 3D FRAME WAS PERFORMED IN CRIMSON. RED= SYSTOLE, BLUE= DIASTOLE

TABLE 9 SYSTOLE AND DIASTOLE COORDINATES FOR THE LEFT CORONARY ARTERY IN 5 HEALTHY VOLUNTEERS (V). THE NET TRANSLATION IS A DIFFERENCE BETWEEN THE SYSTOLIC AND DIASTOLIC POINTS IN THE 3 SPATIAL DIRECTIONS, X, Y AND Z. THE MOTION IS A VECTOR QUANTITY IN MM.

	Systole coordinates			Net Translation			Motion	Diastole coordinates		
V	X	Y	Z	X	Y	Z	mm	X	Y	Z
1	35.94	55.69	24.25	11.4	9.33	-9.31	17.1	24.7	-46.36	-14.94
2	16.31	-43.77	-57.11	3.27	-5.47	-11.43	13.1	13.04	-38.3	-45.68
3	18.01	-21.37	14.99	4.14	-3.31	-9.96	11.3	13.87	-18.06	24.95
4	22.34	-57.83	-37.83	6.39	-2.71	-3.95	7.9	15.95	-55.12	-33.88
5	20.23	-36.53	-46.72	7.26	-0.17	-4.64	8.6	12.97	-36.36	-42.08



### 15.1.1 Circumferential change: volunteers

The average circumferential change in the aorta between systole and diastole by volunteer was 7.9%. Circumferential change by location along the aorta by volunteer is shown in Figure 66 along with a mean change for each location. As can be seen, almost uniformly, overall the greatest change in circumference occurred at the left coronary artery and the least in the descending aorta. The mean change in circumference decreased along the length of the aorta. This is likely due to the relative rigidity of the descending aorta due to fixation to the spine and the tethering effect of the intercostal arteries. Subject 4 was an outlier, showing the greatest variation in circumference at the level of the left common carotid artery.

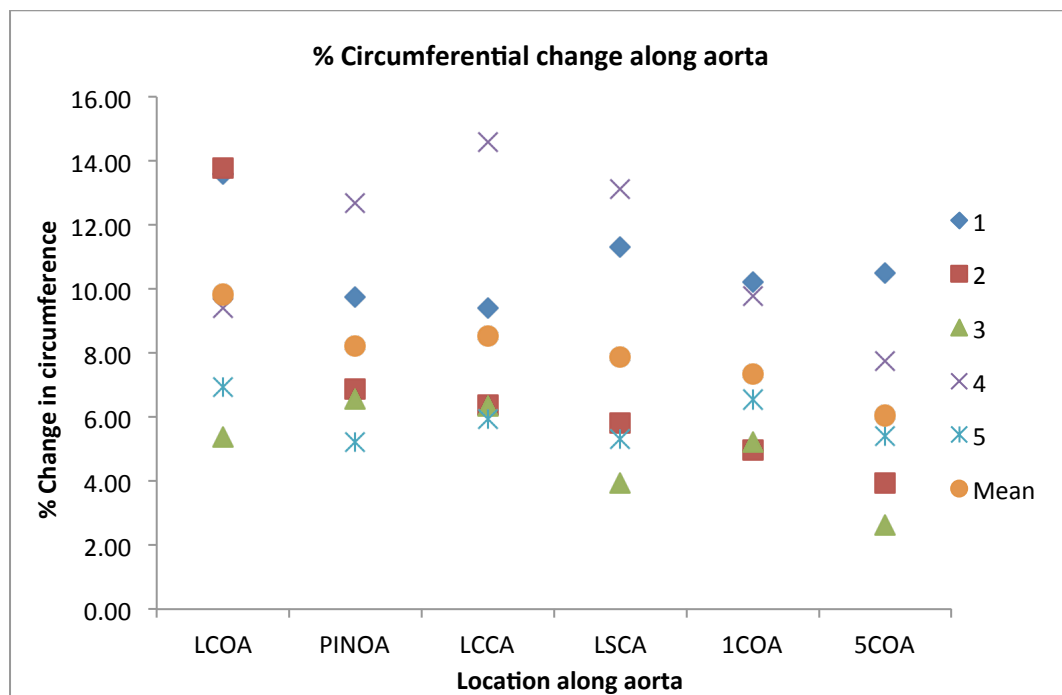


FIGURE 66 PERCENTAGE CIRCUMFERENTIAL CHANGE ALONG THE AORTIC LENGTH BY VOLUNTEER. MEAN VALUES ARE SHOWN IN ORANGE.

## 15.1.2 Circumferential change: patients

For the dissection patients the true and false lumen changes were plotted according the cardiac phase.

### ***15.1.2.1 Patient A***

Figure 67 and Figure 68 for patient A shows a trend for the true lumen to expand in systole and collapse in diastole. The false lumen collapsed in systole for all locations except in the region of the descending aorta at the level of the 1<sup>st</sup> and 5<sup>th</sup> intercostal arteries. Here the false lumen was overall larger in size than the true lumen at both locations and furthermore it increased in circumference in the systolic phase. The false lumen at the level of the LSCA remained approximately the same. These results are shown in Table 10.

Although the TL at 1<sup>st</sup> COA in systole was 40% smaller than the false lumen, in diastole this was 53% smaller. In systole at the 5<sup>th</sup> COA the TL was 20% smaller and in diastole it was 30% smaller. The largest change in circumference was seen in the TL in systole at the level of the 1<sup>st</sup> COA which increased by 30%.

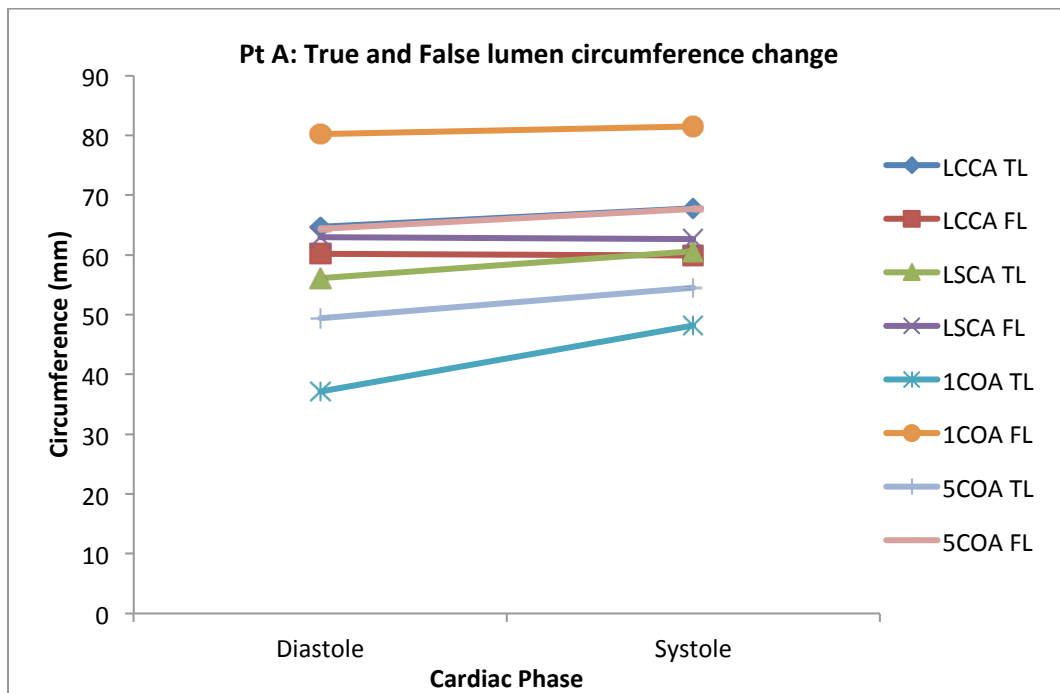


FIGURE 67 TRUE AND FALSE LUMEN CIRCUMFERENTIAL CHANGE FOR DISSECTION PATIENT A

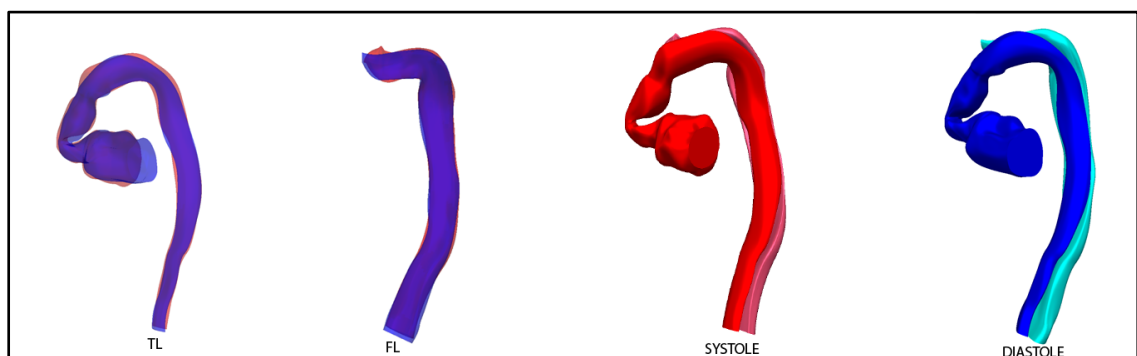


FIGURE 68 DISSECTION PATIENT A. THE MODELS ON THE LEFT SHOW THE TRUE AND FALSE LUMENS CHANGES BETWEEN SYSTOLE AND DIASTOLE. TRUE LUMEN IS SHOWN IN BLUE, FALSE IN PINK. THE FIGURES TO THE RIGHT SHOW THE OVERALL AORTIC CHANGES BETWEEN SYSTOLE AND DIASTOLE

TABLE 10 PATIENT A CIRCUMFERENTIAL CHANGE AND THEREFORE MOTION OF THE INTIMAL FLAP IN THE AORTA DURING THE CARDIAC CYCLE.

Location	Circumference in Diastole mm	Circumference in Systole mm	Change in circumference from diastole to systole	% change in FL compared to TL in diastole	% change in FL compared to TL in systole
LCCA TL	64.7	67.8	3.1	-7.5%	-7.9%
LCCA FL	60.2	59.9	-0.3		
LSCA TL	56.1	60.6	4.5	10.9%	2%
LSCA FL	63	62.6	-0.4		
1st COA TL	37.1	48.2	11.1	54%	33%
1st COA FL	80.2	81.5	1.3		
5th COA TL	49.4	54.5	5.1	30%	13.2%
5th COA FL	64.3	67.7	3.4		

### 15.1.2.2 Patient B

For patient B, there was a trend for the TL to expand in systole and collapse in diastole except for at the region of the 1<sup>st</sup> intercostal artery where the TL remained the same (Figure 69, Figure 70) The largest change of any kind was seen in the LSCA FL which was compressed by 28% in systole. The LSCA FL in diastole is 31% smaller than the LSCA TL and in systole the FL collapses significantly, the TL more than doubling in size. These results are shown in Table 10.

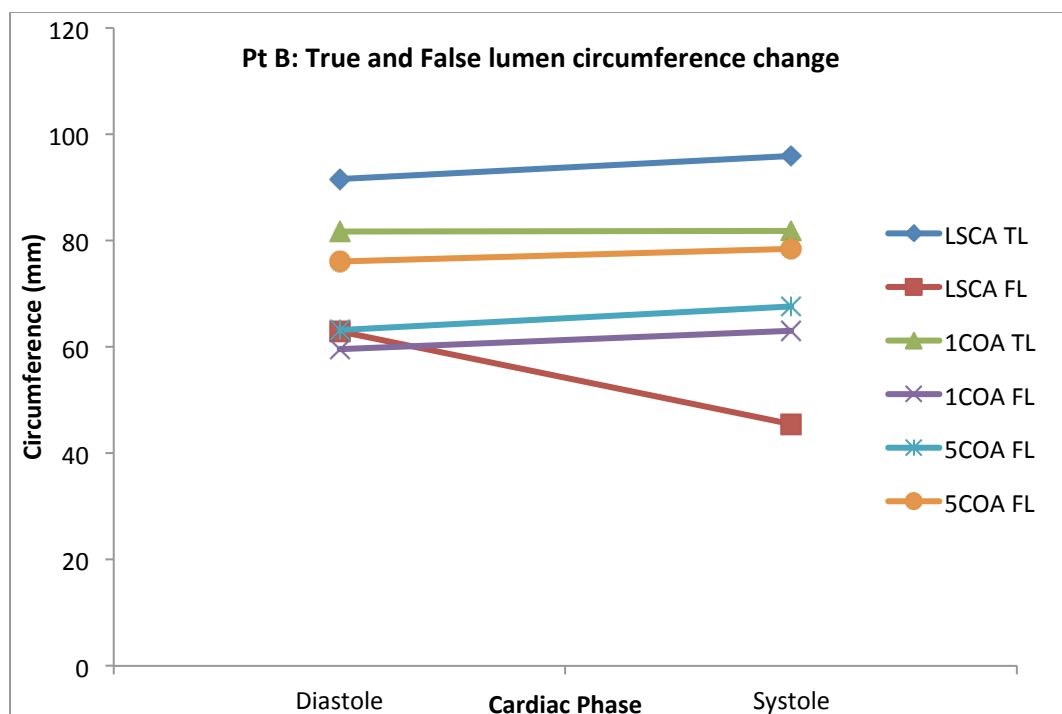


FIGURE 69 TRUE AND FALSE LUMEN CIRCUMFERENTIAL CHANGE FOR DISSECTION PATIENT B

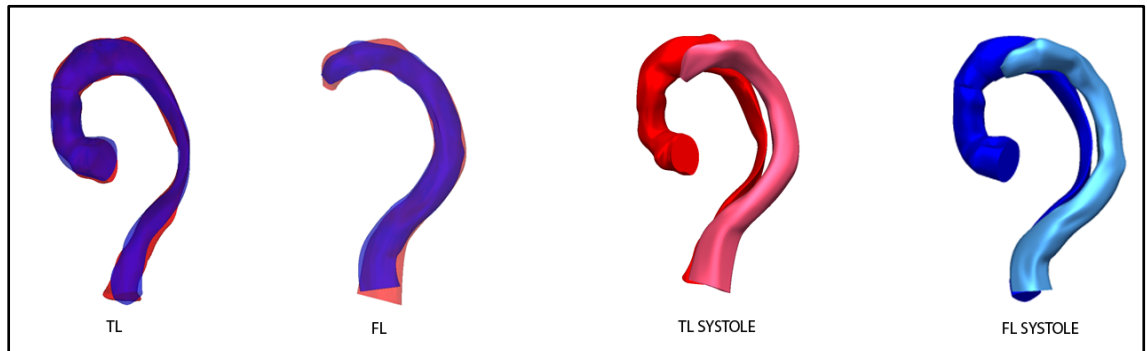


FIGURE 70 DISSECTION PATIENT B. THE MODELS ON THE LEFT SHOW THE TRUE AND FALSE LUMENS CHANGES BETWEEN SYSTOLE AND DIASTOLE. TRUE LUMEN IS SHOWN IN BLUE, FALSE IN PINK. THE FIGURES TO THE RIGHT SHOW THE OVERALL AORTIC CHANGES BETWEEN SYSTOLE AND DIASTOLE.

TABLE 11 PATIENT B CIRCUMFERENTIAL CHANGE AND THEREFORE MOTION OF THE INTIMAL FLAP IN THE AORTA DURING THE CARDIAC CYCLE.

Location	Circumference in Diastole mm	Circumference in Systole mm	Change in circumference from diastole to systole	% difference in FL compared to TL in diastole	% difference in FL compared to TL in systole
LSCA TL	91.6	96.0	4.8	-31.3	-111.0
LSCA FL	62.9	45.5	-27.7		
1st COA TL	81.7	81.9	0.2	-37.1	-30%
1st COA FL	59.6	63.1	5.8		
5th COA TL	63.2	67.6	6.9	16.9	13.9
5th COA FL	76.1	78.5	3.2		

### **15.1.3 Aortic strain: healthy volunteers**

As seen in the healthy volunteers, the mean longitudinal strain experienced was maximal in the aortic arch at 13.2%, 4.2% in the ascending aorta and -1.5% in the descending aorta. The circumferential strain at each chosen location was highest at the level of left coronary artery and lowest at the distal descending aorta at 6.3% (Figure 71). Finally the mean volumetric strain for the ascending aorta was in the region of 24%, 29% at the arch and 16.7% in the descending aorta. Figure 72 shows the changes in the aortic strain by location in one healthy subject.

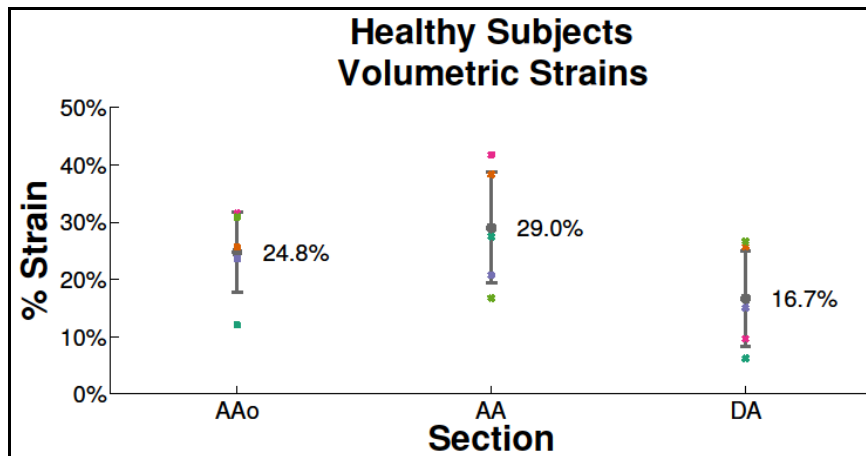
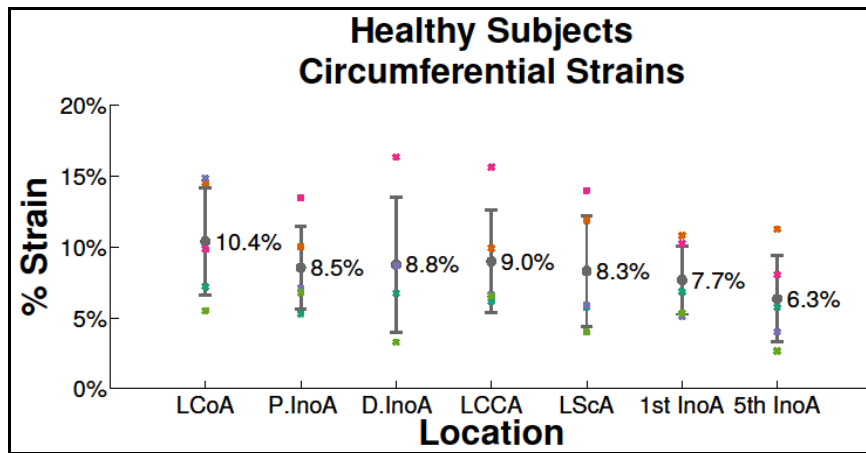
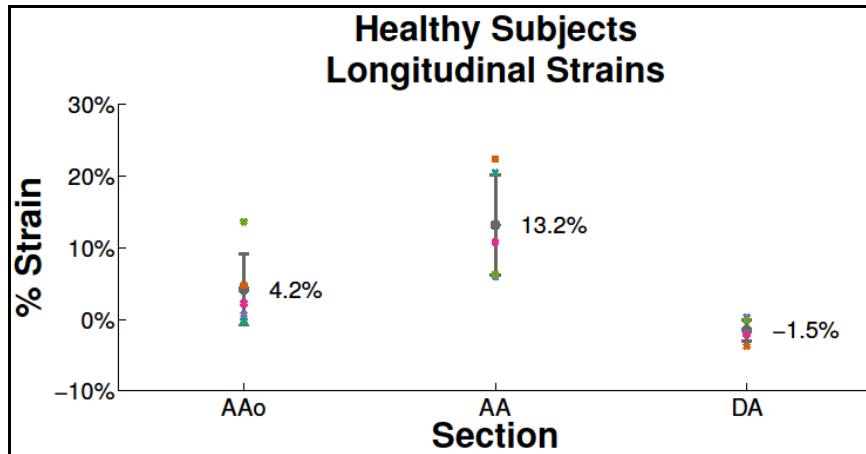


FIGURE 71 HEALTHY SUBJECTS STRAINS. TOP: LONGITUDINAL STRAIN, CENTRE: CIRCUMFERENTIAL STRAIN AND BOTTOM: VOLUMETRIC STRAIN, GREY BARS INDICATE THE STANDARD DEVIATION AND THE MEAN VALUES ARE SHOWN IN THE GREY CIRCLES.



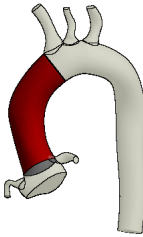
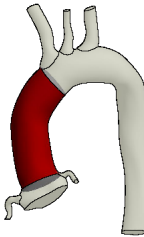
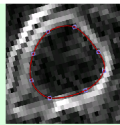
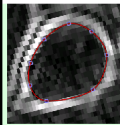
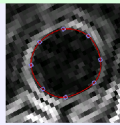
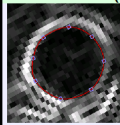
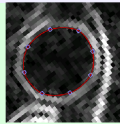
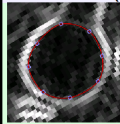
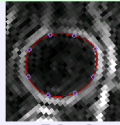
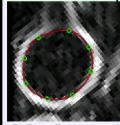
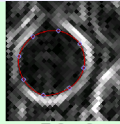
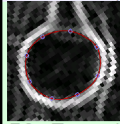
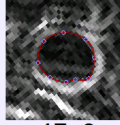
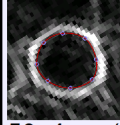
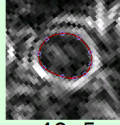
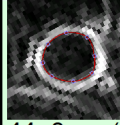
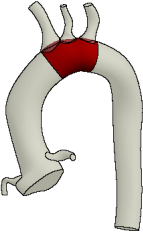
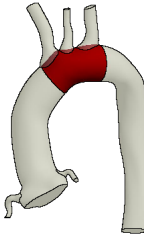
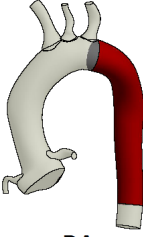
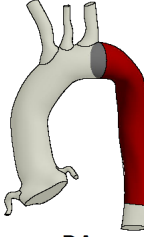
Diastole	Systole	Diastole	Systole
 <p><b>AAo</b> Vol 15.6ml CL 59.4mm</p>	 <p><b>AAo</b> Vol 17.5ml (+12.1%) CL 59.2mm (-0.3%)</p>	<p>LCoA</p>  <p>63.3mm</p>  <p>67.7mm (+7.2%)</p>	
		<p>P.InoA</p>  <p>59.6mm</p>  <p>62.7mm (5.3%)</p>	
		<p>D.InoA</p>  <p>60.3mm</p>  <p>64.2mm (+6.7%)</p>	
		<p>LCCA</p>  <p>58.8mm</p>  <p>62.3mm (+6.2%)</p>	
		<p>LSCA</p>  <p>56.6mm</p>  <p>59.7mm (+5.8%)</p>	
		<p>1st ICoA</p>  <p>47.3mm</p>  <p>50.4mm (+6.8%)</p>	
		<p>5th ICoA</p>  <p>42.5mm</p>  <p>44.8mm (+5.7%)</p>	
 <p><b>AA</b> Vol 6.1ml CL 23.7mm</p>	 <p><b>AA</b> Vol 7.8ml (+27.5%) CL 28.2mm (+20.5%)</p>		
 <p><b>DA</b> Vol 16.0ml CL 95.6mm</p>	 <p><b>DA</b> Vol 17.0ml (+6.2%) CL 93.8mm (-1.9%)</p>		

FIGURE 72 AORTIC STRAIN AS MEASURED IN DIFFERENT SEGMENTS OF THE AORTA DURING DIASTOLE AND SYSTOLE. VOL= VOLUMETRIC STRAIN, CL= CENTRELINE (LONGITUDINAL) STRAIN OF NOTE THE ARCH OF THE AORTA (AA) DEMONSTRATES THE LARGEST VOLUMETRIC AND CIRCUMFERENTIAL STRAIN. CONVERSELY, THE DESCENDING AORTA (DA) EXPERIENCES A COMPRESSIVE STRAIN AS DOES THE ASCENDING AORTA (AA)

## 15.1.4 Aortic strain: dissection patients

### 15.1.4.1 Patient A

The geometry and results for patient A are shown in Figure 73. Volumetric and longitudinal deformations are shown on the left and the image reslices with the aortic circumference at each branching location on the right.

Patient A demonstrated a volumetric strain of 32% in the AAo, 11.2% in the TL and 7.6% in the FL at the level of the arch and a strain of 44.2% in the TL of the DA. The FL of the DA showed a compressive or negative strain of 7.4%.

The longitudinal strain in the AAo (+13.6 %) was larger than that the mean strain observed in the healthy subjects. A compressive longitudinal strain was observed in the AA (-5.1 % in the TL and -5.6 % in the FL). In the DA, the FL experienced a positive longitudinal strain (+12.8 %) while the TL experienced a compressive strain (-1.3 %). Circumferential strain was found to be within the same range as the healthy subjects in the AAo. In the dissected regions of the AA and DA large circumferential strain were noted.

### 15.1.4.2 Patient B

The geometry and results for patient B are shown in Figure 74. Volumetric and longitudinal deformations are shown on the left and the image reslices with the aortic circumference at each branching location on the right.

Patient B also demonstrated significantly greater volumetric strain in AAo (+19.5%) than in AA (TL: +1.6 % FL: -11.9 %). There was a positive volumetric strain in the DA (TL: +6.6 % FL: +8.0%). A positive longitudinal strain was seen in the AAo (+19.5 %) Longitudinal strain was compressive in the AA TL (-2.3 %) and a positive strain was seen in the FL (+15.7 %) (although this section of FL only represents 3.5 % of the total AA volume in systole). In the

DA the TL demonstrates a negligible longitudinal strain (0.1%) while the FL saw a +1.8% strain.

Circumferential strains observed in the AA at D.InoA (3.9%) and LCCA (4.1%) are significantly lower than those seen in the AAo at LCoA (14.2 %) and P.InoA (7.1%). The TL expansion was seen to have a significant influence on the FL, causing it to collapse in places such as at the LSCA where a large compressive circumferential strain (-23.8%) was observed in the FL.

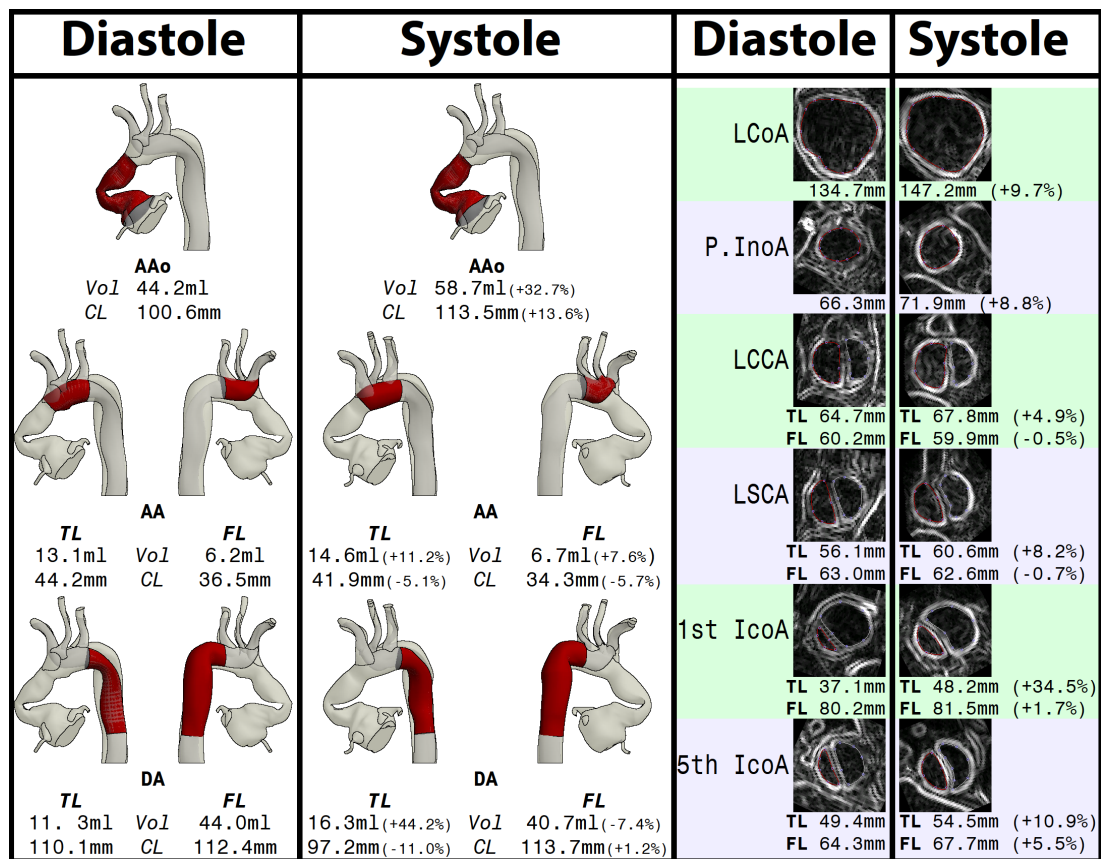


FIGURE 73 PATIENT A AORTIC STRAIN AND MORPHOLOGICAL CHANGES BY LOCATION. THE PANEL ON THE LEFT MIDDLE SHOW SEGMENTATIONS AND CALCULATED VOLUME (VOL) AND LONGITUDINAL (CL) STRAIN IN DIASTOLE AND SYSTOLE. THE PANEL ON THE RIGHT SHOWS THE IMAGE RESLICES AT THE CHOSEN POINTS OF INTEREST SHOWING VESSEL CONTOUR CIRCUMFERENCE AND CIRCUMFERENTIAL CHANGE.



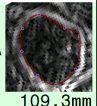
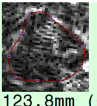


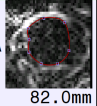
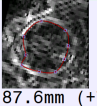


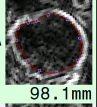
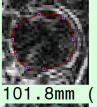
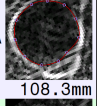
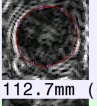
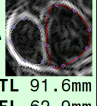
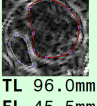
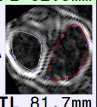
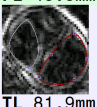
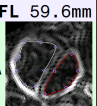
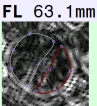
Diastole	Systole	Diastole	Systole
 <p><b>AAo</b> Vol 39.7ml CL 66.5mm</p>	 <p><b>AAo</b> Vol 47.5ml (+19.5%) CL 66.5mm (+19.0%)</p>	<p>LCoA</p>  <p>109.3mm</p>  <p>123.8mm (+14.2%)</p>	
 <p><b>DA</b></p>	 <p><b>DA</b></p>	<p>P.InoA</p>  <p>82.0mm</p>  <p>87.6mm (+7.1%)</p>	
 <p><b>AA</b></p>	 <p><b>AA</b></p>	<p>D.InoA</p>  <p>98.1mm</p>  <p>101.8mm (+3.9%)</p>	
<p><b>TL</b> 41.1ml <b>FL</b> 52.3mm</p>	<p><b>TL</b> 41.8ml (+1.6%) <b>FL</b> 51.1mm (-2.3%)</p>	<p>LCCA</p>  <p>108.3mm</p>  <p>112.7mm (+4.1%)</p>	
<p><b>TL</b> 56.9ml <b>FL</b> 177.3mm</p>	<p><b>TL</b> 60.6ml (+6.6%) <b>FL</b> 179.0mm (+0.1%)</p>	<p>LSCA</p>  <p>TL 91.6mm FL 62.9mm</p>  <p>TL 96.0mm (+4.8%) FL 45.5mm (-23.8%)</p>	
<p><b>TL</b> 56.9ml <b>FL</b> 177.3mm</p>	<p><b>TL</b> 60.6ml (+6.6%) <b>FL</b> 179.0mm (+0.1%)</p>	<p>1st IcoA</p>  <p>TL 81.7mm FL 59.6mm</p>  <p>TL 81.9mm (+0.2%) FL 63.1mm (+6.2%)</p>	
<p><b>TL</b> 56.9ml <b>FL</b> 177.3mm</p>	<p><b>TL</b> 60.6ml (+6.6%) <b>FL</b> 179.0mm (+0.1%)</p>	<p>5th IcoA</p>  <p>TL 63.2mm FL 76.1mm</p>  <p>TL 67.6mm (+7.3%) FL 78.5mm (+3.2%)</p>	

FIGURE 74 PATIENT B AORTIC STRAIN AND MORPHOLOGICAL CHANGES BY LOCATION. THE PANEL ON THE LEFT MIDDLE SHOW SEGMENTATIONS AND CALCULATED VOLUME (VOL) AND LONGITUDINAL (CL) STRAIN IN DIASTOLE AND SYSTOLE. THE PANEL ON THE RIGHT SHOWS THE IMAGE RESLICES AT THE CHOSEN POINTS OF INTEREST SHOWING VESSEL CONTOUR CIRCUMFERENCE AND CIRCUMFERENTIAL CHANGE.

# Chapter 16

## Discussion

### 16.1 Follow up study

Currently, the main criteria that prompt intervention in chronic dissections are size ( $>5.5\text{cm}$ ), rapid growth ( $>1\text{cm/y}$ ), the presence of complications such as organ malperfusion the presence of symptoms such as pain. The follow up currently for stable dissection patients in the UK is by CT scanning, and this occurs on an annual basis.

Although only three patients underwent yearly follow up, simulation results from only one have been developed. Nonetheless, just evaluating the differences in geometry between the three patients gives an indication of how each patient presents a unique pathological process and problem. Lumping these to fit a one-size-for-all management strategy seems inadequate. An individualized approach tailored to the patients requirements and based on the patient's geometry and haemodynamics would be more relevant and more physiologically accurate whereby decisions to intervene are based on haemodynamic parameters and dynamic aortic morphology rather than Patient 1 underwent yearly follow up as well as a CFD simulation to assess the changes in aortic haemodynamics from baseline to the follow up. The main morphological change that was observed in this patient was a healing of tear 4 in the infradiaphragmatic region. Nonetheless there was no change in the volume of thrombus albeit no change in the size of the aorta of the false lumen either. This means that over one year, the false lumen still remains patent and still has flow as seen on MRI.

The simulation results for patient 1 were interesting. These showed that at baseline the mean pressure in the aorta was higher (over  $100\text{mmHg}$ ) compared to  $97\text{mmHg}$  in 2014. Around the area of tear 1, there was turbulent high velocity flow but the actual false lumen had low flow, albeit a high pressure. This may represent a blind pressurized sac.

Interestingly this area in 2014 was still pressurised with a low flow suggesting that the blind sac theory is probably correct and that there may be potential for false lumen growth here. Additionally, all tear areas showed turbulent flow as would be expected, except for the region of tear 4, which already showed low flow and pressure at baseline. It is therefore not surprising that a year on this tear had healed and was no longer visible on the CAD model derived from the follow up imaging data.

Already with a change in local attitudes, clinical follow up with CT scans seems to be losing favour and instead MRI scanning seems to be gaining popularity and momentum. Of course availability of scanners, of trained medical staff to interpret the scans, and the time taken to acquire images all need to be taken into consideration from a diagnosis point of view where CT still trumps MRI. However, it is not before long, that the use of MRI even for diagnosis will become commonplace.

CFD and simulation have the ability to provide clinicians with a wealth of data that can be applied to daily practice. By starting with image data a model is built which is then divided into many smaller parts or subdomains to numerically solve the equations of motion for a fluid. The result provides parameters such as pressure and wall shear stress which are difficult to measure in vivo. These derived parameters are important in understanding diseases pathology, and progression to therefore allow for a tailor made approach to intervention as well as conservative management. (91)

# Chapter 17

## Discussion

### 17.1 Black blood study

In this study the potential utility of  $T_2$ PSIR and  $T_2$ IR sequences in imaging of the thoracic aorta, with respect to scan time, apparent CNR, image sharpness and a qualitative visual scoring was undertaken in eleven volunteers and two patients with aortic dissection. The aim of this study was to devise optimum sequences for black blood imaging to accurately investigate morphology of the aortic intimal flap in dissection.

The  $T_2$ PSIR sequence was shown to be superior with respect to image quality as assessed by CNR, sharpness and visual scores, although the scan time was longer than  $T_2$ IR. The improved image quality is likely due to the ability of  $T_2$ PSIR to provide optimal blood-to-vessel wall contrast for any heart rates, as well as the increased signal that is obtained by performing the non-selective inversion pulse every other cardiac cycle. Based on these results we have found  $T_2$ PSIR to be the more favourable approach, the increased scan time notwithstanding.

In this study, the potential feasibility of using the  $T_2$ PSIR sequence in patients with aortic dissection to visualize the intimal flap as well as the location of tears was also demonstrated. Visual comparison with CT in the dissection patients shows good agreement.

Although slow flowing blood can be adequately suppressed using  $T_2$ IR or  $T_2$ PSIR, the pilot study indicated that rapid blood flow during the application of the  $T_2$  prepared pulses leads to flow-artefacts. Furthermore, by positioning the  $T_2$ -prep pulses in a cardiac phase with low flow, immediately after the R-wave, these flow artefacts can be minimized.

The main drawback of the  $T_2$ PSIR sequence is the increased scan time compared to  $T_2$ IR which augments the susceptibility to respiratory motion induced artefacts due to respiratory



drift or irregular breathing. The use of respiratory gating with an end-expiratory 5 mm window reduces respiratory motion artefacts at the expense of further prolonging the scan time.

Highly efficient respiratory motion compensation techniques have been proposed for coronary magnetic resonance angiography (MRA) to directly track and compensate for bulk respiratory induced motion of the heart (92-94). Similar techniques may be applicable to aortic T<sub>2</sub>PSIR to reduce the total scan time by allowing for data acquisition throughout the whole respiratory cycle. Additional scan time reduction may be obtained using compressed sensing which allows for image acceleration beyond what can be achieved with conventional parallel imaging, which was employed in this study (95).

Several negative prognostic indicators have been identified in aortic dissection. These include tear location (proximal tears fare worse than distal ones), size (larger tears are associated with a worse outcome than smaller tears) number of entry tears (one is worse than many) and partial thrombosis of the false lumen. (33,39,42,96,97) As far as the latter is concerned, ongoing perfusion of the false lumen without an exit tear leads essentially to a blind pressurized sac and aortic dilatation.

For this reason, a detailed evaluation of the tear morphology and geography may facilitate patient specific management, including tailor-made follow up as dictated or indeed intervention (33,42,79,96-99). Based on the promising initial results reported here, further studies are warranted in patients with aortic dissection using T<sub>2</sub>PSIR techniques. The scope of future work using these techniques should focus on the utility of the T<sub>2</sub>PSIR in imaging of aortic dissection, where subtle anatomical features of clinical importance such as tear location and anatomy may well be more accurately visualized compared to conventional CT standards.

# Chapter 18

## Discussion

### 18.1 Dual phase study

The aorta is a complex organ with complex biomechanical properties. Aortic pulsatility and of its associated side branches along with the rapid change in motion direction throughout the cardiac cycle may play a significant role in the management of aortic pathologies. It therefore follows that complex forces are generated and exerted onto stent grafts thereby resulting in graft migration and failure. Therefore, the ideal selection of a graft for a particular patient or pathology is vital. (100,101)

In as much as the aorta being a complex structure, aortic dissection represents an even more intricate morphological and physiological environment. In biomechanical terms, the dissection results in a separation of the elastic layers of the aortic wall occurring when the haemodynamic loads exerted on the aorta exceed the forces holding the aortic layers together. (102)

The intimal flap is but a few millimetres thick and can be expected to experience vast motion throughout the cardiac cycle. This can in turn lead to dynamic obstruction of the true lumen with each heartbeat resulting in branch vessel ischaemia. (103) Although this motion is difficult to assess via a static 2D imaging modality like CT scanning it has been done by previous groups. (104-106) The use of ECG gated CT aortography reduces artefacts and provides functional assessment, albeit with a higher radiation dose. Ganten et al showed that the true lumen collapsed by up to 29% in some cases. This of course can have a significant impact on visceral ischaemia. Other groups' studies have investigated the aortic motion at the level of the aortic root abdominal aorta and the ascending aorta utilising CT scanning. (100,106-108) and have all indicated the variability of aortic motion from beat to beat and its resultant mechanical effects not just on therapeutic endografts placed in these regions but

also the native aorta leading to additional stress. Displacement of the aortic root during the cardiac cycle has been shown to range from 0-22mm in patients with cardiovascular diseases. Those with aortic regurgitation exhibit greater displacement and those with left ventricular hypokinesis show the opposite trend. Additional work has also indicated the increase in mechanical stresses in the aortic wall as a result of aortic root motion, perhaps offering an explanation for the tear location and orientation as seen in aortic dissections. (107,109)

The current dual phase study described has several advantages over the CT scan studies. Firstly, there was no associated radiation. Additionally accurate tracking of cardiac motion was performed using a cine scan and PC-MR flow data. Additional functional data such as velocity and flow were also readily obtainable.

The study focussed on investigating the utility of dual phase aortic imaging to understand the motion and strain on the aorta during the cardiac cycle in normal healthy volunteers and then to investigate the effects in a patient with aortic dissection.

Study of the healthy subjects demonstrated that the ascending aorta was a mobile structure demonstrating a mean longitudinal strain of 4.2%, and a volumetric strain of 24%. For each fixed location the mean circumferential strain was approximately 8%.

The arch was a more mobile structure than the ascending aorta, demonstrating longitudinal strain in the order of 13% and a volumetric strain of 29%. It is possible that the supra-aortic branches serve to restrain the longitudinal motion of the aorta. Finally, the descending aorta in comparison was rather fixed, demonstrating a volumetric strain of 16.7% and a compressive strain of -1.5%. This compressive strain can be explained by the relative fixation of the descending aorta to the spine thereby attenuating its longitudinal motion. Longitudinal and circumferential strain both contribute to volumetric strain which was found to be significantly less in the AAo than in the AA. One reason for this may be the existence of the visceral branches, particularly the ascending vessels. The DA on the other hand is relatively fixed to the spine, as well as being tethered to the ligamentum arteriosum and

attenuates lateral aortic motion from longitudinal strain and a comparable circumferential strain contribution. The AAo is like a rigid body deformation as there are no branching vessels between the coronaries and the innominate artery thereby resulting in lower longitudinal strain and the primary contribution to volumetric strain being circumferential changes. The AA shows a greater volumetric change as there is a larger contribution from longitudinal strain and a similar contribution from circumferential strain.

Results from patients having been treated for TAAD with a residual Type B component were interesting. Here the ascending aorta demonstrated higher strain than in healthy subjects perhaps reflective of the material properties of the Dacron graft used to repair the ascending aorta. Additionally the arch seemed to exhibit lower strain than the healthy subjects perhaps indicative of the stress of the graft proximally and the relatively fixed descending thoracic aorta distally. Of note, patient A seemed to have an excessively long Dacron graft, which seemed to be folding over and causing an apparent stenosis. There is a likely greater pressure differential in this area, with a large pressure proximal to the stenosis and a lower pressure distal to it. This may result in a lowered volumetric strain distally in the distal ascending aorta or the arch. This patient also had suspected Marfan pathology, which may again affect the strain distribution. Clearly the aorta distal to the Dacron repair would have an abnormal infrastructure due to the pathology and this could lead to a lowered strain in this area.

Patient B seemed to have a smaller stenosis in the region just proximal to the P.InoA again leading to a similar distribution of strain as for patient A. A final observation in these two patients is also the increased age compared to the healthy volunteers. (Patient A 46, B 53 at the time of the scan) and age related biomechanical changes occur in the aorta, with reduced distensibility affecting the arch the least. Both patient A and B demonstrated compressive or negligible longitudinal strains in the DA. TL and a positive strain in the DA FL. This is due to the geometry of the dissection. In both cases the FL is on the outer curvature of the arch. During systole, the TL enlarges, which in turn imposes on the FL causing it to distend resulting in a tensile longitudinal strain. It is possible that a false lumen on the inner

curvature may experience a compressive longitudinal strain. Clinical observations noted support for this hypothesis, suggesting a false lumen situated the outer curvature have typically been associated with reduced risk of growth (42,97,110).

# Chapter 19

## Conclusion

### **19.1 Proposed patient pathway for long term management of acute, residual (chronic) Type B dissections**

As an insight into the direction of personalized medical care, this work demonstrates the potential utility of the combination of non-ionizing functional imaging modalities and CFD methodology into clinical practice.

Based on results from this work, it would be feasible to consider that CFD has an important role to play in the management of aortic dissection. Although patients presenting with an acute TAAD will always be excluded from such pathways due to the urgent nature of the intervention required however, patients with acute TBAD are a different cohort.

Dilatation of the false lumen affects 50% of patients over 5 years and survival ranges from 50-82%. Complete thrombosis is associated with a better survival than a fully patent false lumen but partial thrombosis has the worst outcomes. Although the management of uncomplicated TBAD seems to be at present conservative, randomized controlled trials have indicated the utility of stent graft use in stable aortic dissection. There are only 2 prospective randomized controlled trials in uncomplicated dissection the ADSORB for acute dissections up to 14 days and the chronic INSTEAD trial looking at dissections between 14 days to -1 year. The Investigation of stent grafts in aortic dissection trial (INSTEAD) is the first randomized controlled trial to compare best medical therapy (BMT) with stent graft placement in addition to best medical therapy. This trial was designed to compare and evaluate the effects of stent graft placement in Type B patients who would have otherwise been conservatively managed with medication alone.

Although the 2-year results did not show a significant difference in outcomes (survival, vascular, and progression) aortic remodelling and stability were seen in the overwhelming majority of cases (90%) treated with best medical therapy and stent graft placement. Additionally there was up to a 20% crossover from the BMT group to the stenting or surgery group due to false lumen expansion or other late complications.

The amended follow-up study, INSTEAD-XL includes 5-year follow up. In this cohort, the BMT group experienced further ongoing complications and fatalities whereas the stented patients had a stable long term, course and no fatalities up to 5 years. The investigators of INSTEAD postulated that the so called 'uncomplicated' TBAD are actually not so uncomplicated in the years following dissection, and these patients treated conservatively often had further false lumen expansion and aortic rupture. Additionally, these patients deemed stable initially seemed to die suddenly, indicating perhaps that the mechanism of death was due to aortic rupture and this stresses the fact that the current monitoring programme is not able to detect the at risk patient, and more importantly, a static measurement of aortic diameter is not an indicator of safety. Aortic remodelling and healing to allow for morphological correction are crucial to providing stability and stent graft placement is superior at this than best medical treatment alone. (27)

Optimal medical treatment is essential in the acute setting, not forgetting that the haemodynamic insult that results in a weakened aorta is elevated systolic and mean arterial blood pressure. Equally important in patients deemed fit for discharge without intervention is the regular monitoring of blood pressure and a tight control keeping the pulse pressure and heart rate low, as these are factors that propagate the dissection. (111)

These insights suggest that the stable dissection patient is actually not so stable as thought and an detailed understanding of the intra-aortic morphology and haemodynamcis on a personalized basis will be provide accurate information to best manage each patient. Aortic remodelling is the key to stabilizing the dissected aorta offering healing and realignment of all

layers of the aorta. So far data suggest that dissection is never safe under BMT alone for uncomplicated TBAD.

The ADSORB trial, (Acute Dissection: Stent graft OR Best medical therapy aimed to compare freedom from events such as :

1. Incomplete or no false lumen thrombosis in any part of the false lumen
2. Aortic dilatation of greater than 5cm or the max diameter of the descending aorta >55mm.
3. Aortic rupture on CT

In this trial, 61 patients were randomized in 17 European centres from Dec 2009-Dec 2010. There were 29 patients in the BMT plus stent group and 30 in the BMT group alone.

Unpublished results (at the time of writing) of the trial demonstrated a statistically significant greater freedom from the composite end point at the end of the 1-year study in the BMT plus TEVAR group as compared to those in the BMT alone cohort (57% vs 3%;  $P < .001$ ). One reason for this is that there was a significant difference in false lumen thrombosis between groups, as no significant difference was seen in the aortic dilatation and rupture components of the composite end point. Secondary aortic remodelling end points were improved in the BMT plus TEVAR group, with a statistically significant larger true lumen and smaller false lumen, and generally a smaller overall aortic diameter, as compared to the BMT alone cohort.

It is important to realise that the composite end point does not provide clinically useful information, which can steer clinical decisions.

Another group has published long-term follow-up data for endovascular repair of acute complicated TBAD and here over 20% of patients required additional (one or more) adjunctive procedures in addition to the original TEVAR, to treat malperfusion as a result of the dissection. Over the follow up period (median 34 months) 26% of patients required re-intervention for a number of reasons although there was no difference in survival between



those who required re-intervention and those who did not. This itself highlights the true complexity of this condition compared to TEVAR for a more 'stable' pathology such as aneurysm.(110) The high re-intervention rate itself is an indication that lifelong aortic surveillance by an experienced aortic centre is undertaken to identify and treat complications.

Based on these observations and studies, the potential utility of CFD in the preoperative work up and the post-operative result can be imagined. A proposed patient pathway is shown in Figure 75.

Patients with an acute TBAD would undergo MRI scanning if stable, to ascertain flow data from PC-MRI. CT image data will provide the morphological basis for development of a CAD model although strictly speaking the MRI can suffice alone. Combining the two using cardiovascular modelling software like CRIMSON would lead to a patient specific model of the dissection. Next, using flow data from the patients MRI and non-invasive BP measurements taken during the MRI scan one has the boundary conditions to inform the CAD model. This will then give an indication of real time intra-aortic haemodynamics, better informing us about the dynamic behaviour of the dissection. Additionally MRI methods as described can be relied upon to give detailed tear information on morphology. Dual phase scanning can give an indication of aortic strain. All these methods combined aim to give a dynamic assessment for patients with a TBAD rather than relying on static image data or dimension change that is currently employed in the treatment planning for these patients.

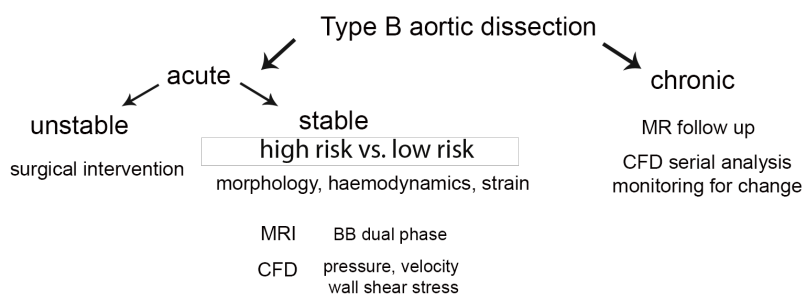


FIGURE 75 PROPOSED PATIENT PATHWAY FOR TBAD PATIENTS.

# Chapter 20

## Limitations

### 20.1 TEVAR Study

Inclusion of invasive haemodynamic pressure wire readings for three patients was not given approval in this body of work. This was a major setback to the study as it was aimed at providing the first in vivo confirmation of simulation results for aortic dissection. Despite retrospective ethical approval the inclusion was not permitted. In addition to this major setback, a change in the local surgical practice, led to a shift away from TEVAR for TBAD unless there were complications or haemodynamic instability. Although several other patients were identified on the wards, none underwent TEVAR and therefore no further recruitment into this arm of the study was possible.

### 20.2 Follow up study

The aim of follow up study was to image patients at a one year interval from their original recruitment date and develop models ready for simulation. Several changes occurred during this period. The MRI protocol initially developed was deemed too long with not all sequences providing relevant information. This protocol was therefore modified. The major limitation of performing the MRI scans on these patients was degradation in image quality due to individual patient factors such as arrhythmias or discomfort and therefore motion artefacts several scans had to be abandoned. Model development proved to be quite laborious, as the development of a new in house package, CRIMSON required several bug fixes and updates. The software used prior to the implementation of CRIMSON (SimVascular) was slow and obsolete and therefore all models had to be rebuilt in CRIMSON.

Time wise it took several weeks and quite frequently months develop a single model that seemed accurate, as previous model building had been done for a simple tubular structure without the addition of a complex dissection flap.

All three dissection patients with a one year follow up had extremely challenging geometries which took months to develop. Further problems were encountered when the blending and meshing operations took place as the complex geometry meant a workable model required several iterations. Unfortunately for one patient the (patient 3) initial and follow up models were extremely tricky, and despite best efforts a workable meshed model was unable to be developed.

Finally, the simulation process was time consuming and expensive, thereby limiting the number of simulations to be developed. The first hurdle was to extract usable PC-MRI data for flow and velocity measurements. This was tricky in the regions of the true and false lumens. Flow patterns in the false lumen were difficult to interpret due to turbulence.

Previous work within the lab had suggested developing coarse meshes initially to define workable parameters for each model as development of a fine mesh although led to a more physiologically correct interpretation of haemodynamics it was expensive and mistakes in the mesh had financial implications. For this reason simulation was performed using a coarse mesh in just one patient.

## 20.3 Black blood

A fundamental limitation of the  $T_2$  prepared inversion recovery sequence is that the  $T_2$ prep prepulse (in general 30-50ms in duration) has to be performed during a cardiac phase with low flow to ensure homogeneous blood suppression, which may be difficult in patients with high heart rates. However, a phase contrast scan can be performed prior to the  $T_2$ IR or  $T_2$ PSIR to measure blood flow to ensure that the  $T_2$ prep pulse is performed in the phase with lowest flow.

The negative factor associated with the T2PSIR sequence is the length of time it currently takes to acquire scans. Clearly in the clinical setting it would not be feasible to undertake such long scans. Further optimization however will lead to quicker data acquisition.

## **20.4 Dual phase**

The main limitation of the dual phase study was realising that the cardiac phases of systole and diastole were only clearly visualised when a cine scan was performed and the state contraction or relaxation were physically sought for by eye. This meant that previous scans in 5 volunteers had to be repeated.

# References

1. Clough RE, Nienaber C a. Management of acute aortic syndrome. Nat Rev Cardiol [Internet]. Nature Publishing Group; 2014;12(2):103-14. Available from: <http://www.nature.com/doifinder/10.1038/nrcardio.2014.203>
2. Pyeritz RE, Gasner C. The Marfan syndrome [Internet]. National Marfan Foundation; 1999 [cited 2015 Nov 16]. 44 p. Available from: [https://books.google.co.uk/books/about/The\\_Marfan\\_syndrome.html?id=dtRrAAAAMAAJ&pgis=1](https://books.google.co.uk/books/about/The_Marfan_syndrome.html?id=dtRrAAAAMAAJ&pgis=1)
3. Nichols F. Observations concerning the body of His Late Majesty [Internet]. Philos Trans London. p. 265-74. Available from: <http://www.scopus.com/inward/record.url?eid=2-s2.0-0001234794&partnerID=tZOtx3y1>
4. Criado FJ. Aortic dissection: a 250-year perspective. Tex Heart Inst J [Internet]. 2011;38(6):694-700. Available from: <http://www.pubmedcentral.nih.gov/articlerender.fcgi?artid=3233335&tool=pmcentrez&rendertype=abstract>
5. DEBAKEY ME, HENLY WS, COOLEY DA, MORRIS GC, CRAWFORD ES, BEALL AC. SURGICAL MANAGEMENT OF DISSECTING ANEURYSMS OF AORTA. J Thorac Cardiovasc Surg. 1965;49(1):130 - &.
6. Holzapfel GA, Gasser TC, Ogden RW. A New Constitutive Framework for Arterial Wall Mechanics and a Comparative Study of Material Models. J Elast Phys Sci solids [Internet]. Kluwer Academic Publishers; [cited 2015 Aug 25];61(1-3):1-48. Available from: <http://link.springer.com/article/10.1023/A%3A1010835316564>
7. Nienaber C a, Powell JT. Management of acute aortic syndromes. Eur Heart J. 2012 Jan;33(1):26-35b.
8. LeMaire SA, Russell L. Epidemiology of thoracic aortic dissection. Nat Rev Cardiol. 2011;8(2):103-13.
9. Pape LA, Tsai TT, Isselbacher EM, Oh JK, O’Gara PT, Evangelista A, et al. Aortic diameter  $\geq 5.5$  cm is not a good predictor of type A aortic dissection: Observations

from the International Registry of Acute Aortic Dissection (IRAD). *Circulation*. 2007;116(10):1120-7.

10. Juvonen T, Ergin MA, Galla JD, Lansman SL, McCullough JN, Nguyen K, et al. Risk factors for rupture of chronic type B dissections. *J Thorac Cardiovasc Surg* [Internet]. 1999 Apr [cited 2015 Aug 6];117(4):776-86. Available from: <http://www.ncbi.nlm.nih.gov/pubmed/10096974>
11. Marfan AB. A case of congenital deformity of the four limbs, most pronounced at the extremities, and characterized by elongation of the bones, along with some degree of thinning. *Bull Mem Soc Med Hop Paris*. 1896;13:220.
12. Loeys BL, Chen J, Neptune ER, Judge DP, Podowski M, Holm T, et al. A syndrome of altered cardiovascular, craniofacial, neurocognitive and skeletal development caused by mutations in TGFBR1 or TGFBR2. *Nat Genet* [Internet]. 2005 Mar;37(3):275-81. Available from: <http://dx.doi.org/10.1038/ng1511>
13. Beighton P, De Paepe A, Steinmann B, Tsipouras P, Wenstrup RJ. Ehlers-Danlos syndromes: revised nosology, Villefranche, 1997. Ehlers-Danlos National Foundation (USA) and Ehlers-Danlos Support Group (UK). *Am J Med Genet*. 1998;77:31-7.
14. Loscalzo ML, Goh DLM, Loeys B, Kent KC, Spevak PJ, Dietz HC. Familial thoracic aortic dilation and bicommissural aortic valve: A prospective analysis of natural history and inheritance. *Am J Med Genet Part A* [Internet]. Wiley Subscription Services, Inc., A Wiley Company; 2007;143A(17):1960-7. Available from: <http://dx.doi.org/10.1002/ajmg.a.31872>
15. Hagan PG, Nienaber CA, Isselbacher EM, Bruckman D, Karavite DJ, Russman PL, et al. The International Registry of Acute Aortic Dissection (IRAD): new insights into an old disease. *Jama J Am Med Assoc*. 2000;283:897-903.
16. Elefteriades J a, Farkas E a. Thoracic aortic aneurysm clinically pertinent controversies and uncertainties. *J Am Coll Cardiol* [Internet]. Elsevier Inc.; 2010 Mar 2 [cited 2013 May 23];55(9):841-57. Available from: <http://www.ncbi.nlm.nih.gov/pubmed/20185035>
17. Daily PO, Trueblood HW, Stinson EB, Wuerflein RD, Shumway NE. Management of Acute Aortic Dissections. *Ann Thorac Surg* [Internet]. The Society of Thoracic Surgeons; 1970 Sep [cited 2013 Aug 15];10(3):237-47. Available from:

18. Thrumurthy SG, Karthikesalingam A, Patterson BO, Holt PJE, Thompson MM. The diagnosis and management of aortic dissection. 2012;8290(January):1-7.
19. Lempel J, Frazier A, Jeudy J. Aortic Arch Dissection: A Controversy of Classification. *Radiology* [Internet]. 2014;271(3):131457. Available from: <http://www.ncbi.nlm.nih.gov/pubmed/24617732> \n <http://pubs.rsna.org/doi/abs/10.1148/radiol.14131457>
20. Halpern EJ. Triple-rule-out CT angiography for evaluation of acute chest pain and possible acute coronary syndrome. *Radiology*. 2009;252:332-45.
21. Krüger T, Conzelmann LO, Bonser RS, Borger M a, Czerny M, Wildhirt S, et al. Acute aortic dissection type A. *Br J Surg* [Internet]. 2012 Oct [cited 2013 Jul 30];99(10):1331-44. Available from: <http://www.ncbi.nlm.nih.gov/pubmed/22961510>
22. Eggebrecht H, Nienaber CA, Neuhäuser M, Baumgart D, Kische S, Schmermund A, et al. Endovascular stent-graft placement in aortic dissection: a meta-analysis. *Eur Heart J*. 2006;27:489-98.
23. Moulakakis KG, Mylonas SN, Dalainas I, Kakisis J, Kotsis T, Liapis CD. Management of complicated and uncomplicated acute type B dissection. A systematic review and meta-analysis [Internet]. *Annals of Cardiothoracic Surgery*. 2014 [cited 2015 Aug 7]. p. 234-46. Available from: <http://www.annalscts.com/article/view/3871/html>
24. Nienaber C a, Rousseau H, Eggebrecht H, Kische S, Fattori R, Rehders TC, et al. Randomized comparison of strategies for type B aortic dissection: the INvestigation of STEnt Grafts in Aortic Dissection (INSTEAD) trial. *Circulation* [Internet]. 2009 Dec 22 [cited 2013 May 22];120(25):2519-28. Available from: <http://www.ncbi.nlm.nih.gov/pubmed/19996018>
25. Fattori R, Montgomery D, Lovato L, Kische S, Di Eusanio M, Ince H, et al. Survival after endovascular therapy in patients with type B aortic dissection: a report from the International Registry of Acute Aortic Dissection (IRAD). *JACC Cardiovasc Interv* [Internet]. 2013 Aug [cited 2015 Aug 7];6(8):876-82. Available from: <http://www.sciencedirect.com/science/article/pii/S1936879813009916>

26. Svensson LG, Kouchoukos NT, Miller DC, Bavaria JE, Coselli JS, Curi MA, et al. Expert consensus document on the treatment of descending thoracic aortic disease using endovascular stent-grafts. *Ann Thorac Surg* [Internet]. Elsevier; 2008 Jan 1 [cited 2015 Aug 25];85(1 Suppl):S1-41. Available from: <http://www.annalsthoracicsurgery.org/article/S0003497507022540/fulltext>
  
27. Nienaber CA, Kische S, Rousseau H, Eggebrecht H, Rehders TC, Kundt G, et al. Endovascular repair of type B aortic dissection: long-term results of the randomized investigation of stent grafts in aortic dissection trial. *Circ Cardiovasc Interv* [Internet]. 2013 Aug [cited 2015 Aug 7];6(4):407-16. Available from: <http://www.ncbi.nlm.nih.gov/pubmed/23922146>
  
28. Nienaber CA, Zannetti S, Barbieri B, Kische S, Schareck W, Rehders TC. INvestigation of STEnt grafts in patients with type B Aortic Dissection: design of the INSTEAD trial--a prospective, multicenter, European randomized trial. *Am Heart J* [Internet]. 2005 Apr [cited 2015 Aug 7];149(4):592-9. Available from: <http://www.ncbi.nlm.nih.gov/pubmed/15990739>
  
29. Brunkwall J, Lammer J, Verhoeven E, Taylor P. ADSORB: a study on the efficacy of endovascular grafting in uncomplicated acute dissection of the descending aorta. *Eur J Vasc Endovasc Surg*. Elsevier Ltd; 2012 Jul;44(1):31-6.
  
30. Coady M a, Ikonomidis JS, Cheung AT, Matsumoto AH, Dake MD, Chaikof EL, et al. Surgical management of descending thoracic aortic disease: open and endovascular approaches: a scientific statement from the American Heart Association. *Circulation*. 2010 Jun 29;121(25):2780-804.
  
31. Tsai TT, Evangelista A, Nienaber C a, Trimarchi S, Sechtem U, Fattori R, et al. Long-term survival in patients presenting with type A acute aortic dissection: insights from the International Registry of Acute Aortic Dissection (IRAD). *Circulation*. 2006 Jul 4;114(1 Suppl):I350-6.
  
32. Tsai TT, Fattori R, Trimarchi S, Isselbacher E, Myrmel T, Evangelista A, et al. Long-term survival in patients presenting with type B acute aortic dissection: insights from the International Registry of Acute Aortic Dissection. *Circulation*. 2006 Nov 21;114(21):2226-31.
  
33. Trimarchi S, Tolenaar JL, Jonker FHW, Murray B, Tsai TT, Eagle K a, et al. Importance of false lumen thrombosis in type B aortic dissection prognosis. *J Thorac Cardiovasc Surg*. The American Association for Thoracic Surgery; 2013 Mar;145(3 Suppl):S208-12.



34. Kimura N, Tanaka M, Kawahito K, Yamaguchi A, Ino T, Adachi H. Influence of patent false lumen on long-term outcome after surgery for acute type A aortic dissection. *J Thorac Cardiovasc Surg. The American Association for Thoracic Surgery*; 2008 Nov;136(5):1160-6, 1166.e1-3.
35. Blount KJ, Hagspiel KD. Aortic diameter, true lumen, and false lumen growth rates in chronic type B aortic dissection. *Ajr Am J Roentgenol*. 2009 May;192(5):W222-9.
36. Farber M a. Commentary. Partial thrombosis of the false lumen in patients with acute type B aortic dissection. *Perspect Vasc Surg Endovasc Ther*. 2008 Sep;20(3):316-8.
37. Chang C-P, Liu J-C, Liou Y-M, Chang S-S, Chen J-Y. The role of false lumen size in prediction of in-hospital complications after acute type B aortic dissection. *J Am Coll Cardiol*. 2008 Sep 30;52(14):1170-6.
38. Erbel R, Alfonso F, Boileau C, Dirsch O, Eber B, Haverich a, et al. Diagnosis and management of aortic dissection. *Eur Heart J [Internet]*. 2001 Sep [cited 2013 Jul 30];22(18):1642-81. Available from: <http://www.ncbi.nlm.nih.gov/pubmed/11511117>
39. Tsai TT, Evangelista A, Nienaber C a, Myrmel T, Meinhardt G, Cooper J V, et al. Partial thrombosis of the false lumen in patients with acute type B aortic dissection. *N Engl J Med*. 2007;357(4):349-59.
40. van Prehn J, Vincken KL, Muhs BE, Barwegen GKW, Bartels LW, Prokop M, et al. Toward endografting of the ascending aorta: insight into dynamics using dynamic cine-CTA. *J Endovasc Ther [Internet]*. 2007 Aug [cited 2015 Oct 22];14(4):551-60. Available from: <http://www.ncbi.nlm.nih.gov/pubmed/17696632>
41. Muhs BE, Vincken KL, van Prehn J, Stone MKC, Bartels LW, Prokop M, et al. Dynamic Cine-CT Angiography for the Evaluation of the Thoracic Aorta; Insight in Dynamic Changes with Implications for Thoracic Endograft Treatment. *Eur J Vasc Endovasc Surg [Internet]*. Elsevier; 2006 Nov 11 [cited 2015 Oct 22];32(5):532-6. Available from: <http://www.ejves.com/article/S107858840600284X/fulltext>
42. Tolenaar JL, van Keulen JW, Trimarchi S, Jonker FHW, van Herwaarden J a, Verhagen HJM, et al. Number of entry tears is associated with aortic growth in type B dissections. *Ann Thorac Surg [Internet]*. Elsevier Inc; 2013 Jul [cited 2013 Oct 9];96(1):39-42. Available from: <http://www.ncbi.nlm.nih.gov/pubmed/23684160>

43. Weiss G, Wolner I, Folkmann S, Sodeck G, Schmidli J, Grabenwöger M, et al. The location of the primary entry tear in acute type B aortic dissection affects early outcome. *Eur J Cardiothorac Surg Off J Eur Assoc Cardiothorac Surg*. 2012;0:1-6.
44. Quint LE, Platt JF, Sonnad SS, Deeb GM, Williams DM. Aortic intimal tears: detection with spiral computed tomography. *J Endovasc Ther an Off J Int Soc Endovasc Spec*. 2003;10:505-10.
45. Clough RE, Waltham M, Giese D, Taylor PR, Schaeffter T. A new imaging method for assessment of aortic dissection using four-dimensional phase contrast magnetic resonance imaging. *J Vasc Surg [Internet]*. 2012 Apr;55(4):914-23. Available from: <http://linkinghub.elsevier.com/retrieve/pii/S0741521411026085>
46. Taylor CA, Figueroa CA. Patient-specific modeling of cardiovascular mechanics. *Annu Rev Biomed Eng*. 2009;11:109-34.
47. Freeman LA, Young PM, Foley TA, Williamson EE, Bruce CJ, Greason KL. CT and MRI assessment of the aortic root and ascending aorta. *AJR Am J Roentgenol [Internet]*. American Roentgen Ray Society; 2013 Jun 23 [cited 2015 Aug 26];200(6):W581-92. Available from: <http://www.ajronline.org/doi/full/10.2214/AJR.12.9531>
48. Tumlin J, Stacul F, Adam A, Becker CR, Davidson C, Lameire N, et al. Pathophysiology of contrast-induced nephropathy. *Am J Cardiol [Internet]*. 2006 Sep 18 [cited 2015 Aug 26];98(6A):14K - 20K. Available from: <http://www.ncbi.nlm.nih.gov/pubmed/16949376>
49. Martin DR, Semelka RC. Health effects of ionising radiation from diagnostic CT. *Lancet (London, England) [Internet]*. Elsevier; 2006 May 27 [cited 2015 Aug 26];367(9524):1712-4. Available from: <http://www.thelancet.com/article/S0140673606687485/fulltext>
50. Schlaudecker JD, Bernheisel CR. Gadolinium-associated nephrogenic systemic fibrosis. *Am Fam Physician [Internet]*. 2009 Oct 1 [cited 2015 Aug 26];80(7):711-4. Available from: <http://www.ncbi.nlm.nih.gov/pubmed/19817341>
51. Gonsalves CF. The Hyperattenuating Crescent Sign<sup>1</sup>. *Radiology [Internet]*. Radiological Society of North America; 1999 Apr 1 [cited 2015 Aug 26];211(1):37-8.

52. Ueda T, Chin A, Petrovitch I, Fleischmann D. A pictorial review of acute aortic syndrome: discriminating and overlapping features as revealed by ECG-gated multidetector-row CT angiography. *Insights Imaging* [Internet]. 2012 Dec [cited 2015 Aug 26];3(6):561-71. Available from: <http://www.pubmedcentral.nih.gov/articlerender.fcgi?artid=3505562&tool=pmcentrez&rendertype=abstract>
  
53. Ketelsen D, Fenchel M, Thomas C, Buchgeister M, Boehringer N, Tsiflikas I, et al. Estimation of radiation exposure of retrospective gated and prospective triggered 128-slice triple-rule-out CT angiography. *Acta Radiol* [Internet]. SAGE Publications; 2011 Sep 1 [cited 2015 Aug 26];52(7):762-6. Available from: <http://acr.sagepub.com/content/52/7/762.full>
  
54. Yoshida S, Akiba H, Tamakawa M, Yama N, Hareyama M, Morishita K, et al. Thoracic involvement of type A aortic dissection and intramural hematoma: diagnostic accuracy--comparison of emergency helical CT and surgical findings. *Radiology* [Internet]. 2003 Aug [cited 2015 Aug 26];228(2):430-5. Available from: <http://www.ncbi.nlm.nih.gov/pubmed/12819341>
  
55. Cayne NS, Veith FJ, Lipsitz EC, Ohki T, Mehta M, Gargiulo N, et al. Variability of maximal aortic aneurysm diameter measurements on CT scan: Significance and methods to minimize. *J Vasc Surg*. 2004;39(4):811-5.
  
56. Nienaber CA, Clough RE. Management of acute aortic dissection. *Lancet* (London, England) [Internet]. 2015 Feb 28 [cited 2015 Aug 25];385(9970):800-11. Available from: <http://www.sciencedirect.com/science/article/pii/S0140673614610059>
  
57. Baliga RR, Nienaber C a, Bossone E, Oh JK, Isselbacher EM, Sechtem U, et al. The role of imaging in aortic dissection and related syndromes. *JACC Cardiovasc Imaging* [Internet]. 2014 Apr [cited 2014 Jun 2];7(4):406-24. Available from: <http://www.ncbi.nlm.nih.gov/pubmed/24742892>
  
58. Nienaber CA, von Kodolitsch Y, Nicolas V, Siglow V, Piepho A, Brockhoff C, et al. The Diagnosis of Thoracic Aortic Dissection by Noninvasive Imaging Procedures. *N Engl J Med* [Internet]. 1993;328(1):1-9. Available from: <http://dx.doi.org/10.1056/NEJM199301073280101>

59. Herédia V, Ramalho M, Duarte S, Campos ROP De, Hernandez M. Magnetic Resonance Imaging of the Thoracic Aorta : A Review of Technical and Clinical Aspects , Including Its Use in the Evaluation of Aneurysms and Acute Vascular Conditions.
60. Sakamoto I, Sueyoshi E, Uetani M. MR Imaging of the Aorta. Radiol Clin North Am [Internet]. 2007 May [cited 2015 Oct 17];45(3):485-97. Available from: <http://www.ncbi.nlm.nih.gov/pubmed/17601504>
61. Stemerman DH, Krinsky GA, Lee VS, Johnson G, Yang BM, Rofsky NM. Thoracic aorta: rapid black-blood MR imaging with half-Fourier rapid acquisition with relaxation enhancement with or without electrocardiographic triggering. Radiology. 1999;213:185-91.
62. Urban B a, Bluemke D a, Johnson KM, Fishman EK. Imaging of thoracic aortic disease. Cardiol Clin. 1999 Dec;17(4):659-82, viii.
63. Lin K, Bi X, Liu Y, Taimen K, Lu B, Li D, et al. Black-blood steady-state free precession (SSFP) coronary wall MRI for cardiac allografts: a feasibility study. J Magn Reson Imaging [Internet]. 2012 May [cited 2014 Jun 26];35(5):1210-5. Available from: <http://www.ncbi.nlm.nih.gov/pubmed/22282170>
64. Liu C-Y, Bley TA, Wieben O, Brittain JH, Reeder SB. Flow-independent T(2)-prepared inversion recovery black-blood MR imaging. J Magn Reson Imaging [Internet]. 2010 Jan [cited 2014 Jun 30];31(1):248-54. Available from: <http://www.ncbi.nlm.nih.gov/pubmed/20027595>
65. Brittain JH, Olcott EW, Szuba A, Gold GE, Wright GA, Irarrazaval P, et al. Three-dimensional flow-independent peripheral angiography. Magn Reson Med. 1997;38(3):343-54.
66. Kellman P, Arai AE, McVeigh ER, Aletras AH. Phase-sensitive inversion recovery for detecting myocardial infarction using gadolinium-delayed hyperenhancement. Magn Reson Med [Internet]. 2002 Feb [cited 2014 Jun 26];47(2):372-83. Available from: <http://www.pubmedcentral.nih.gov/articlerender.fcgi?artid=2041905&tool=pmcentrez&rendertype=abstract>
67. Xie J, Bi X, Fan Z, Bhat H, Shah S, Zuehlsdorff S, et al. 3D flow-independent peripheral vessel wall imaging using T(2)-prepared phase-sensitive inversion-

recovery steady-state free precession. J Magn Reson Imaging [Internet]. 2010 Aug [cited 2014 Jun 30];32(2):399-408. Available from: <http://www.pubmedcentral.nih.gov/articlerender.fcgi?artid=2915467&tool=pmcentrez&rendertype=abstract>

68. Evangelista A. Acute Intramural Hematoma of the Aorta: A Mystery in Evolution. Circulation [Internet]. 2005 Feb 14 [cited 2015 Oct 20];111(8):1063-70. Available from: <http://www.ncbi.nlm.nih.gov/pubmed/15710757>
69. Sommer T, Fehske W, Holzknecht N, Smekal A V, Keller E, Lutterbey G, et al. Aortic dissection: a comparative study of diagnosis with spiral CT, multiplanar transesophageal echocardiography, and MR imaging. Radiology [Internet]. 1996;199(2):347-52. Available from: <http://dx.doi.org/10.1148/radiology.199.2.8668776>
70. Milner JS, Moore JA, Rutt BK, Steinman DA. Hemodynamics of human carotid artery bifurcations: Computational studies with models reconstructed from magnetic resonance imaging of normal subjects. J Vasc Surg [Internet]. Elsevier; 1998 Jul 7 [cited 2015 Aug 27];28(1):143-56. Available from: <http://www.jvascsurg.org/article/S0741521498702101/fulltext>
71. Taylor CA, Hughes TJR, Zarins CK. Finite element modeling of blood flow in arteries. Comput Methods Appl Mech Eng [Internet]. 1998 May [cited 2015 Aug 20];158(1-2):155-96. Available from: <http://www.sciencedirect.com/science/article/pii/S004578259880008X>
72. Kim HJ, Vignon-Clementel IE, Coogan JS, Figueroa CA, Jansen KE, Taylor CA. Patient-specific modeling of blood flow and pressure in human coronary arteries. Ann Biomed Eng [Internet]. 2010 Oct [cited 2015 Aug 27];38(10):3195-209. Available from: <http://www.ncbi.nlm.nih.gov/pubmed/20559732>
73. Long Q, Xu XY, Ariff B, Thom SA, Hughes AD, Stanton A V. Reconstruction of blood flow patterns in a human carotid bifurcation: a combined CFD and MRI study. J Magn Reson Imaging [Internet]. 2000 Mar [cited 2015 Aug 27];11(3):299-311. Available from: <http://www.ncbi.nlm.nih.gov/pubmed/10739562>
74. Cebal JR, Castro MA, Burgess JE, Pergolizzi RS, Sheridan MJ, Putman CM. Characterization of Cerebral Aneurysms for Assessing Risk of Rupture By Using Patient-Specific Computational Hemodynamics Models. AJNR Am J Neuroradiol [Internet]. 2005 Nov 1 [cited 2015 Aug 27];26(10):2550-9. Available from: <http://www.ajnr.org/content/26/10/2550.long>

75. Vorp DA. Biomechanics of abdominal aortic aneurysm. *J Biomech* [Internet]. Elsevier; 2007 Jan 1 [cited 2015 Jul 1];40(9):1887-902. Available from: <http://www.jbiomech.com/article/S002192900600323X/fulltext>
  
76. Karmonik C, Bismuth J, Redel T, Anaya-Ayala JE, Davies MG, Shah DJ, et al. Impact of tear location on hemodynamics in a type B aortic dissection investigated with computational fluid dynamics. *Conf Proc IEEE Eng Med Biol Soc* [Internet]. 2010 Jan [cited 2014 Mar 6];2010:3138-41. Available from: <http://www.ncbi.nlm.nih.gov/pubmed/21096590>
  
77. Karmonik C, Bismuth J, Davies MG, Shah DJ, Younes HK, Lumsden AB. A computational fluid dynamics study pre- and post-stent graft placement in an acute type B aortic dissection. *Vasc Endovascular Surg* [Internet]. 2011 Feb [cited 2014 Mar 6];45(2):157-64. Available from: <http://www.ncbi.nlm.nih.gov/pubmed/21156714>
  
78. Karmonik C, Müller-Eschner M, Partovi S, Geisbüsch P, Ganten M-K, Bismuth J, et al. Computational fluid dynamics investigation of chronic aortic dissection hemodynamics versus normal aorta. *Vasc Endovascular Surg* [Internet]. 2013 Nov [cited 2014 Feb 12];47(8):625-31. Available from: <http://www.ncbi.nlm.nih.gov/pubmed/24048257>
  
79. Rudenick PA, Bijlens BH, García-dorado D, Evangelista A. An in vitro phantom study on the influence of tear size and configuration on the hemodynamics of the lumina in chronic type B aortic dissections. *YMVA* [Internet]. Elsevier; 57(2):464-74.e5. Available from: <http://dx.doi.org/10.1016/j.jvs.2012.07.008>
  
80. Tse KM, Chiu P, Lee HP, Ho P. Investigation of hemodynamics in the development of dissecting aneurysm within patient-specific dissecting aneurysmal aortas using computational fluid dynamics (CFD) simulations. *J Biomech* [Internet]. Elsevier; 2011 Mar 15 [cited 2015 Oct 21];44(5):827-36. Available from: <http://www.jbiomech.com/article/S0021929011000133/fulltext>
  
81. Chen D, Müller-Eschner M, Kotelis D, Böckler D, Ventikos Y, von Tengg-Kobligh H. A longitudinal study of Type-B aortic dissection and endovascular repair scenarios: computational analyses. *Med Eng Phys* [Internet]. 2013 Sep [cited 2014 Mar 6];35(9):1321-30. Available from: <http://www.ncbi.nlm.nih.gov/pubmed/23523079>
  
82. Dillon-Murphy D, Noorani A, Nordsletten D, Figueroa CA. Multi-modality image-based computational analysis of haemodynamics in aortic dissection. *Biomech Model*

Mechanobiol [Internet]. 2015 Sep 28 [cited 2015 Oct 21]; Available from:  
<http://www.ncbi.nlm.nih.gov/pubmed/26416312>

83. Wang KC, Dutton RW, Taylor CA. Improving geometric model construction for blood flow modeling. IEEE Eng Med Biol Mag [Internet]. 1999 [cited 2015 Aug 28];18(6):33-9. Available from:  
<http://ieeexplore.ieee.org/lpdocs/epic03/wrapper.htm?arnumber=805142>
84. PressureWire<sup>TM</sup> Certus.
85. Look DC. Time Saving in Measurement of NMR and EPR Relaxation Times. Rev Sci Instrum [Internet]. 1970 [cited 2014 Dec 29];41(2):250. Available from:  
<http://scitation.aip.org/content/aip/journal/rsi/41/2/10.1063/1.1684482>
86. Nezafat R, Stuber M, Ouwerkerk R, Gharib AM, Desai MY, Pettigrew RI. B1-insensitive T2 preparation for improved coronary magnetic resonance angiography at 3 T. Magn Reson Med [Internet]. 2006 Apr [cited 2015 Aug 4];55(4):858-64. Available from: <http://www.ncbi.nlm.nih.gov/pubmed/16538606>
87. Jenista ER, Rehwald WG, Chen E-L, Kim HW, Klem I, Parker MA, et al. Motion and flow insensitive adiabatic T2 -preparation module for cardiac MR imaging at 3 Tesla. Magn Reson Med [Internet]. 2013 Nov [cited 2014 Jun 30];70(5):1360-8. Available from: <http://www.ncbi.nlm.nih.gov/pubmed/23213005>
88. Etienne A, Botnar RM, Van Muiswinkel AMC, Boesiger P, Manning WJ, Stuber M. "Soap-Bubble" visualization and quantitative analysis of 3D coronary magnetic resonance angiograms. Magn Reson Med [Internet]. 2002 Oct [cited 2014 Aug 22];48(4):658-66. Available from: <http://www.ncbi.nlm.nih.gov/pubmed/12353283>
89. Kim WY, Danias PG, Stuber M, Flamm SD, Plein S, Nagel E, et al. Coronary magnetic resonance angiography for the detection of coronary stenoses. N Engl J Med [Internet]. 2001 Dec 27 [cited 2014 Aug 12];345(26):1863-9. Available from: <http://www.ncbi.nlm.nih.gov/pubmed/11756576>
90. vmtk - the Vascular Modelling Toolkit [Internet]. [cited 2015 Dec 3]. Available from: <http://www.vmtk.org/>
91. Lee JJ, D'Ancona G, Amaducci A, Follis F, Pilato M, Pasta S. Role of computational

modeling in thoracic aortic pathology: a review. *J Card Surg* [Internet]. 2014 Sep [cited 2015 Aug 27];29(5):653-62. Available from: <http://www.ncbi.nlm.nih.gov/pubmed/25080972>

92. Prieto C, Doneva M, Usman M, Henningsson M, Greil G, Schaeffter T, et al. Highly efficient respiratory motion compensated free-breathing coronary mra using golden-step Cartesian acquisition. *Journal of Magnetic Resonance Imaging*. 2014;
93. Piccini D, Littmann A, Nielles-Vallespin S, Zenge MO. Respiratory self-navigation for whole-heart bright-blood coronary MRI: methods for robust isolation and automatic segmentation of the blood pool. *Magn Reson Med* [Internet]. 2012 Aug [cited 2015 Jul 3];68(2):571-9. Available from: <http://www.ncbi.nlm.nih.gov/pubmed/22213169>
94. Pang J, Bhat H, Sharif B, Fan Z, Thomson LEJ, LaBounty T, et al. Whole-heart coronary MRA with 100% respiratory gating efficiency: self-navigated three-dimensional retrospective image-based motion correction (TRIM). *Magn Reson Med* [Internet]. 2014 Jan [cited 2015 May 20];71(1):67-74. Available from: <http://www.pubmedcentral.nih.gov/articlerender.fcgi?artid=3655135&tool=pmcentrez&rendertype=abstract>
95. Lustig M, Donoho D, Pauly JM. Sparse MRI: The application of compressed sensing for rapid MR imaging. *Magn Reson Med*. 2007;58:1182-95.
96. Tolenaar JL, Keulen JW Van, Jonker FHW. Morphologic predictors of aortic dilatation in type B aortic dissection. *J Vasc Surg* [Internet]. Society for Vascular Surgery; 2010;58(5):1220-5. Available from: <http://dx.doi.org/10.1016/j.jvs.2013.05.031>
97. Bogerijen GHW Van, Tolenaar JL, Rampoldi V. Predictors of aortic growth in uncomplicated type B aortic dissection. *J Vasc Surg* [Internet]. Society for Vascular Surgery; 2013;59(4):1134-43. Available from: <http://dx.doi.org/10.1016/j.jvs.2014.01.042>
98. Tsai TT, Schlicht MS, Khanafer K, Bull JL, Valassis DT, Williams DM, et al. Tear size and location impacts false lumen pressure in an ex vivo model of chronic type B aortic dissection. *J Vasc Surg*. 2008;47(4):844-51.
99. Trimarchi S, Jonker FHW, Bogerijen GHW Van, Tolenaar JL, Frans L, Czerny M, et al. Predicting aortic enlargement in type B aortic dissection. 2014;3(3):285-91.



100. van Bogerijen GHW, van Herwaarden JA, Conti M, Auricchio F, Rampoldi V, Trimarchi S, et al. Importance of dynamic aortic evaluation in planning TEVAR [Internet]. *Annals of Cardiothoracic Surgery*. [cited 2015 Oct 22]. p. 300-6. Available from: <http://www.annalscts.com/article/view/3810/html>
101. Figueroa CA, Taylor CA, Chiou AJ, Yeh V, Zarins CK. Magnitude and Direction of Pulsatile Displacement Forces Acting on Thoracic Aortic Endografts. *J Endovasc Ther an Off J Int Soc Endovasc Spec*. 2009;16:350-8.
102. Pasta S, Phillippi JA, Gleason TG, Vorp DA. Effect of aneurysm on the mechanical dissection properties of the human ascending thoracic aorta. *J Thorac Cardiovasc Surg* [Internet]. Elsevier; 2012 Feb 2 [cited 2015 Nov 19];143(2):460-7. Available from: <http://www.jtcvsonline.org/article/S0022522311008348/fulltext>
103. Williams DM, Lee DY, Hamilton BH, Marx M V, Narasimham DL, Kazanjian SN, et al. The dissected aorta: part III. Anatomy and radiologic diagnosis of branch-vessel compromise. *Radiology* [Internet]. 1997 Apr [cited 2015 Nov 19];203(1):37-44. Available from: <http://www.ncbi.nlm.nih.gov/pubmed/9122414>
104. Beller CJ, Labrosse MR, Thubrikar MJ, Robicsek F. Role of aortic root motion in the pathogenesis of aortic dissection. *Circulation* [Internet]. 2004 Feb 17 [cited 2015 Aug 27];109(6):763-9. Available from: <http://circ.ahajournals.org/cgi/content/long/109/6/763>
105. Ganten MK, Weber TF, von Tengg-Koblighk H, Böckler D, Stiller W, Geisbüsch P, et al. Motion characterization of aortic wall and intimal flap by ECG-gated CT in patients with chronic B-dissection. *Eur J Radiol*. 2009;72(1):146-53.
106. Yang S, Li X, Chao B, Wu L, Cheng Z, Duan Y, et al. Abdominal aortic intimal flap motion characterization in acute aortic dissection: assessed with retrospective ECG-gated thoracoabdominal aorta dual-source CT angiography. *PLoS One* [Internet]. Public Library of Science; 2014 Jan 4 [cited 2015 Oct 23];9(2):e87664. Available from: <http://journals.plos.org/plosone/article?id=10.1371/journal.pone.0087664>
107. Beller CJ, Labrosse MR, Thubrikar MJ, Robicsek F. Role of Aortic Root Motion in the Pathogenesis of Aortic Dissection. *Circulation*. 2004;109(6):763-9.
108. Bell V, Mitchell WA, Sigurðsson S, Westenberg JJM, Gotal JD, Torjesen AA, et al. Longitudinal and circumferential strain of the proximal aorta. *J Am Heart Assoc*

[Internet]. 2014 Dec 18 [cited 2015 Aug 27];3(6):e001536. Available from:  
<http://jaha.ahajournals.org/content/3/6/e001536.abstract>

109. Beller CJ, Labrosse MR, Hagl S, Gebhard MM, Karck M. Aortic root motion remodeling after aortic valve replacement--implications for late aortic dissection. *Interact Cardiovasc Thorac Surg* [Internet]. 2008 May [cited 2015 Oct 23];7(3):407-11; discussion 411. Available from: <http://www.ncbi.nlm.nih.gov/pubmed/18334521>
110. Hughes GC. Management of acute type B aortic dissection; ADSORB trial. *J Thorac Cardiovasc Surg* [Internet]. 2015 Feb [cited 2015 Nov 16];149(2 Suppl):S158-62. Available from: <http://www.sciencedirect.com/science/article/pii/S0022522314012884>
111. Rajagopal K, Bridges C, Rajagopal KR. Towards an understanding of the mechanics underlying aortic dissection. *Biomech Model Mechanobiol* [Internet]. 2007 Mar 14 [cited 2015 Aug 27];6(5):345-59. Available from: <http://www.ncbi.nlm.nih.gov/pubmed/17356838>
112. Nienaber C a, Rousseau H, Eggebrecht H, Kische S, Fattori R, Rehders TC, et al. Randomized comparison of strategies for type B aortic dissection: the INvestigation of STEnt Grafts in Aortic Dissection (INSTEAD) trial. *Circulation*. 2009 Dec 22;120(25):2519-28.

# List of Tables

Table 1 mortality rates for aortic dissection by type and management.....	32
Table 2 Demographics of the TEVAR population patients .....	87
Table 3 Follow up patients demographics and scan details .....	103
Table 4 morphological changes over the period of one year for patient 1. The false lumen volume has decreased and thrombus volume has increased. ....	107
Table 5 volume of true & false lumens and tears .....	114
Table 6 Demographics of study subjects. V= healthy volunteer, P= Patient .....	124
Table 7 Visual score results for each of the sequences .....	125
Table 8 study population demographics. V=Volunteer, P=Patient .....	128
Table 9 Systole and diastole coordinates for the left coronary artery in 5 healthy volunteers. The net translation is a difference between the systolic and diastolic points in the 3 spatial directions, x, y and z. The motion is a vector quantity in mm. ....	131
Table 10 Patient A Circumferential change and therefore motion of the intimal flap in the aorta during the cardiac cycle. ....	135
Table 11 Patient B Circumferential change and therefore motion of the intimal flap in the aorta during the cardiac cycle. ....	137

# List of Figures

Figure 1 An intimal tear results in a true and false lumen for blood flow (2) .....	11
Figure 2 segments of the aorta. The aortic root extends from the aortic annulus to the sinotubular junction. The ascending aorta commences at the sinotubular junction and extends to the origin of the innominate artery. the arch of the aorta extends from the origin of the innominate artery to the left subclavian artery. The descending aorta extends from the left subclavian to the diaphragmatic hiatus where it crosses to become the abdominal aorta .....	13
Figure 3 Components of the arterial wall (6). The monolayered intima is a thin basal membrane with a subendothelial layer, the thickness of which varies with age and disease. The media is composed of smooth muscle cells, a network of elastic and collagen fibrils and elastic laminae which separate the media into a number of fibre-reinforced layers. The adventitia is the outermost layer and primarily consists of thick bundles of collagen fibrils.....	14
Figure 4 Manifestations of the acute aortic syndrome. TL= true lumen, FL= false lumen, PAU = penetrating aortic ulcer, IMH = intramural haematoma (7) .....	16
Figure 5 classification of aortic dissection, Debakey and Stanford. In Stanford Type A the ascending aorta is involved in the dissection. In Stanford Type B the descending aorta is involved. In the Debakey system the location of the tear is important, and in Type I and II the tear is located in the ascending aorta whereas in Type III the tear is in the descending aorta. ....	20
Figure 6 toe images from a patient with acute TAAD. yellow arrow indicates position of intimal flap. fl=false lumen, tl=true lumen, lvot= left ventricular outflow tract .....	24
Figure 7 CT angiogram (A&B) images from a patient with acute TAAD. yellow arrow indicates position of intimal flap. fl= false lumen, tl= true lumen. ....	24

Figure 8 operations for TAAO. a) replacement of the supra-commissural ascending aorta. b) hemi-arch replacement. c) arch replacement. d) trifurcated graft and arch debranchment (21).....	27
Figure 9 TEVAR aims to seal off the entry tear and promote aortic remodelling. (24) .....	29
Figure 10 In-hospital mortality for medically managed and surgically managed aortic dissection. Medically managed TAAO has the worst in hospital mortality at over 50% at 30 days.(15) .....	32
Figure 11 A Unadjusted Kaplan-Meier survival curve stratified by in-hospital management from date of hospital discharge in patients with TAAO dissection. (31) B. Unadjusted Kaplan-Meier survival curve stratified by in-hospital management of patients with acute TBAD who survive to hospital discharge (32) .....	33
Figure 12 Five-year survival rates for medically treated TBAD versus endovascular therapy. (25).....	33
Figure 13 A proposed model of the physiological consequences of false-lumen patency or thrombosis, based on hemodynamic studies in ex vivo models and in patients with Type B aortic dissection.....	37
Figure 14 CT image of a normal aorta in a 54 year old man. The different lines represent the landmarks used in reporting a clinical scan. Black solid line= aortic root, white solid line= sinuses of Valsalva, black dashed line= sinotubular junction. White dashed line= mid ascending aorta. Black dotted line= distal ascending aorta. (47).....	39
Figure 15 CT images from a patient with acute TAAO. ....	41
Figure 16 CE-MRA in a patient with chronic TBAD. red arrow shows the position of the true lumen, green arrow shows the intimal flap, yellow arrow shows the false lumen and blue arrow the area of thrombus. ....	43
Figure 17 with black blood mri techniques the vessel wall appears bright and blood black. this allows for clearer visualization of vessel wall pathology. These images are from healthy volunteers.....	44

Figure 18 t2PSIR and t2IR sequences. To minimize flow artefacts originating flowing blood during the performance of the T2prep this pre-pulse is performed in early systole immediately after R-wave detection. The inversion time is determined such that blood signal is nulled for T2IR while for T2PSIR blood signal can be nulled for a wide range of inversion times due to the phase sensitive reconstruction.....	46
Figure 19 Toe long axis view of the aortic root showing the intimal flap (yellow arrow) and true and false lumens (TL, FL). LVOT = left ventricular outflow tract, LV= Left ventricle. ....	48
Figure 20 A. patient-specific ascending aortic flow waveform measured by PC-MRI is mapped to the inflow face of the CAD model. A 3-element Windkessel model with a proximal resistance ( $R_p$ ), capacitance (C), distal resistance ( $R_d$ ) boundary condition is used to represent the resistance and compliance of the vasculature downstream of each outlet. B. haemodynamic results from CFD in a patient with aortic dissection. figures represent early systole maps of blood velocity (left) blood pressure (centre) and wall shear stress (right). ....	50
Figure 21 pathline creation from path points using image data in crimson.....	59
Figure 22 Contouring operation along the vessel pathline .....	61
Figure 23 lofting and blending operations .....	63
Figure 24 Meshing operation.....	65
Figure 25 A close-up view of Certus PressureWire (84).....	67
Figure 26 A snapshot of the RadiAnalyzer monitor (A) and screen recordings during a TEVAR case (B) are shown. Red trace = aortic pressure, green trace = false lumen pressure (84).....	68
Figure 27 Set up in the hybrid theatre. With the C-arm in position, the RadiAnalyzer is attached to the operating table. Both the PressureWire (PW, green) and the pigtail (Ao, red) are connected to the transducer at the height of the patient's right atrium. ....	69
Figure 28 Proforma for individualized patient specific intraoperative pressure .....	70

Figure 29 T <sub>2</sub> PSIR and T <sub>2</sub> IR sequences. T <sub>2</sub> PSIR and T <sub>2</sub> IR sequences (b). In both sequences an inversion pulse is performed to null the signal from blood and a T <sub>2</sub> prep, using 2 adiabatic refocussing pulses (a), is performed to improve the contrast between blood and vessel wall. In the T <sub>2</sub> PSIR sequence an additional image acquisition is performed in the subsequent cardiac cycle to calculate the polarity of the signal (c). To minimize flow artefacts originating flowing blood during the performance of the T <sub>2</sub> prep this pre-pulse is performed in early systole immediately after R-wave detection. The inversion time is determined such that blood signal is nulled for T <sub>2</sub> IR while for T <sub>2</sub> PSIR blood signal can be nulled for a wide range of inversion times due to the phase sensitive reconstruction....	75
Figure 30 Images obtained from one of the two pilot study subjects demonstrating flow dependence of T <sub>2</sub> PSIR. The chart on the right demonstrates flow in the ascending (red, AA) and descending aorta (blue, DA), over time and the time-points in the cardiac cycle when the T <sub>2</sub> prep were performed for the low and high flow conditions. ES= early systole, low flow (0-50ms) MS= mid systole, high flow (200-250ms).....	77
Figure 31 Image segmentation for the dual phase study.....	81
Figure 32 Systolic and diastolic images from the same subject. Not much difference in cardiac and aortic motion was visible between the two phases. ....	82
Figure 33 Cine triggered scans show a difference in systolic and diastolic states of the heart. ....	82
Figure 34 An alternate strategy of including a cine image with dynamic cardiac imaging to determine systole and diastole was included in addition to calculating flow in the ascending aorta above the level of the aortic valve with pc-mri. systolic imaging was then triggered as shown by the red arrow and diastolic by the blue arrow. ....	83
Figure 35 representation of the aorta in the dual phase study. the aorta was divided into segments to allow for comparative analysis. The points 1-4 serve to distinguish between the ascending aorta (1-2), arch (2-3) and descending aorta (3-4). ....	85
Figure 36 CT library of images for all TEVAR patients 1-4,.....	88

Figure 37 Patient 1. Acute TBAD Images from CT scans at presentation. blue arrow indicates thrombus formation. red arrow indicates the position of the true lumen. green arrow indicates location of intimal tear.....	90
Figure 38 workflow for creating a 3d cad model for simulation. a. image data is used to create geometry in crimson. b a 3d cad model is developed. c. flow data is acquired from pc-mri using gt-flow. d. flow data is converted into graphical format.....	91
Figure 39 Ct images of patient 2. The red arrow shows the true lumen, the yellow arrow indicates the false lumen. ....	93
Figure 40 workflow for preparing a model for simulation. a. 3d geometry from image data results in b. an anatomically accurate model. c and d. gt flow is used to extract relevant flow data at various points in the aorta. e. the flow data is converted into excel ready for use in simulation. ....	94
Figure 41 Patient 3. A: Pre-operative CT scan with red arrow highlighting the true lumen and the yellow arrow highlighting the false lumen. ....	96
Figure 42 CT scan images from a 30-year old male with an acute TBAD. the green arrow indicates the position of the intimal flap. the yellow arrow indicates the false lumen and the red arrow the true lumen. ....	97
Figure 43 a 3d model of patient 4 Showing the true (blue) and false lumen (pink). No thrombus was present due to the acute nature of the dissection. ....	98
Figure 44 Patient 4. 3d model with area of tear (green arrow) highlighted and corresponding CT image showing the same.....	99
Figure 45 proforma from an example of a hypothetical tevar case showing recording of intra-aortic haemodynamics. pressure wire results were plotted over the aortic length for each patient. ....	101
Figure 46 Patient 1 in 2013. The true lumen is shown in blue, false in pink and thrombus in brown. ....	105
Figure 47 Patient 1 in 2014. The true lumen is shown in blue, false in pink and thrombus in brown. ....	106



Figure 48 patient 1 thrombus volume is 2014 with corresponding CT image depicting thrombus. ....	106
Figure 49 CAD models for patient 1 in 2013. The tears are marked in yellow and black arrows. ....	107
Figure 50 CAD models for patient 1 in 2014. These models show the change in tear morphology at one year post follow up at location. Tear at location 4 has healed.....	108
Figure 51 Simulation results from patient 1. mean Pressure is shown on the left and maximum velocity on the right. Top: 2013 results, Bottom: 2014 results. Of immediate note is the overall low mean pressure throughout the aorta and in particular the false lumen distally when compared to the previous year. Additionally a lower velocity profile is evident in the area of healed tear 4. ....	109
Figure 52 simulation results for 2013 left: pressure, centre: velocity and right tear morphology. Of note: Area of tear 1 has a high pressure but low velocity potentially representing a partial thrombosis of the proximal false lumen. Tears 2,3 and 5 show a turbulent flow pattern whereas tear 4 has very low if any flow. ....	110
Figure 53 simulation results for 2014 left: pressure, centre: velocity and right tear morphology. Of note: the overall mean pressure seems to be lower in 2014. in particular this is true for the distal false lumen. Tears 2,3 and 5 still show a turbulent flow pattern whereas tear 4 has now healed fully and is not seen in the CAD image on the right...	111
Figure 54 Agreement between PC-MRI and CFD simulation flow results for patient 1. Top: 2013 results. Bottom: 2014 results.....	112
Figure 55 Patient 2. CAD models of aortic dissection over the period of one year. The false lumen is widely patent with not much change in size over the year and no healing of tears. ....	114
Figure 56 Patient 2. CAD model development in crimson. true lumen is shown in blue, false in pink. tears are shown in yellow. ....	115
Figure 57 tear morphology for patient 2. Nine tears were found and no thrombus had developed since the original acute dissection 5 years ago. ....	116

Figure 58 Tear morphology for patient 2. All 9 tears were fully patent one year on, with no thrombus formation. ....	117
Figure 59 Baseline CAD model for Patient 3 and corresponding CT Scan. This was a complex dissection extending into the arch and the superior mesenteric artery. Accurate realization of the geometry was difficult and a blended model was not developed.....	119
Figure 60 Patient 4. CAD model of aortic dissection. The picture on the top shows the thrombus lofted in (Brown).....	121
Figure 61 patient 4. cad models showing location of tears (yellow). There were four tears in total. ....	122
Figure 62 Reformatted images from three healthy volunteers using T <sub>2</sub> IR and T <sub>2</sub> PSIR. A clearer image with better vessel wall visualization is obtained when using the T <sub>2</sub> PSIR sequence. ....	126
Figure 63 Sagittal section images showing T <sub>2</sub> PSIR sequences performed in two patients with chronic TBAD. The white arrows show the position of the intimal flap, which is clearly visualized. Cross-sections of each patient's a) CT scan and b) MRI (T <sub>2</sub> PSIR) sequence are shown below the sagittal images. The red arrows indicate the position of the intimal tear in each of the imaging modalities.....	127
Figure 64 dual phase models. Blue diastole, red, systole. The superimposed image on the far right shows the changes in aortic motion with the cardiac cycle. The aortic root is seen to be travelling in the inferior-lateral direction during systole. this is due to the force of cardiac contraction and twisting motion of the heart. ....	129
Figure 65 enlarged version of the aortic root of a volunteer. here the motion of the left coronary artery is visualized and highlighted by the yellow arrows. quantification of this in the 3d frame was performed in crimson. red= systole, blue= diastole .....	130
Figure 66 Percentage circumferential change along the aortic length by volunteer. Mean values are shown in orange. ....	132
Figure 67 true and false lumen circumferential change for dissection patient a.....	134

Figure 68 dissection patient A. the models on the left show the true and false lumens changes between systole and diastole. true lumen is shown in blue, false in pink. The figures to the right show the overall aortic changes between systole and diastole .....	134
Figure 69 true and false lumen circumferential change for dissection patient B .....	136
Figure 70 dissection patient B. the models on the left show the true and false lumens changes between systole and diastole. true lumen is shown in blue, false in pink. The figures to the right show the overall aortic changes between systole and diastole. ....	137
Figure 71 Healthy subjects strains. Top: longitudinal strain, Centre: circumferential strain and Bottom: volumetric strain, Grey bars indicate the standard deviation and the mean values are shown in the grey circles. ....	139
Figure 72 aortic strain as measured in different segments of the aorta during diastole and systole. Vol= volumetric strain, CL= centreline (longitudinal) strain of note the arch of the aorta (AA) demonstrates the largest volumetric and circumferential strain. conversely, the descending aorta (DA) experiences a compressive strain as does the ascending aorta (AA).....	140
Figure 73 Patient A Aortic strain and morphological changes by location. The panel on the left middle show segmentations and calculated volume (vol) and longitudinal (CL) strain in diastole and systole. The panel on the right shows the image RESLICES AT the chosen points of interest showing vessel contour circumference and circumferential change. ....	143
Figure 74 Patient B Aortic strain and morphological changes by location. The panel on the left middle show segmentations and calculated volume (vol) and longitudinal (CL) strain in diastole and systole. The panel on the right shows the image reslices at the chosen points of interest showing vessel contour circumference and circumferential change.	144
Figure 75 Proposed patient pathway for TBAD patients.....	156

# Appendix

## A1 Patient invitation letters: pressure wire study



Date: Feb 2014

Version: 2

Dear Mr. / Mrs.

You have been informed by the vascular surgery team that you will benefit from an operation to manage your aortic dissection.

To help us understand this condition in more detail and improve our treatment options in the future, I am writing to invite you to consider participation in a study whilst you are undergoing your planned operation.

I have enclosed an information leaflet detailing the study along with my contact details. If you are interested in participating, I would be grateful if you contact me by completing and posting the enclosed stamped reply slip, or by phone, email or text, details below.

Thank you in advance, for your time and efforts in helping us understand this condition better and enabling us to improve our service.

Many thanks,

Yours sincerely,

Dr. Alia Noorani

On behalf of Prof. Taylor and the research team,

**Write:** Division of Imaging Sciences

3<sup>rd</sup> Floor Lambeth Wing,

St. Thomas' Hospital,

London

SE1 7EH

**Phone or Text:** 07715802408

**Email:** alia.noorani@kcl.ac.uk

## A1 Patient invitation letters - MRI study



Date: Feb 2014

Version 2

Dear Mr. / Mrs.

Aortic dissection is a complex condition and we are investigating the use of magnetic resonance imaging (MRI) scans to help us understand it in more detail, with the potential to improve our treatment options in the future.

The enclosed information leaflet details the study and explains the MRI procedure.

If you are interested in participating, I would be grateful if you would contact me by completing and posting the enclosed stamped reply slip, or by email, phone or text on the number below. We will reimburse your travel costs to and from the hospital.

Thank you in advance, for your time and efforts in helping us understand this condition better and enabling us to improve our service

Many thanks

Yours sincerely

Dr. Alia Noorani

On behalf of Prof. Taylor and the research team,

**Write:**

Division of Imaging Sciences

3<sup>rd</sup> Floor Lambeth Wing,

St. Thomas' Hospital,

London

SE1 7EH

**Phone or Text:** 07715802408

**Email:** [alia.noorani@kcl.ac.uk](mailto:alia.noorani@kcl.ac.uk)

## **A2 Patient information - invasive study**

# **PARTICIPANT INFORMATION SHEET**

### **A study of haemodynamics in aortic dissection**

**PROTOCOL REFERENCE NUMBER: 14/LO/0286**

**VERSION NUMBER: 2**

**DATE: February 2014**

We would like you invite you to take part in our research study. Before you decide we would like you to understand why the research is being done and what it will involve for you. Please take time to read the following information carefully. Talk to others about the study if you wish. The research doctor (name below) will go through the information when they meet with you.

Part 1 tells you the purpose of this study and what will happen to you if you take part.

Part 2 gives you more detailed information about the conduct of the study.

Ask us if there is anything that is not clear or if you would like more information. Take time to decide whether or not you wish to take part.

# **PART 1**

## **1. What is the purpose of the study?**

Aortic dissection is a tear in the lining of the main artery from the heart. This can happen for a number of reasons, commonly due to high blood pressure. Typically, patients experience severe chest pain. When a tear occurs, a second false channel or lumen for blood flow can develop. Blood flow can be diverted into this false channel and can affect the blood supply to other vital organs. The management of dissection depends on the location of the tear in the aorta (upper or lower part) and the presence of any other complicating factors.

Patients with complications are offered an operation, called a stent graft procedure whereby a mesh-tube is inserted into the aorta via the groin blood vessels. This provides stability to the aorta and seals the tear. Some patients have poor outcomes after their dissection and we need to understand why this is the case. High blood pressure in the false lumen is thought to be an important factor, although this has not been proven as yet. In this study we intend to take accurate blood pressure readings using a specialized catheter while you are having your stent graft procedure.

## **2. Why have I been chosen?**

You have been chosen because you have an aortic dissection, which is being treated with a stent graft operation.

## **3. Do I have to take part?**

No. It is up to you to decide whether or not to take part. Your clinical team (vascular surgery) will describe the study. If you agree to take part, a member of the research team will approach you on admission, to go through this information sheet, discuss any questions and ask you to sign a consent form. You are still free to withdraw at any time and without giving a

reason. A decision to withdraw at any time, or a decision not to take part, will not affect the standard or type of care you receive.

#### **4. What will happen to me if I take part?**

Patients enrolled in this study will be consented by the clinical vascular surgical team for their stent graft operation. Additionally the research team will seek your consent for this research study. With your consent, we would invite you to undergo an MRI scan prior to the operation and plan to take pressure measurements from your aorta whilst you are undergoing your stent graft procedure. We anticipate will add a further 5 minutes to the overall operation.

#### **5. What do I have to do?**

You need read this information leaflet and decide if this study may be of interest to you. In addition, if you are part of any other experimental studies you should make this known. If you would like to take part, please contact Miss Alia Noorani, (co-investigator) by completing and returning the enclosed reply slip by post, by email on [alia.noorani@kcl.ac.uk](mailto:alia.noorani@kcl.ac.uk) or by phone or text on 07715802408.

#### **6. What are the side effects of any treatment received?**

There is a small (less than 0.5%) chance that the pressure catheter causes damage to the aorta. It is important to remember that the catheter itself is small and is commonly used to detect problems in the blood vessels of the heart, which are extremely fragile. If any damage to the aorta occurs, it will be treated in the same way as originally planned, i.e with a stent graft, as this effectively seals the tear.

There is also a theoretical, very small, less than 0.1% chance of stroke associated with the pressure wire. It is important to remember that the stent graft procedure itself is associated with a risk of stroke (less than 5%) and that this risk is outweighed by the benefits of the operation to treat the dissection.



Because your operation is minimally invasive (like a key hole procedure), it does not involve big incisions or cuts on the body. Therefore, in order to be able to perform the procedure, X-ray guidance is used to inform the surgeons the exact location of the tear in the aorta and where it is ideal to place the stent graft. During the operation, you will be exposed to X-rays as routine and the research study will add a further 5 minutes to the exposure. We all have a 1 in 3 chance of getting cancer, even if we never have an X-ray. It is important to consider that these extra X-ray examinations still represent a very small addition to this underlying risk from all causes.

## **7. What are the other possible disadvantages and risks of taking part?**

The only disadvantage as mentioned above is additional, short X-ray exposure during your existing stent graft procedure, although the extra exposure represents a very a very small additional risk.

## **8. What are the possible benefits of taking part?**

We cannot promise that the study will help you, but the information we gain from this study will potentially help us improve the treatment of patients with aortic dissection in the future.

## **9. What happens when the research study stops?**

Results from this study will then be used to understand the importance of pressure in the false lumen and help target our management of patients who may be at greatest risk at the time of their original presentation.

## **10. What if there is a problem?**

Any complaint about the way you have been dealt with during the study or any possible harm you might suffer will be addressed.

The contact details are:

Miss Alia Noorani (Co-Investigator)

Division of Imaging Sciences

3<sup>rd</sup> Floor Lambeth Wing,

St Thomas' Hospital

London

SE1 7EH

Telephone: Department of Imaging Sciences: 020 71885441

Direct line: 07715802408 Email: alia.noorani@kcl.ac.uk

## **11. Will my taking part in the study be kept confidential?**

Yes. All the information about your participation in this study will be kept confidential. The details are included in Part 2.

## **12. Contact Details:**

For further information please contact:

Miss Alia Noorani (Co-Investigator)

Division of Imaging Sciences

3<sup>rd</sup> Floor Lambeth Wing,

St Thomas' Hospital

London SE1 7EH

Telephone: Department of Imaging Sciences: 020 71885441 Direct line: 07715802408

Email: [alia.noorani@kcl.ac.uk](mailto:alia.noorani@kcl.ac.uk)

*This completes Part 1 of the Information Sheet.*

*If the information in Part 1 has interested you and you are considering participation, please continue to read the additional information in Part 2 before making any decision.*

## PART 2

### 13. What will happen if I don't want to carry on with the study?

This will in no way affect any further medical treatment you receive within the Trust.

### 14. What if there is a problem?

#### A - Complaints:

If you have a concern about any aspect of this study, you should ask to speak with the researchers who will do their best to answer your questions (Miss Alia Noorani: 07715802408). If you remain unhappy and wish to complain formally, you can do this by contacting the **Patient Advice and Liaison Service (PALS)** based at St. Thomas' Hospital. Details are as follows:

Visit PALS at:

The Knowledge and Information Centre (KIC)

Ground Floor, North Wing, St. Thomas' Hospital.

Timings: Monday- Friday 10am-12pm and 2pm-4pm.

Tel: 020 7188 8801 / 020 7188 8803

Fax: 020 7188 1651

Email: [pals@gstt.nhs.uk](mailto:pals@gstt.nhs.uk)

Write: Patient Information Team, KIC, Ground Floor, North Wing, St Thomas' Hospital,  
Westminster Bridge Road, London SE1 7EH.

## **B - Harm:**

In the event that something does go wrong and you are harmed during the research study there are no special compensation arrangements. If you are harmed and this is due to someone's negligence then you may have grounds for a legal action for compensation against King's College London but you may have to pay your legal costs. The normal National Health Service complaints mechanisms will still be available to you.

### **15. Will my taking part in this study be kept confidential?**

All information that is collected about you during the course of the research will be kept strictly confidential and anonymous. It may become necessary to access your hospital medical records.

Access to data collected in the study will securely be held on computers with access restricted to members of the research team. It will be used to develop further studies, which will need to be approved by an ethics committee. Results may be used in presentations or publications, but they will be anonymous. Procedures for handling, processing, storage and destruction of data will be compliant with the Data Protection Act 1998.

### **16. Involvement of the General Practitioner/Family doctor (GP)**

Your GP will be notified of your participation in the study. In addition, it will also be recorded in your hospital medical records.

### **17. Will any genetic tests be done?**

No genetic tests will be done.

### **18. What will happen to the results of the research study?**

It is hoped that the results of this study will be used to provide information for a larger study looking at non-invasive methods of pressure assessment. It is possible that the results will be published and presented both nationally and internationally. If this occurs, it will not be possible to trace individual patient data.

## **19. Who is organising and funding the research?**

The research is being organised by King's College London and by Guy's and St. Thomas' NHS Trust and is funded by the Royal College of Surgeons of England and Heart Research UK. The doctors conducting the research receive no direct funding for co-ordination of the study.

## **20. Who has reviewed the study?**

All research in the NHS is looked at by independent group of people, called a Research Ethics Committee, to protect your interests. This study has been given a favourable review by the Bromley Research Ethics Committee.

**MAY WE THANK YOU FOR CONSIDERING TAKING PART IN  
THIS STUDY**

## **A2 Patient information- MRI study**

# **PARTICIPANT INFORMATION SHEET**

## **A study of haemodynamics in aortic dissection (MRI scans)**

**PROTOCOL REFERENCE NUMBER: 14/LO/0286**

**VERSION NUMBER: 2**

**DATE: February 2014**

We would like you invite you to take part in our research study. Before you decide we would like you to understand why the research is being done and what it will involve for you. Please take time to read the following information carefully. Talk to others about the study if you wish. The research doctor (name below) will go through the information when they meet with you.

- Part 1 tells you the purpose of this study and what will happen to you if you take part.
- Part 2 gives you more detailed information about the conduct of the study.

Ask us if there is anything that is not clear or if you would like more information. Take time to decide whether or not you wish to take part.

# **PART 1**

## **1. What is the purpose of the study?**

Aortic dissection is a tear in the lining of the aorta, which is the main artery branching from the heart. This can happen for a number of reasons, commonly due to high blood pressure. Typically, patients experience severe chest pain. When a tear occurs, a second false channel (or lumen) for blood flow can develop. Blood flow can be diverted into this false channel and affect the blood supply to other vital organs. The management of dissection depends on the location of the tear in the aorta (upper or lower part) and the presence of any other complicating factors.

Some patients have poor outcomes after their dissection and we need to understand why this is the case. High blood pressure in the false lumen is thought to be an important factor, although this is not proven as yet. In this study we want to develop a non-invasive method of studying aortic pressures using MRI and computer simulation methods.

## **2. Why have I been chosen?**

You have been chosen because you have an aortic dissection, which is being monitored with regular Computed Tomography (CT) (and / or MRI scans).

## **3. Do I have to take part?**

No. It is up to you to decide whether or not to take part. We will describe the study and go through this information sheet. If you agree to take part, we will ask you to sign a consent form. You are still free to withdraw at any time and without giving a reason. A decision to withdraw at any time, or a decision not to take part, will not affect the standard or type of care you receive.



#### **4. What will happen to me if I take part?**

Patients enrolled in this study will be asked to have a total of 3 MRI scans over a period of 1 year. The scans will take about one hour each and we will check your most recent kidney function tests (via the hospital system or your GP). During the scan we may also site an intravenous cannula so a contrast agent (dye) can be given. We will reimburse your travel costs to and from the hospital.

#### **5. What do I have to do?**

You need to read this information leaflet and decide if this study may be of interest to you. In addition, if you are part of any other experimental studies you should make this known. If you would like to take part, please contact Miss Alia Noorani, (co-investigator), by completing and returning the enclosed reply slip by post, by email, on [alia.noorani@kcl.ac.uk](mailto:alia.noorani@kcl.ac.uk) or by phone or text on 07715802408.

#### **6. What are the side effects of any treatment received?**

MRI does not have any known adverse effects. If you have a pacemaker or other implanted metallic device or metallic foreign body we will ask you very specific questions about these before considering putting you in the MRI scanner.

The contrast agent (dye) used for the MRI scan can potentially cause allergic reactions. A mild reaction such as nausea, headache or a temporary funny taste in the mouth can occur in one in a hundred people (1%). Severe reactions such as anaphylaxis are very rare (<0.00001%).

In patients with severe kidney impairment (defined as  $GFR < 30 \text{ mL/min/1.73m}^2$ ) there is a risk of a contrast-based reaction called nephrogenic systemic fibrosis (NSF) but this is very rare (<0.00001%). Administration of these agents is considered to be safe in patients without severe impairment of renal function.

## **7. What are the other possible disadvantages and risks of taking part?**

It is important that you inform us if you are or could be pregnant.

If you have private medical insurance you should check with the company before agreeing to take part in the study to ensure that your cover will not be affected.

## **8. What are the possible benefits of taking part?**

We cannot promise that the study will help you, but the information we gain from this study will potentially help us improve the treatment of patients with aortic dissection in the future. It is however possible that other conditions you were not aware of will be discovered during the study. If this occurs then further follow up arrangements will be made.

## **9. What happens when the research study stops?**

Results from this study will be used to understand the importance of pressure in the false lumen and develop a non-invasive method of studying these pressures. The overall hope of this project is to improve how to target and manage patients who may be at greatest risk at the time of their original presentation.

## **10. What if there is a problem?**

Any complaint about the way you have been dealt with during the study or any possible harm you might suffer will be addressed.

The contact details are:

Miss Alia Noorani (Co-Investigator)

Division of Imaging Sciences

3<sup>rd</sup> Floor, Lambeth Wing

St Thomas' Hospital

London

SE1 7EH

Department of Imaging Sciences: 020 71885441

Direct line: 07715802408

Email: [alia.noorani@kcl.ac.uk](mailto:alia.noorani@kcl.ac.uk)

## **11. Will my taking part in the study be kept confidential?**

Yes. All the information about your participation in this study will be kept confidential. The details are included in Part 2.

## **12. Contact Details:**

For further information please contact:

Miss Alia Noorani (Co-Investigator)

Division of Imaging Sciences

3<sup>rd</sup> Floor Lambeth Wing,

St Thomas' Hospital

London

SE1 7EH

Telephone:

Department of Imaging Sciences: 020 71885441

Direct line: 07715802408

Email: [alia.noorani@kcl.ac.uk](mailto:alia.noorani@kcl.ac.uk)

*This completes Part 1 of the Information Sheet.*

*If the information in Part 1 has interested you and you are considering participation, please continue to read the additional information in Part 2 before making any decision.*

## PART 2

### 13. What will happen if I don't want to carry on with the study?

This will in no way affect any further medical treatment you receive within the Trust.

### 14. What if there is a problem?

#### A - Complaints:

If you have a concern about any aspect of this study, you should ask to speak with the researchers who will do their best to answer your questions

(Miss Alia Noorani: direct line 07715802408). If you remain unhappy and wish to complain formally, you can do this by contacting the **Patient Advice and Liaison Service (PALS)** based at St. Thomas' Hospital. Details are as follows:

Visit PALS at:

The Knowledge and Information Centre (KIC)

Ground Floor, North Wing, St. Thomas' Hospital.

Timings: Monday- Friday 10am-12pm and 2pm-4pm.

Tel: 020 7188 8801 / 020 7188 8803

Fax: 020 7188 1651

Email: [pals@gstt.nhs.uk](mailto:pals@gstt.nhs.uk)

Write: Patient Information Team, KIC, Ground Floor, North Wing, St Thomas' Hospital, Westminster Bridge Road, London SE1 7EH.

## ***B - Harm:***

In the event that something does go wrong and you are harmed during the research study there are no special compensation arrangements. If you are harmed and this is due to someone's negligence then you may have grounds for a legal action for compensation against King's College London but you may have to pay your legal costs. The normal National Health Service complaints mechanisms will still be available to you.

### **15. Will my taking part in this study be kept confidential?**

All information that is collected about you during the course of the research will be kept strictly confidential and anonymous. It may become necessary to access your hospital medical records.

Access to data collected in the study will securely be held on computers with access restricted to members of the research team. It will be used to develop further studies, which will need to be approved by an ethics committee. Results may be used in presentations or publications, but they will be anonymous. Procedures for handling, processing, storage and destruction of data will be compliant with the Data Protection Act 1998.

### **16. Involvement of the General Practitioner/Family doctor (GP)**

Your GP will be notified of your participation in the study. In addition, it will also be recorded in your hospital medical records.

### **17. Will any genetic tests be done?**

No genetic tests will be done.

### **18. What will happen to the results of the research study?**

It is hoped that the results of this study will be used to provide information to develop a non-invasive method of pressure assessment. It is possible that the results will be published and

presented both nationally and internationally. If this occurs, it will not be possible to trace individual patient data.

## **19. Who is organising and funding the research?**

The research is being organised by King's College London and by Guy's and St. Thomas' NHS Trust and is funded by the Royal College of Surgeons of England and Heart Research UK. The doctors conducting the research receive no direct funding for co-ordination of the study.

## **20. Who has reviewed the study?**

All research in the NHS is looked at by independent group of people, called a Research Ethics Committee to protect your interests. This study has been given a favourable opinion by the Bromley Research Ethics Committee.

**MAY WE THANK YOU FOR CONSIDERING TAKING PART IN THIS STUDY**

## A3 Research protocol- invasive study

# An investigation of intra-aortic haemodynamics in aortic dissection

---

Research Study Protocol

September 2013

Version 1



## Abstract

Aortic dissection is a major cardiovascular emergency and the commonest aortic catastrophe. Management of this disease depends on the morphology of the dissection, in particular, whether it involves the ascending (Stanford Type A) or descending aorta (Stanford Type B) and the presence of complications such as rupture, rapid growth and end organ ischaemic events.

Emergency surgery is the treatment of choice for Type A dissection although not every patient may be a candidate for surgery in view of pre-existing co-morbidities. Patients with Type B dissection are generally managed with strict pharmacological blood pressure control, although surgery is necessary in those with complications.

Outcomes of patients with chronic, residual, non-surgically treated Type B dissection (as well as surgically repaired Type A with a residual Type B component) are variable with 1 in 4 patients dead at 5 years from their original presentation. Predictors of outcomes are therefore needed to improve the prognosis in this population by identifying the at-risk group earlier.

## Rationale of the project

The treatment of aortic dissection is largely dependent on the morphology of the dissection and the presence of complicating factors. Involvement of the ascending aorta (Type A) requires emergency surgery if co-morbidities allow. Patients with Type B dissection (not involving the ascending aorta) are usually managed conservatively, with blood pressure control. However, the presence of complicating factors such as end-organ ischaemia, rapid aortic growth, on-going pain or rupture, necessitate intervention with an endovascular device (stent-graft), to effectively seal the entry tear and promote thrombosis. Patients with repaired Type A dissection may still have a residual false lumen distally (residual Type B dissection) which may expand over time.

Overall, stable patients are discharged with anti-hypertensives and require regular clinical review and imaging in the form of CT scans. These are performed to monitor overall aortic growth (defined as > 5mm growth between scans). An aorta that has a maximum diameter of 5.5 cm will also require endovascular repair.

Expansion of the false lumen is associated with adverse outcomes and false lumen haemodynamics may hold the answer to why some patients remain stable and others do not. A non-invasive method of determining these haemodynamic parameters would provide important insight into this complex disease and a greater understanding of how to best manage it. Non-invasive methods include using CT and MRI imaging and computational fluid dynamics (CFD) to estimate intra-aortic haemodynamics. However, these need to be validated against invasive methods that provide the ground truth. One such invasive, gold standard method is pressure wire monitoring similar to that performed in the coronary vasculature to physiologically assess coronary lesions.

## **Aim**

To determine invasive intra-aortic haemodynamics in patients with aortic dissection using pressure catheters.

## **Experimental Design and Methods**

### **Introduction**

All patients who demonstrate rapid aortic growth (>5mm between clinical CT scans), or have a maximum aortic diameter of 5.5cm or have on-going symptoms or development of flow related complications are considered for endovascular repair. The stent graft procedure involves careful pre-planning between the vascular and interventional radiology teams to ensure appropriate device selection and access to the aorta. All endovascular procedures, by nature of being minimally invasive require fluoroscopic guidance.

The research study will use a Certus PressureWire (St. Jude, MN, USA) which is a strengthened 0.014 inch wire with high-fidelity sensor technology which allows for simultaneous measurement of intravascular pressure, temperature and thermodilution (Figure 1). The presence of a hydrophilic coating enhances manoeuvrability and device compatibility. The sensor element of the wire is located 3 cm proximal to the tip and three electrical cables run from the sensor to the proximal end of the wire.

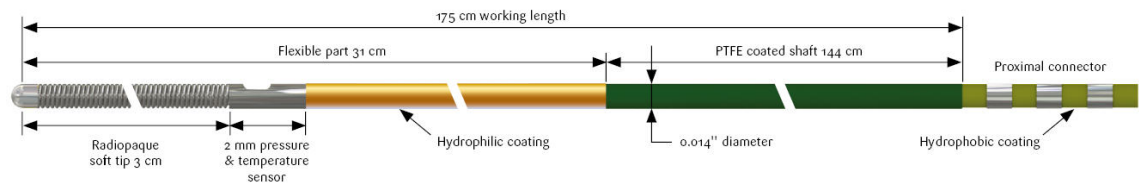


Figure 1

In conjunction with the Radianalyzer (St. Jude, MN, USA) monitor, accurate ( $\pm 1$  mmHg) readings of intravascular pressure can be made and recordings taken for further analysis using the RadiView software (St. Jude, MN, USA) (Figure 2).

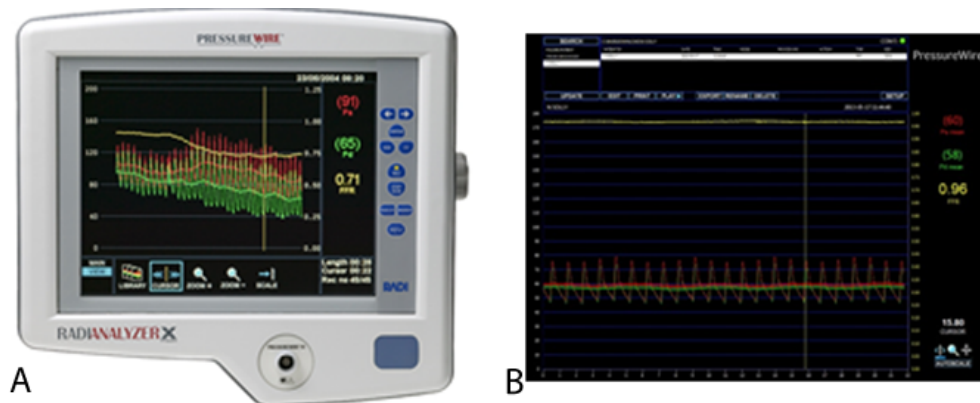


Figure 2 A snapshot of the RadiAnalyzer monitor (A) and screen recordings during a TEVAR case (B) are shown. Red trace = aortic pressure, green trace= false lumen pressure.

## Patient Identification

All clinical patients are discussed at bi-weekly multi disciplinary meetings (MDTs) involving radiologists and vascular surgeons. Only those dissection patients who are identified as requiring an endovascular procedure in view of their increasing aortic dimensions or presence of symptoms are approached and consented for the operation by the vascular surgical team. All these patients are potential candidates for the research study if they are willing to participate.

As this is a pilot study, no formal power calculation has been performed. It is estimated that data will be collected from a maximum of 15 patients

## **Patient Inclusion**

All adult patients (18-80y) with an aortic dissection that requires stent graft insertion to treat their dissection.

## **Patient Exclusion**

Patient choice.

## **Operators**

Consultant interventional radiologists and consultant surgeons. Supervised interventional radiology and surgical trainees.

## **Protocol**

### **a. Pre-procedure/ Information provision and consent**

Once a patient has been identified by the clinical team, they will be contacted to discuss the study. If they are at home, this will be by means of a patient information leaflet and telephone call. Admission for surgery is usually 3-4 days before the endovascular procedure and at this stage they will be approached once again to confirm their interest in participating in the study. After a period of 24 hours to consider participation, written consent will be sought by a clinical member of the research team and recorded in the notes.

### **b. Peri-operative**

On the day of the procedure, the patient will be prepared for theatre as is routine, by the ward and theatre staff. No special considerations need apply for the research study. All thoracic endovascular procedures usually take place in the hybrid theatre suites at St. Thomas' Hospital. Figure 3 shows the expected set-up in the hybrid suite. During anaesthesia, one of the co-investigators will arrange and set up all the required equipment that is needed to record the pressure wire data. Preoperative CT scans will be reviewed with the clinical team

to determine the anatomical location from which readings will be taken to ensure efficient data collection. Once intravascular access has been achieved by means of usually an 8Fr sheath (via a femoral artery) a catheter is placed in the aorta around to the aortic valve. This is the same as would happen in the stent graft procedure. At this point a pressure wire catheter is opened, and passed to the operating team, in a sterile fashion.

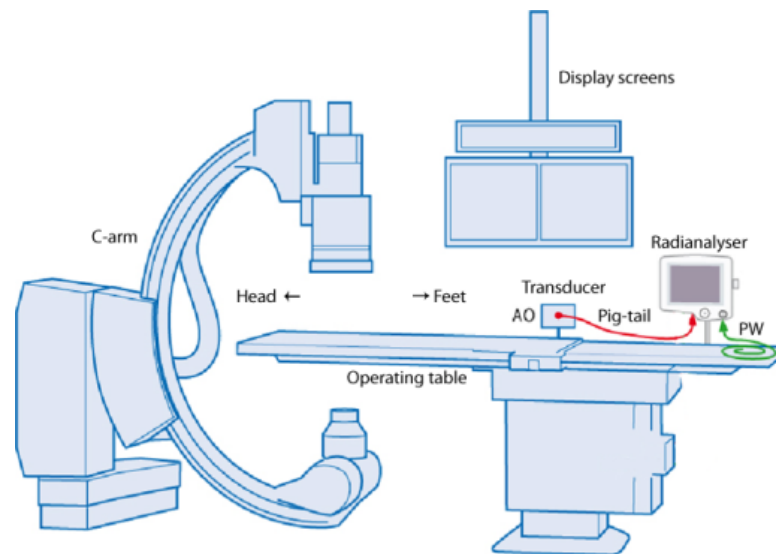


Figure 3 Set up in the hybrid theatre. With the C-arm in position, the RadiAnalyzer is attached to the operating table. Both the PressureWire (PW, green) and the pigtail (Ao, red) are connected to the transducer at the height of the patient's right atrium.

Calibration is then performed as per manufacturer's instructions by placing the catheter flat on the sterile operating field and by pressing the calibrate button on the recording monitor. As part of the operative procedure a pigtail catheter is passed into the aorta to serve as a (fixed) reference catheter for the pressure measurements. Once this is done, a Y connector (Minvasys, France) is connected to the intravascular sheath. This allows simultaneous

access for the pressure wire and the pig-tail aortic catheter, providing a reference reading for every intra-aortic pressure reading.

Next, depending on the anatomical location into which the pressure wire is inserted (true or false lumen), pressure wire readings are acquired. The maximum time taken for these will be 5 minutes.

Once the readings are complete the wire is withdrawn and the stent graft procedure continues as per routine. It is estimated that the entire data collection part of the study will take no more than 5 minutes.

## **List of equipment**

Pressure wire (St. Jude, MN, USA)

Y-connector (Minvasys, France)

Transducer (Edwards LifeSciences, CA)

Heparinised sodium chloride 1L, for transducer

Pressure wire monitor (St. Jude, MN, USA)

Connector tubing to connect to transducer

## **Ethical considerations**

The pressure wire study is an invasive study that has a small but potential risk of stroke. We estimate this to be very small, probably less than an additional 0.1%. There is a very small risk of perforation of the aortic wall. It is important to consider that the patient is already undergoing a major invasive procedure with an inherent risk of aortic rupture. Overall the risk of rupture from the pressure wire is thought to be less than 0.5% and the treatment involves

sealing the rupture with a stent graft. The endovascular procedure requires ionising radiation and the pressure wire study will add an estimated maximum of 5 minutes, pulsed radiation.

## Benefits of the study

It is unlikely that patients undergoing this procedure will benefit directly from this study but information collected here will be used to develop accurate non-invasive methods of vascular haemodynamic assessment, which future patients will benefit from.

## Resources and costs

1x Pressure wire £350

1x Transducer £ 10.20

1x Y Connector £19.50

1x Radiview monitor free of charge

Total    £379.7 per case

Signature

---

Chief investigator

---

Date



## **A3 Research protocol- MRI study**

### **An investigation of haemodynamics in aortic dissection**

---

**Research Study Protocol  
(Magnetic Resonance (MR) imaging)**

**September 2013**

**Version 1**

## Abstract

Aortic dissection is a major cardiovascular emergency and the commonest aortic catastrophe. Management of this disease depends on the morphology of the dissection, in particular, whether it involves the ascending (Stanford Type A) or descending aorta (Stanford Type B) and the presence of complications such as rupture, rapid growth and end organ ischaemic events.

Emergency surgery is the treatment of choice for Type A dissection although not every patient may be a candidate for surgery in view of pre-existing co-morbidities. Patients with Type B dissection are generally managed with strict pharmacological blood pressure control, although surgery is necessary in those with complications.

Outcomes of patients with chronic, residual, non-surgically treated Type B dissection (as well as surgically repaired Type A with a residual Type B component) are variable with more than 1 in 4 patients dead at 5 years from their original presentation. Predictors of outcomes are therefore needed to improve the prognosis in this population by identifying the at-risk group earlier.

## Rationale of the project

The treatment of aortic dissection is largely dependent on the morphology of the dissection and the presence of complicating factors. Involvement of the ascending aorta (Type A) requires emergency surgery if co-morbidities allow. Patients with Type B dissection (not involving the ascending aorta) are usually managed conservatively, with blood pressure control. The presence of complicating factors however, (end-organ ischaemia, rapid aortic growth, on-going pain or rupture) necessitate intervention with an endovascular device (stent-graft), to effectively seal the entry tear and promote thrombosis. Patients with repaired Type A dissection may still have a residual false lumen distally (residual Type B dissection) which may expand over time.

Overall, stable patients are discharged with anti-hypertensives and require regular clinical review and imaging in the form of CT scans. These are performed to monitor overall aortic growth (defined as > 5mm growth between scans). An aorta that has a maximum diameter of 5.5 cm will also require endovascular repair.

Expansion of the false lumen is associated with adverse outcomes and false lumen haemodynamics may hold the answer to why some patients remain stable and others do not. A non-invasive method of determining these haemodynamic parameters will provide important insight into this complex disease and a greater understanding of how to best manage it. Non-invasive methods include using CT and MR imaging and computational fluid dynamics (CFD) to estimate intra-aortic haemodynamics.

## **Aims**

To develop a non-invasive method for assessing intra-aortic haemodynamics in patients with aortic dissection using CT and MR imaging and Computational Fluid Dynamics (CFD) simulation.

## **Experimental Design and Methods**

### **Introduction**

All patients who present with aortic dissection who are considered to be stable are discharged home with stringent blood pressure control, and return for regular follow up CT scans. These patients will be invited for a maximum of 3 MR scans (if not already clinically performed).

## **Patient Identification**

All clinical patients are discussed at bi-weekly multi disciplinary meetings (MDTs) involving radiologists and vascular surgeons. As this is a pilot study, no formal power calculation has been performed. It is estimated that data will be collected from a maximum of 15 patients.

## **Patient Inclusion**

All adult patients (18-80y) with a medically managed aortic dissection are eligible to participate.

## **Patient Exclusion**

Patient choice and contra-indications to MR imaging, listed below.

## **Risks and burdens**

MR imaging does not have any known adverse effects. There are well-established contraindications for MR imaging, including pacemakers and other implanted metallic devices or metallic foreign bodies. Procedures in place in the MR unit will be used in this study to screen for and exclude such subjects.

A small proportion of people (<5%) experience claustrophobia on entering an MR scanner. It will be made clear to patients that they can terminate the study at any time if they are affected. No other discomfort or distress should be caused.

Gadolinium MR contrast agents can potentially cause allergic reactions although severe reactions are very rare. Administration of these agents is considered to be safe in patients without severe impairment of renal function.

Patients with acute or chronic severe renal impairment (i.e, GFR <30mL/min/1.73m<sup>2</sup>) will be excluded. In accordance with current recommendations we will screen all patients for renal dysfunction by checking the most recent blood tests on the hospital system or via the GP.

## Protocol

Once a patient has been identified by the clinical team, they will be contacted by the research team to discuss participation in the study. If they are at home, this will be by means of a patient information leaflet and telephone call. Patients who are considered stable and nearing discharge will be approached on the wards.

All MR scans will take place at the King's College 3T scanner Research scanner based at St. Thomas' hospital using standard clinical protocols.

A contrast agent will be required to enhance the images to improve anatomical detail and quantification of flow and false lumen thrombosis. Commonly used agents are either Gadovist (standard agent) or Vasovist (blood pool agent).

## Monitoring and safety

During the entire examination the patients will be monitored closely. All serious adverse event (SAE), serious adverse reaction (SAR) or unexpected adverse reaction (UAR) will be reported immediately by the Chief Investigator to King's College London (sponsor). As appropriate, these will then be reported to the regulatory authorities. This research is associated with the NHS indemnity scheme.

## Confidentiality

Person-identifiable image data may be stored on the MRI scanner. Data and image data will be identified by anonymous study number when transferred to computers for further analysis. Only the trial investigators will have access to the linkage between study number to patient identity. Data used for dissemination of results by presentation or publication will be anonymous.

## **Ethics and Regulatory Approval**

Application for ethical approval has been made in conjunction with this document.

## **Quality assurance, data handling, publication policy & finance**

Quality assurance will be maintained by Trust Clinical and Research Governance. Data protection will be maintained according to Trust guidelines. The Data Protection Act 1998 will be complied with. All information collected during the course of the study will be kept strictly confidential. Information will be held securely electronically with encryption of any transfer data.

## **Benefits to participants**

It is unlikely that patients undergoing this procedure will benefit directly from this study but information collected here will be used to develop accurate non-invasive methods of vascular haemodynamic assessment, which future patients will benefit from.

## **Resources and costs**

1x MRI scan £300

1x contrast agent £50

**Total** £350 per case

## A4 Consent form- invasive study

Centre Number:

Study Number: 14/LO/0286

Patient Identification Number for this trial:

Version: 1

Date: 16<sup>th</sup> Jan 2014

### CONSENT FORM

**Title of Project: An investigation of intra-aortic haemodynamics in aortic dissection**

Name of Researcher: **Alia Noorani**

**Please initial box**

1. I confirm that I have read and understand the information sheet dated .....  
(version 2 for the above study. I have had the opportunity to consider the information, ask questions and have had these answered satisfactorily.

☐

2. I understand there is a risk of a tear in the aorta approximately less than 0.5% and that the treatment for this will be the same as my planned stent graft procedure

☐

3. I understand that there is a very small risk of stroke (0.1%).

☐

4. I understand that my participation is voluntary and that I am free to withdraw at anytime, without giving any reason, without my medical care or legal rights being affected.

☐

5. I understand that relevant sections of any of my medical notes and data collected during the study may be looked at by responsible individuals from King's College London, from regulatory authorities or from the NHS Trust, where it is relevant to my taking part in this research. I give permission for these individuals to have access to my records.

☐

6. I agree to my GP being informed of my participation in the study.

☐

7. I agree to take part in the above study.

☐

_____	_____	_____	_____
Name of Patient	Date	Signature	
_____	_____	_____	Signature
Name of Person taking consent (if different from researcher)	Date		
_____	_____	_____	Researcher



# A4 Consent form- MRI study

Centre Number:

Study Number: 14/LO/0286

Patient Identification Number for this trial:

Version:2

Date: 3<sup>rd</sup> April 2014

## CONSENT FORM

**Title of Project: An investigation of haemodynamics in aortic dissection  
(MRI study)**

Name of Researcher: **Alia Noorani**

**Please initial box**

1. I confirm that I have read and understood the information sheet dated .....  
(version 2) for the above study. I have had the opportunity to consider the information, ask  
questions and have had these answered satisfactorily.

☐

2. I understand there is a risk of an allergic reaction to the contrast agent used in the MRI  
scan (mild approx.1%, severe <0.00001%) and nephrogenic systemic fibrosis (NSF) in  
severe renal impairment (<1%)

☐

3. I understand that I may feel claustrophobic (<5%) and that if I have metal fillings in my  
teeth I may feel tingling during the scan (<1%).

☐

4. I understand that my participation is voluntary and that I am free to withdraw at any time,  
without giving any reason, without my medical care or legal rights being affected.

☐

5. I understand that relevant sections of any of my medical notes and data collected during the study may be looked at by responsible individuals from King's College London, from regulatory authorities or from the NHS Trust, where it is relevant to my taking part in this research. I give permission for these individuals to have access to my records.

☐

6. I agree to my GP being informed of my participation in the study.

☐

7. I agree to take part in the above study.

☐

_____	_____	_____
Name of Patient	Date	Signature

_____	_____	_____
Name of Person taking consent (if different from researcher)	Date	Signature

_____	_____	_____
Researcher	Date	Signature